The Potential Role of Posttranslational Modifications on Angiotensin II Types 2 (AT2) Receptor Trafficking

JIANG, Lili

A thesis Submitted in Partial Fulfillment of the Requirements for the Degree of

Doctor of Philosophy

In

Biochemistry (Medicine)

The Chinese University of Hong Kong

April 2011

Thesis/Assessment Committee

Professor Helen Wise (Chair of Committee)

Professor Wing-Tai Cheung (Thesis Supervisor)

Professor Shannon Wing-Ngor Au (Committee member)

Professor Karl Wah-Keung Tsim (External examiner)

Declaration

I declare that the assignment here submitted is original except for source material explicitly acknowledged, and that the same or related material has not been previously submitted for the same or different courses. I also acknowledge that I am aware of University policy and regulations on honesty in academic work, and of the disciplinary guidelines and procedures applicable to breaches of such policy and regulations, as contained in the website http://www.cuhk.edu.hk/policy/academichonesty/.

Li Li	2011.4.21
Signature	Date
JIANG LI LI	1007038370
Name	Student ID
	Thesis
Course code	Course title

Abstract

Angiotensin II type 2 (AT2) receptor, belonging to G protein-coupled receptor (GPCR), is an important component of the renin-angiotensin system (RAS). What controls surface expression of AT2 receptor is still unknown. In the present study, to investigate the relationship between post-translational modifications and the trafficking of AT2 receptor, several N- or C- terminal tagged AT2 receptor variants were expressed in three different cell lines. AT2 receptor expression in mouse embryo tissue was also examined for comparison.

AT2 receptors tagged with GFP (AT2-GFP), Myc (Myc-AT2), HA (HA-AT2) and FLAG (AT2-FLAG) were transiently and stably expressed in three cell lines: HEK293, CHO-K1, and PC12. For tissue expression, mouse embryo on day 19 was used. AT2 receptor expression was examined by Western blot and confocal microscopy. Confocal microscopy demonstrated that AT2 receptor mainly expressed on cell membrane and perinuclear region in transfected cells. Although AT2 receptors were reported to undergo different post-translational modifications in different cell types, our Western blot results indicated that in stable cell lines, a tagged AT2 receptor variant always gave a similar molecular mass, suggesting similar post-translational modification occurred in different cells. Interestingly, the expression of AT2 receptor in mouse embryo tissue in Western protein analysis was similar to that of AT2 receptor transiently expressed in HEK293 cells.

The activity of expressed AT2 receptors was determined in stably-transfected cell lines. DNA fragmentation assay showed that AT2 receptor stably expressing CHO cells underwent apoptosis after serum starvation. Proliferation of AT2 receptor-expressing HEK293 and PC12 cells was inhibited in comparison to respective control cells. Flow cytometry analysis showed that AT2 receptor-expressing HEK293 cells accumulated in G1 phase, while AT2 receptor-expressing PC12 cells accumulated in S phase.

Both sumoylation and ubiquitination are involved in protein subcellular localization. To determine whether AT2 receptor was modified by SUMO or ubiquitin protein, HA-tagged SUMO or ubiquitin was co-expressed with AT2 receptor. Immunoprecipitation and Western protein analysis showed that AT2 receptor was not modified by SUMO protein under any circumstance. AT2 receptor was ubiquitinated only when AT2 receptor was transiently expressed in cells. Ubiquitination on AT2 receptor was also detected in brain tissue of Day 19 mouse embryo.

Surface expression of AT2 receptor was examined using purified membrane followed by Western protein analysis. It is of interest to note that glycosylation affected the membrane expression of Myc-AT2 in stably expressed HEK cells but had no effect on AT2-GFP. In contrast, oligomerization affected cell membrane expression of AT2-GFP in HEK cells. Mass spectrometry analysis of immunoprecipitated AT2 receptor complex found that β-actin was a specific AT2 receptor interacting protein in transfected cells.

摘　要

血管緊張素二型受體(AT2 受體)，一個 G 蛋白偶聯受體，是腎素-血管收縮素系統的重要組成成分。影響 AT2 受體在細胞表面表達的機理至今不明。為了研究 AT2 的翻譯後修飾與 AT2 在細胞內的轉運之間的關系，不同的 N-端與 C-端標記的 AT2 受體被表達在不同的細胞系中。小鼠胚胎組織中表達的 AT2 受體 被用來作為對照。

不同標記的 AT2 受體，包括 AT2-GFP, Myc-AT2, HA-AT2 以及 AT2-FLAG 被瞬時以及穩定地轉染在 HEK293, CHO-K1 以及 PC12 三種細胞系中。小鼠第 19 天的胚胎被作為組織研究的對象。AT2 受體的表達主要通過 Western 印記以及激光共聚焦顯微鏡技術來研究。激光共聚焦顯微鏡所得圖像顯示，在被轉染的細胞中 AT2 受體主要表達在細胞膜以及細胞核附近。雖然文獻報道 AT2 受體有各種不同的翻譯後修飾，Western 印記的結果顯示相同標記的 AT2 受體在不同的細胞系中表現為相同的分子量，暗示在不同的細胞系中 AT2 的翻譯後修飾是相似的。有趣的是，在胚胎組織中 AT2 的表達模式與瞬時轉染在 HEK293 細胞中的 AT2 相似。

AT2 受體在穩定表達的細胞系中的活性被檢測。DNA 片段分析顯示穩定表達 AT2 的 CHO 細胞在無血清培養後雕亡。穩定表達 AT2 的 HEK 以及 PC12 細胞的生長被抑制。流式細胞技術顯示與對照細胞相比，穩定表達 AT2 的 HEK 細胞更多的聚集在 G1 期，而穩定表達 AT2 的 PC12 細胞更多的聚集在 S 期。

泛素化修飾（ubiquitination）以及小泛素相關蛋白修飾（sumoylation）都與蛋白質在細胞中的定位有關。為了檢測 AT2 受體是否被 ubiquitin 或者 SUMO 修飾，HA 標記的 SUMO 以及 ubiquitin 與 AT2 受體同時表達在細胞系中。免疫沈澱以及 Western 印記顯示，SUMO 在任何情況下都不參與修飾 AT2 受體；相反，將 AT2 與 ubiquitin 同時瞬時表達在細胞中時，ubiquitin 修飾 AT2 受體。在小鼠 19 天胚胎的腦組織中也檢測到了 AT2 受體的泛素化修飾。

細胞膜表達的 AT2 受體被純化之後經過 Western 印記分析。結果顯示，糖基化修飾影響 Myc-AT2 在 HEK 細胞膜上的表達，但不影響 AT2-GFP 的表達。相反，多聚體的形成影響 AT2-GFP 在 HEK 細胞膜上的表達。質譜分析免疫沈澱的樣品發現了一個 AT2 的相互作用蛋白：β-acitn。

Acknowledgements

I would like to express my deep and sincere gratitude to my supervisor, Prof. Cheung Wing-tai. He, himself is a model for me on how to be a good scientist. He is strict and precise on science. In contrast, I am usually satisfied with "OK". I am really grateful for his constant guidance, patience and support on my research and presentation skills. His attitudes towards science and logical way of thinking have been of great value to me.

I also take this opportunity to thank my thesis committee Prof. Helen Wise, Prof. Shannon Wing Ngor Au, Prof. Karl Wah-Keung Tsim and my supervisor for review and suggestion on my thesis.

I would like to thank all my labmates in SC194: Elaine Chan, Wang Da-kui, Qi Wei, Zhao Qi, Li Zhou-fang, Shirley Chan, Sun Jing-xin and Sherman Cheng for their help and encouragement.

Finally, I give my deep gratitude to my parents and my boyfriend. Thanks for their love and support.

List of table

List of Figures

Table of Contents

Chapter 3 Functional characterization of AT2 receptor variants in stable cell lines

List of Abbreviations

ANGII	Angiotensin II
AT1 receptor	Type 1 angiotensin receptor
AT2 receptor	Type 2 angiotensin receptor
BCA	Bi-cinchoninic acid
BICP	5-Bromo-4-chloro-3-indolyl-phoshate, 4-toluidine salt
bp	Base pair
BSA	Bovine Serum Albumin
$CaCl_2$	Calcium chloride
CHO-K1	Chinese hamster ovary cell
CMV	Cytomegalovirus
CO_2	Carbon dioxide
DEPC	Diethyl Pyrocarbonate
DMEM	Dulbecco's Modified Eagle Medium
DNA	Deoxyribonucleoside triphosphate
dNTP	Deoxynucleotide Triphosphate
EB	Ethidium Bromide
EDTA	Ethylenediaminetetraacetic acid
EGFP	Enhance green fluorescent protein
ER	Endoplasmic reticulum

FBS	Fetal Bovine Serum
GFP	Green fluorescent protein
GPCR	G protein coupled receptor
HEK-293	Human embryonic kidney cells
kb	Kilobase
LB	Luria Bertani medium
NaCl	Sodium chloride
NBT	Nitroblue Tetrazolium Chloride
Ni-NTA	Nickel nitrilotriacetic
PAGE	Polyacrylamide Gel Electrophoresis
PBS	Phosphate buffered saline
PCR	Polymerase Chain Reaction
SDS	Sodium Dodecyl Sulfate
SUMO	Small ubiquitin like modifier
TAE	Tris-acetic acid-EDTA

Chapter 1 Introduction

1.1 GPCR

Guanine nucleotide binding proteins (G proteins) are a family of proteins which transmit outside chemical signal into cells and triggers cellular response. Heterotrimeric G proteins consist of three subunits: α, β and γ. Membrane proteins that transmit external signals via G protein activation are known as G protein coupled receptor (GPCR). There are two main requirements for a protein to be classified as a GPCR: 1) a seven transmembrane α helical structure with an extracellular N terminal and an intracellular C terminal (Baldwin, 1993); 2) bind to G proteins. Angiotensin II type 2 receptor (AT2 receptor) belongs to the GPCR family (Zhang and Pratt, 1996).

1.1.1 Characterization of GPCR

GPCRs comprise the largest family of transmembrane proteins in eukaryotic organism. The ligands that bind to and activate GPCR include hormones, neurotransmitters, lipids, peptides, ions and photons (Gether and Kobilka, 1998). Nearly half of the therapeutic drugs prescribed in the world target GPCRs (Bridges and Lindsley, 2008). There are about 1000 members in the super family which can be divided into six groups based on sequence similarity. They are rhodopsin like receptors, secretin receptor family, metabolic glutamate receptors, cyclic AMP receptors, fungal mating pheromone receptors and frizzled/smoothened receptors (Attwood and Findlay, 1994). AT2 receptor belongs to the rhodopsin like family, which is the largest group.

In the inactive state, the GDP-bound Gα subunit is associated with the Gβγ dimer. Once an extracellular ligand binds to a GPCR, the conformation of GPCR is changed from an inactive state to an active state. Activated receptor catalyzes the exchange of GDP for GTP on the Gα subunit. The Gα subunit bound with GTP dissociates from the Gβγ dimer. The Gα and Gβγ dimer then could independently interact and activate series of effectors, such as adenylyl cyclases, phospholipases and ion channels (Dupre et al., 2009).

There are 15 Gα, 5 Gβ and 12 Gγ subunits in humans. Heterotrimeric G proteins are generally referred to their Gα proteins, which are responsible for GDP/GTP binding. Gα proteins can be divided into four families based on sequence homology and functional similarities: Gαs, Gαi, Gαq/Gα11, and Gα12/13 (Dupre et al., 2009). It is commonly believed that AT2 coupled to Gαi proteins (Zhang and Pratt, 1996).

1.1.2 GPCR trafficking in cells

GPCRs are firstly synthesized, folded and assembled in the endoplasmic reticulum (ER). The properly folded GPCRs are packaged and transported by the ER-derived vesicles from ER to the trans-Golgi network (TGN), ER-Golgi intermediate complex and at last into Golgi apparatus. During transportation GPCRs undergo series of posttranslational modification such as N-glycosylation. The mature GPCRs are transported to cell membrane for function (Dong et al., 2007).

As shown in Figure 1.1, agonist stimulation of GPCR causes receptor activation, phosphorylation, β-arrestin binding and receptor internalization. It is a general property of activated GPCRs. Take angiotensin type I receptor (AT1 receptor) as an example: ANGII-stimulated AT1 receptors cause protein kinase C (PKC) activation and increase cytoplasmic calcium concentration. Furthermore mitogen-activated protein kinases (MAPK), Janus kinase-signal transducers and activators of transcription pathway (JAK/STAT) are also activated by AT1 receptors. At the same time ANGII also causes desensitization and subsequent sequestration of AT1 receptors. Activated AT1 receptors are phosphorylated by GPCR kinases (GRK) and PKC. Phosphorylated AT1 receptors form stable complex with β–arrestin and internalize in a β–arrestin and dynamin dependent manner into endosomes. Internalized AT1 receptors will be transported back to membrane in short term or degraded in long term (Oakley et al., 2000). However, activated AT2 receptors are not bound to β-arrestin or internalized (Pucell et al., 1991; Turu et al., 2006).

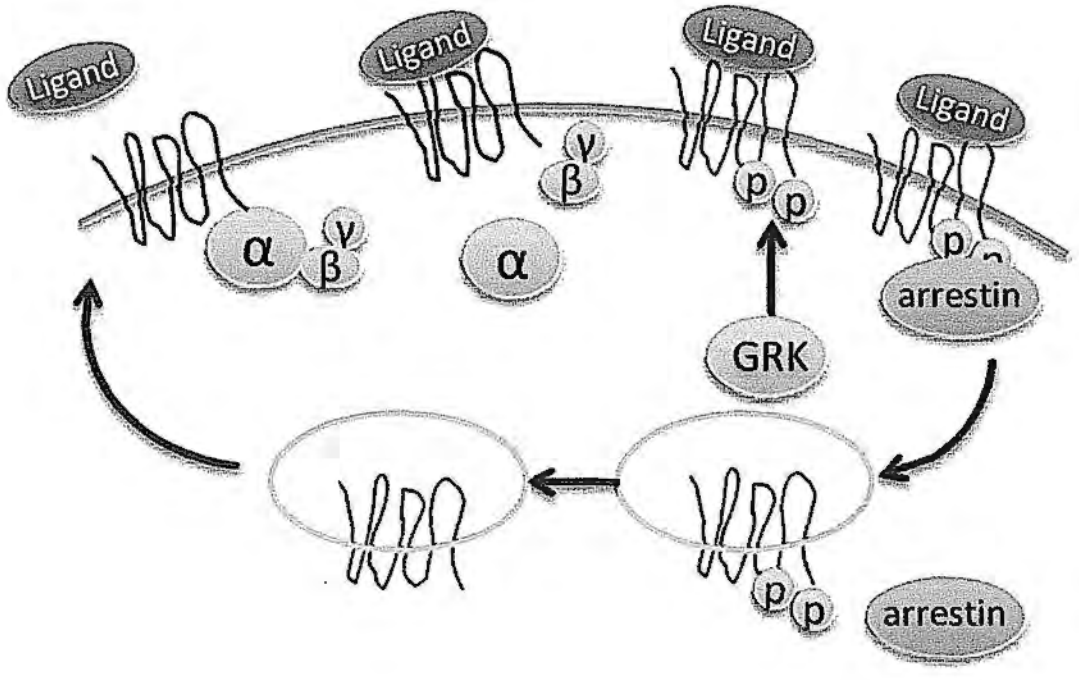

Figure 1.1 Activation and desensitization of GPCRs. After ligand binding, Gα dissociates from the dimer of Gβ and Gγ. The receptor was then phosphorylated by GRK and the phosphorylated receptor binds to β-arrestin followed by internalization. The internalized receptor could be recycled to cell surface. α, β and γ: G proteins; GRK: GPCR kinases; P: phosphate.

1.2 Renin-angiotensin system

1.2.1 RAS

The renin-angiotensin system (RAS) is a hormone system which plays a vital role in regulation of blood pressure and salt balance. The classic RAS mainly focuses on the processing of precursor angiotensinogen into the active peptide angiotensin II (ANGII) and the interactions between ANGII and its receptors.

Liver derived angiotensinogen is firstly cleaved by circulating renin into angiotensin I. Renin is a 45 kDa enzyme produced by granular cells of the renal juxtaglomerular apparatus. Angiotensin I is not yet active. It has to be cleaved into smaller molecular by different enzymes. The most important fragment generated from angiotensin I is ANGII, a major effector in RAS. The enzyme responsible for the conversion of angiotensin I into ANGII is angiotensin-converting enzyme (ACE) (Velez, 2009). ANGII binds to two types of receptors: AT1 and AT2 receptors, to elicit multiple functions (Figure 1.2).

The RAS becomes increasing complicated in the past few years. Firstly a homologue of ACE, named ACE2, was discovered. ACE2 convert ANGII into ANG1-7 by cleaving the C terminal amino acid of ANGII. ANG1-7 was suggested to act through Mas receptor to antagonize the actions of ANGII, including vasodilatation and anti-proliferation. Another fragment of ANGII: ANG3-8 and its receptor AT4 are also added to RAS regulating cognition and memory (George et al., 2010).

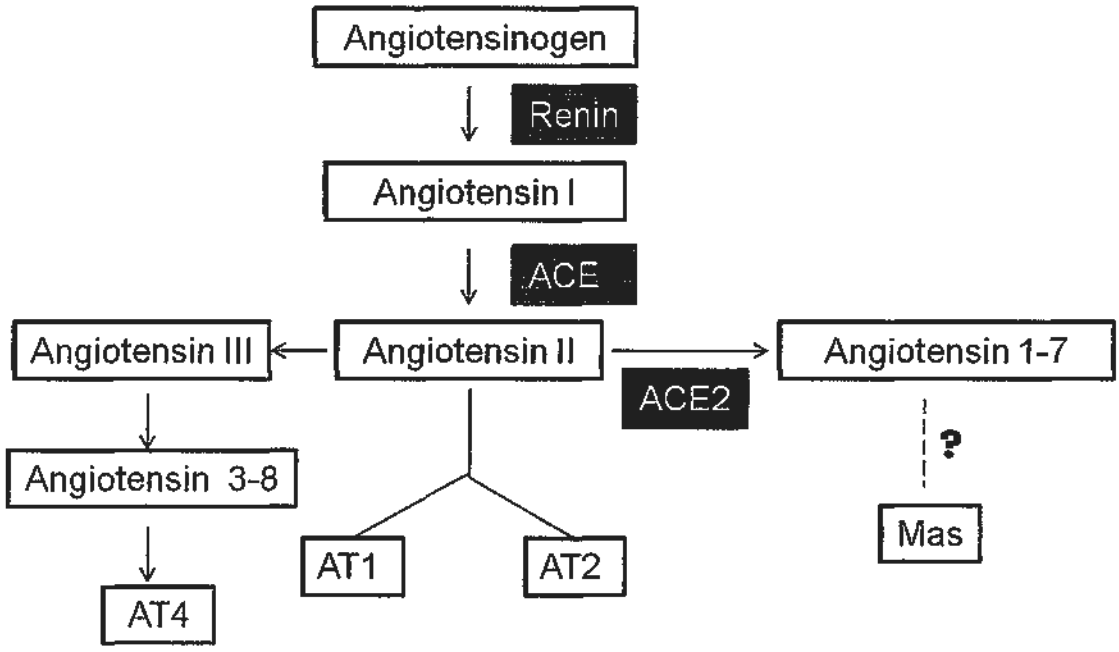

Figure 1.2 Schematic illustration of renin –angiotensin system (RAS). Angiotensinogen is cleaved into angiotensin I by renin. Angiotensin I is cleaved into angiotensin II (ANGII) by ACE. ANGII binds to AT1 receptor and AT2 receptor. Angiotensin 1-7 and angiotensin 3-8 was cleaved from ANGII. Angiotensin 1-7 was suggested as a ligand of Mas receptor. Angiotensin 3-8 binds to AT4 receptor.

The classic concept of RAS was referred to circulating RAS. However in recent years it is well recognized that local RAS exists in many tissues including brain, kidney, heart and blood vessels. The main components of RAS including angiotensinogen, renin, ACE and ANGII receptors were found co-expressed in all these tissues. The idea that local RAS function independent of circulating RAS was established (Ferreira et al., 2008).

Dysregulation of RAS is involved in different kinds of diseases including cancer, renal and cardiovascular disease. Angiotensin II receptor blocker and ACE blocker are commonly used for treatment of patients with hypertension and heart failure (Brown and Hall, 2005).

1.2.2 Physiological roles of ANGII

The RAS is a complicated system. The effects of ANGII can be divided into long term and short term. The short term effects are usually mediated by circulating RAS in seconds to minutes. These actions include contraction of vascular smooth muscle cells, release of other hormone and absorption of salt and water. For example, in case of sodium depletion, the secretion of renin increases immediately. The resulting elevation of plasma ANGII levels induces drinking and sodium appetite which will increase the absorption of water and Na^+ to compensate the loss. In meanwhile secretion of aldosterone and vasopressin induced by ANGII further regulate the balance of sodium and water (Hunyady and Catt, 2006).

The long-term effects are mediated by the local renin-angiotensin system instead. ANGII displays cytokine-like effects in end organs. These effects include cell growth and migration promotion, extracellular matrix deposition and vascular and electrical remodeling. For example, ANGII promotes vascular growth and cardiac hypertrophy (Munzenmaier and Greene, 1996); ANGII promotes Na^+/H^+ exchange in the apical membrane of proximal tubular cells in kidney which subsequently increase the reabsorption of NaCl (Tamura et al., 1998); In hearts, regulation of local RAS increase the efficiency of cardiovascular dynamics and help achieve sodium balance without large alterations in blood pressure (Mattiazzi, 1997).

1.2.3 Biochemistry of ANGII receptor

The effects of ANGII are mediated through two subtypes of receptor: AT1 receptor and AT2 receptor. Both receptors belong to the GPCR superfamily but share only about 34%

homology in amino acid sequence. They can be distinguished according to their affinities to selective non-peptide ligands and different sensitivity towards reducing reagents. Losartan, an antagonist of AT1, is selectively recognized by AT1 and has been used to treat for hypertension. Non-peptide antagonists PD123319 and CGP42112 are only specially recognized by AT2 receptor (Kambayashi et al., 1993). Sulfhydryl reducing reagents such as dithiothreitol (DTT), suppress AT1 receptor activities but have no effects or even enhance the activities of AT2 receptor (Song et al., 1992). However, Ang II has a similar affinity for both AT1 and AT2 receptors (de Godoy and Rattan, 2006).

Most of the classic functions of ANGII including vasoconstriction, antinatriuresis, aldosterone secretion, salt appetite, thirst and fibrotic process are mediated through AT1 receptors. In mammals, AT1 receptor is widely expressed in endocrine, renal and nervous system (Aldred et al., 1993; Edwards and Aiyar, 1993; Matsubara et al., 1993). Apart from the physiological effects, AT1 receptor is commonly involved in pathophysiological process through activation of the transcription factor nuclear factor-κB (NF-κB) which participates in a variety of inflammatory responses (Muller et al., 2000).

AT2 receptor is abundantly expressed in whole bodies of fetus in late gestation and its expression is dramatically decreased after birth (Matsubara et al., 1998). These findings suggest a possible role for AT2 receptor in development and differentiation. In adult AT2 receptor expression is detectable in adrenals, distinct area of brain, kidney and pancreas (Lenkei et al., 1997; Leung et al., 1997; Miyata et al., 1999; Pernollet et al.,

1979). Expression of AT2 receptor is increased under pathological condition such as renal and heart failure (Volpe and De Paolis, 2000). It is commonly believed that AT2 receptor acts against AT1 receptor in vasoconstriction, antigrowth and apoptosis. In AT2 receptor knockout mice (AT2-/-), AT1 expression is increased in kidney and heart which shifts the pressure-natriuresis rightward (Gross et al., 2004). Although AT2 receptor deficient mice appear normal, they showed a markedly reduced exploratory behavior when placed in a new environment (Ichiki et al., 1995). AT2 receptor deficient in human is linked to mental retardation (Vervoort et al., 2002).

1.3 AT2 receptor

1.3.1 Characterization of AT2 receptor

The cDNA of AT2 receptor was cloned from a cDNA library of PC12W cells (rat phenochromocytoma cell line) and a cDNA library of mouse fetus (Kambayashi et al., 1993; Nakajima et al., 1993). Soon after the human AT2 receptor gene was isolated from a genomic DNA library from human placenta (Tsuzuki et al., 1994). In human and mice, AT2 receptor exists as a single copy localized on the X chromosome and has no intron. The cDNA of AT2 receptor encodes a 363-amino acid protein in rat and human. AT2 receptor in different mammalian species are highly homologous (>91%) in amino acid sequence (Figure 1.3); most variations of amino acids are located in the short

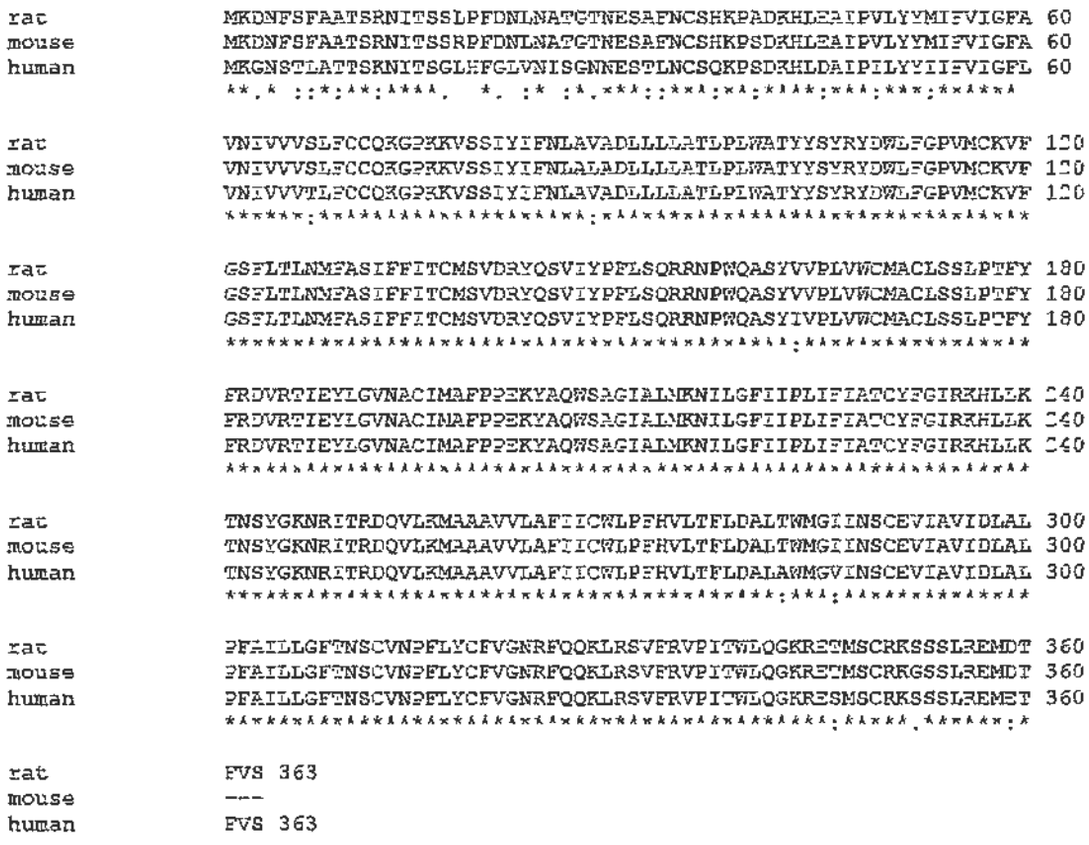

Figure 1.3 Protein sequence alignment of the rat, mouse and human AT2 receptor. The protein sequences of rat and human AT2 receptor contain 363 amino acids, while mouse AT2 receptor contains 360 amino acids. NCBI accession numbers of rat, mouse and human AT2 receptor protein sequence are NP 036626.1, NP 031455.1 and NP 000677.2 respectively.

N-terminal region (Feng et al., 2005). Predicted structure of AT2 receptor shows the characteristic structure of GPCR: a seven transmembrane domain.

There are five potential glycosylation sites in AT2 receptor. Glycosylation is an enzymatic process that attached glycans to target proteins or lipids. Most of proteins undergo glycosylation in ER. Glycosylation of AT2 receptor has been demonstrated by different molecular weight of AT2 receptor in different tissues and different cell lines analyzed by reducing SDS-PAGE (Ouali et al., 1993; Servant et al., 1994, 1996). Different degrees of glycosylation of AT2 receptor caused marked divergence of molecular weight ranging from 40~200kDa.

There are four conserved cysteine (C) residues located on the extracellular domains of AT2 receptor. It was reported that AT2-GFP expressed in CHO cells formed dimer through C35 and C290 (Miura et al., 2005).

There is a potential protein kinase C (PKC) phosphorylation site in the second intracellular loop of AT2 receptor and three potential PKC phosphorylation sites, one potential cyclic AMP (cAMP)-dependent protein kinase site in the C-terminal of AT2 predicted by EXPASY tools (http://expasy.org/tools/). It has been proved that AT2 receptor is linked to PKC but not cAMP-dependent pathways in the cardiomyocyte (Rabkin, 1996). AT2 receptor expressed in COS-7 cells is rapidly phosphorylated via PKC during activation by ANGII (Olivares-Reyes et al., 2000). Unlike other GPCRs, AT2 receptors are not phosphorylated by any GPCR kinases (Turu et al., 2006).

1.3.2 Signaling pathways of AT2 receptor

Four major signal transduction pathways are activated by AT2 receptor:

(1) Nitric oxide (NO)-cyclic guanosine monophosphate (cGMP) activation. NO is an important mediator of AT2 receptor. AT2 receptor activation stimulates NO production and cGMP increase (Siragy and Carey, 1997). NO-cGMP is involved in ANGII/AT2-induced vasodilatation (Savoia et al., 2006), sodium and water absorption (Carey et al., 2000) and differentiation in PC12W cells (Zhao et al., 2003)

(2) Phospholipase-A2 (PLA2) activation with subsequent release of arachidonic acid (AA). ANGII/AT2 binding releases Gβγ which in turn activates PLA2. PLA2 catalyzes release of AA (Haithcock et al., 1999). AA could be metabolized by a cytochrome P450-dependent monooxygenase to products that affect ion transport, Na^+, K^+-ATPase, ion transport, Na^+-H^+ exchange and mitogenesis (Jacobs and Douglas, 1996).

(3) Protein kinase C (PKC) activation. AT2 receptor-mediated cardioprotection effects are due to PKC activation in the cadiomyocytes (Xu et al., 2000). In transfected COS7 cells, PKC is activated through AT2 receptor after ANGII stimulation (Olivares-Reyes et al., 2000). However, in NG108-15 cells AT2 receptor inhibits PKC and promotes cell differentiation (Beaudry et al., 2006).

(4) Protein phosphatase activation. Three specific phosphatases have been reported to be activated downstream of AT2 receptor: (a) protein phosphatase 2A; (b) mitogen-

activated protein kinase phosphatase (MKPs); (c) SH2-domain containing phosphatases (SHP-1). Protein phosphatase activation is usually linked to AT2 receptor-induced cell proliferation inhibition and apoptosis (Lee et al., 2010). However AT2 receptor-induced MAPK activation was also reported in NG108-15 cells (Gendron et al., 1999)

1.3.3 AT2 interacting proteins

Direct physical protein interacting partners of the AT2 receptor described so far include the following:

1) G proteins. In 1996 it was discovered that the AT2 receptor coupled to both Gαi2 and Gαi3, which proved that this receptor was G-protein coupled (Zhang and Pratt, 1996). Recently AT2 receptor was reported to interact with Gαs through a tyrosine phosphatase: SHP-1 (Feng et al., 2002).

2) Transcription factor promyelocytic zinc finger protein (PLZF). The interaction between AT2 receptor and PLZF was revealed by yeast-two-hybrid screening of a human heart library. Confocal microscopy showed that ANGII stimulation induced cytosolic PLZF to co-localize with AT2 receptor at cell membrane and drove AT2 receptor to perinuclear region. AT2 receptor enhances expression of PI3K p85α subunit through PLZF (Senbonmatsu et al., 2003).

3) SH2 domain containing phosphatase 1 (SHP-1). AT2 receptor mediated protein phosphatase activation was reported in 1995 (Mukoyama et al., 1995). Direct physical association with SHP-1 was discovered in 2002. The association required

the presence of Gαs alone rather than the G protein heterotrimer. SHP-1 decreased cellular tyrosine phosphorylation (Feng et al., 2002).

4) AT2 receptor binding protein (ATBP). The interaction between AT2 receptor and ATBP was discovered through yeast-two-hybrid by screening of a mouse embryo library. ATBP localized in Golgi membrane and regulated AT2 receptor transport from ER to cell membrane. mRNA levels of ATBP was increased after AT2 receptor activation and decreased in AT2 receptor knock-out mice (Wruck et al., 2005). However ATBP is ubiquitously expressed not restricted to the expression pattern of AT2 receptor.

5) Na^+/H^+ exchanger (NHE 6). NHE6 was also discovered through yeast-two-hybrid by screening of a mouse 17-day fetus cDNA library. NHE are integral plasma membrane proteins that exchange extracellular Na^+ for intracellular H^+. They regulated multiple cellular functions including intracellular pH homeostasis, cell volume control, and electro neutral NaCl absorption in epithelia. In transfected COS-7 cells AT2 receptor was precipitated with HA tagged NHE6 after ANGII treatment (Pulakat et al., 2005).

6) ErbB3 receptor. ErbB3 was discovered to interact with AT2 receptor through yeast-based two-hybrid protein-protein interaction assay by screening random peptide library. ErbB3, which is also expressed during fetal development, belongs to the epidermal growth factor receptor family. However the interaction was only proved in

yeast-based two-hybrid assays, no more evidence has been reported (Knowle et al., 2000).

1.3.4 Trafficking of AT2 receptor

To interact with exogenous ligands, GPCRs need to be expressed on plasma membrane. The trafficking mechanism of AT2 receptor to cell membrane is largely unknown. AT2 receptors have no N-terminal hydrophobic signal sequence characteristic of many membrane proteins for their insertion into membrane (Wickner and Lodish, 1985). A Golgi membrane associated protein ATBP was reported to regulate the transport of the AT2 receptor from ER to cell membrane through binding to the C terminal of AT2 receptor. When ATBP was silenced by siRNA in N1E-115 cells, membrane expression of transfected AT2-GFP was disrupted (Wruck et al., 2005). Alternatively, insertion of AT2 receptor into the membrane may spontaneously happen due to its hydrophobic nature (Engelman and Steitz, 1981).

AT2 receptor trafficking induced by ANGII has been reported in smooth muscle cells. In basal state, AT1 receptor resides in cell membrane while AT2 receptor is present in cytosol. Higher concentration of ANGII (10 μM, usually 1 μM for physiological concentration) causes AT1 receptor internalization and AT2 receptor transport to cell membrane. The authors also suggested that AT1 receptor was activated by low concentration of ANGII and AT2 receptor was activated by high concentration of ANGII (de Godoy and Rattan, 2006).

Studies in primary cells and expression system suggest that in contrast to common GPCR, ANGII-stimulated AT2 receptors are not internalized (Pucell et al., 1991). Consistent to this, no interaction between AT2 receptor and arrestin was detected in transfected cells (Turu et al., 2006). In 2003, a group found that AT2 receptor stimulated by ANGII internalized into cytosol when coexpressed with a transcription factor promyelocytic zinc finger protein (PLZF). Upon ANGII stimulation, PLZF bound to the C terminal of AT2 receptor and brought AT2 receptor back to perinuclear region (Senbonmatsu et al., 2003).

1.3.5 Post-translational modification related to AT2 receptor cell membrane expression

As mentioned in section 1.3.1, there are several potential glycosylation and phosphorylation sites predicted in AT2 receptors. Indeed lines of evidence indicated that AT2 receptors are subjected to the following post-translational modifications:

1.3.5.1 Phosphorylation

There are two kinds of phosphorylation on GPCR: a) phosphorylation mediated by second messenger dependent serine-threonine kinases (protein kinase A and PKC) which also could occur on inactive receptors; b) phosphorylation of activated receptor by GPCR kinase (GRK) which causes subsequent coupling of GPCR with arrestin for internalization (Turu et al., 2006).

Phosphorylation of the AT2 receptor by PKC has already been demonstrated, but GRK-mediated phosphorylation of the AT2 receptor has not been detected (Olivares-Reyes et

al., 2000). GRK mediated phosphorylation has an important role in β-arrestin binding to activated GPCR and subsequent internalization. This might explain why activated AT2 receptor is not internalized quickly like a normal GPCR.

1.3.5.2 N-glycosylation

N-glycosylation is one type of glycosylation which is important for folding of eukaryotic proteins. It is also responsible for localization of some GPCRs. For example, after putative N-linked glycosylation consensus motif was mutated, AT1 receptor distributed at a much higher density to the ER-Golgi complex than to the plasma membrane in HEK293 cells (Lanctot et al., 1999). Although AT2 receptor undergoes extensive N-glycosylation, previous report showed that in PC12W cells, a subline of PC12 rat pheochromocytoma cell line (Speth and Kim, 1990), deglycosylated form of AT2 receptor still could be detected in plasma membrane (Servant et al., 1996).

1.3.5.3 Dimer or oligomerization

GPCR are able to form both homodimer and heterodimer. For example, β2-adrenergic, dopamine D2 and opioid receptors undergo homo-dimerization following agonist stimulation (Franco et al., 2007). AT1 and AT2 receptor dimerization led to AT1 receptor signal inhibition (AbdAlla et al., 2001). Homodimer and oligomer of AT2 receptor was detected in prefrontal cortex membranes of AD patients (AbdAlla et al., 2009). Furthermore, homo-dimer of AT2 receptor localized in the cell membrane and induced apoptosis without ANGII stimulation. Cys mutant form of AT2-GFP lost cell membrane expression in CHO cells (Miura et al., 2005). However, on cell membrane,

AT2 receptor mainly formed homo-dimers, rather than hetero-dimers with AT1 receptors (Miura et al., 2010).

1.4 Ubiquitination and sumoylation

Both ubiquitination and sumoylation occurs through the sequential activation of a cascade of reactions catalyzed by three classes of enzymes (E1, E2 and E3), resulting in the covalent attachment of ubiquitin or SUMO (small ubiquitin like modifier) to a lysine residue in the target proteins. Both ubiquitination and sumoylation regulate proteins by altering the surface of target protein which in turn affects interaction with other proteins. Despite these common features there are still some significant differences between the two posttranslational modifications.

1.4.1 Ubiquitin and Ubiquitin like modifiers

Ubiquitin and Ubiquitin-like modifiers (the best known of which is SUMO) are a group of small molecular weight proteins. All these proteins share similar 3-D structure and a similar conjugation mechanism, through their C-terminal to a particular lysine residue of their substrates. Both ubiquitin and SUMO proteins can be covalently and reversibly conjugated to the target proteins.

1.4.2 Ubiquitin

Ubiquitin is a small protein which consists of 76 amino acids. It has a C terminal glycine which can form an isopeptide bond with the ε-amino group of a lysine in target proteins. Covalent conjugation of ubiquitin to targets begins with ubiquitin activation by binding to E1 enzymes in an ATP dependent manner. Then ubiquitin is transferred to E2 enzymes. A substrate is selected in cells by an E3 ligase and ligated to E2 enzymes. As a result, a ubiquitin protein is added to a lysine residue in substrate (monoubiquitination). A single protein can be modified by multiple ubiquitins at different sites (multiubiquitination). Since ubiquitin itself contains lysine residues in seven positions, all of these sites could be modified by another ubiquitin (polyubiquitination). Ubiquitin can be removed and recycled by deubiquitinating enzymes (DUBs). The human genome encodes two E1s, about 40 E2s and more than 600 E3 ligases. About 95 DUBs have been identified in humans (Deshaies and Joazeiro, 2009). The ubiquitination pathway is shown in Figure 1.4.

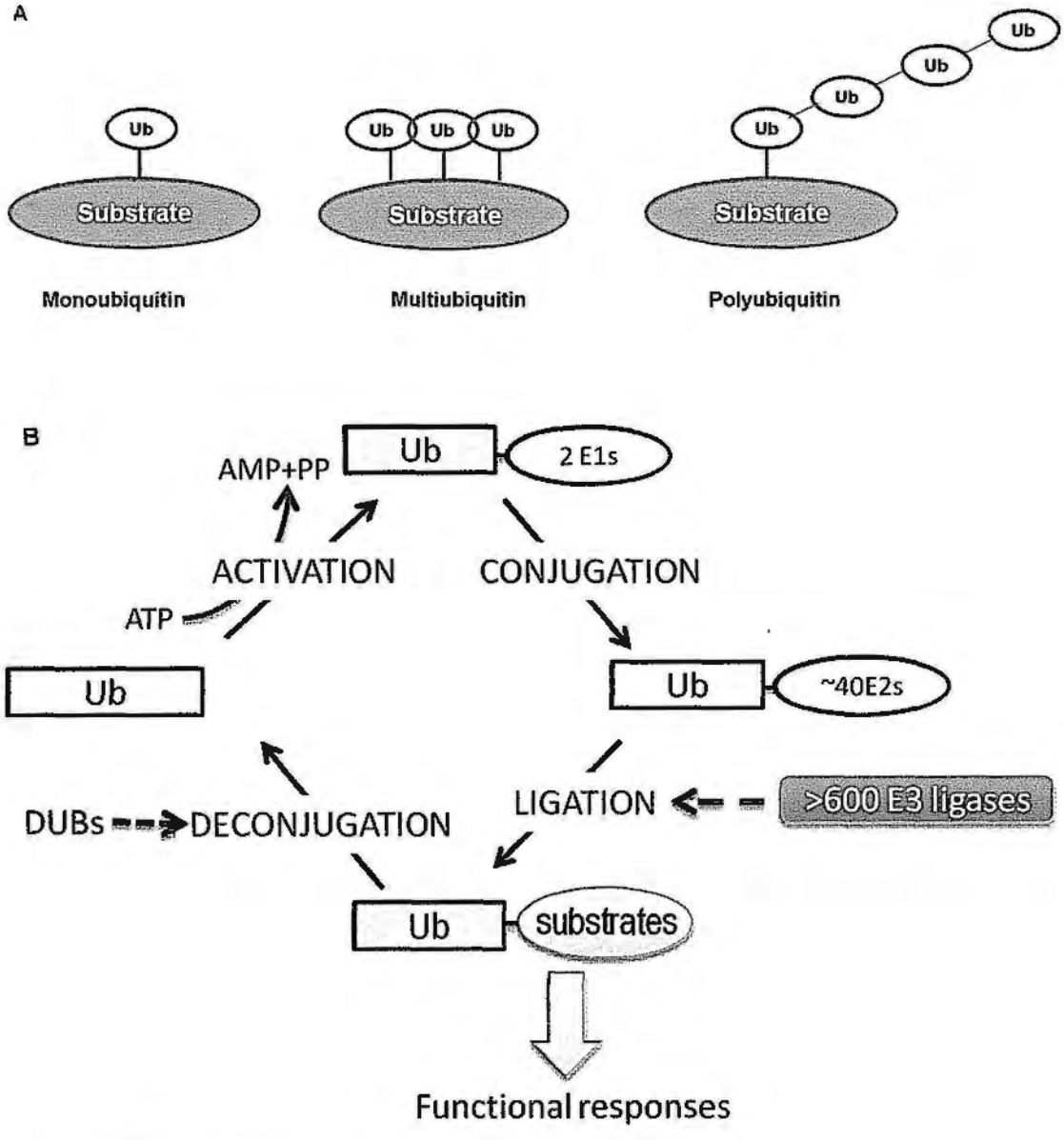

Figure 1.4 Ubiquitination pathway.

A) Different types of ubiquitination. B) Ubiquitination initiation, conjugation and ligation. Ub: ubiquitin, E1, activating enzyme; E2, conjugating enzyme; E3, ligation enzyme; DUB: deubiquitinating enzyme. Modified from Liu and Walters (2010).

Ubiquitin is well known for targeting protein degradation. Misfolded and abnormal proteins could form insoluble aggregates which are toxic to cells. The ubiquitin-proteasome system (UPS), which resides both in the nucleus and in the cytosol, recognizes and targets protein for degradation. Poly-Ubiquitin chain on proteins is a signal of protein degradation. The length of the chains is variable. Poly-ubiquitin modified proteins are transport to proteasome in which proteins are degraded into oligopeptides. The oligopeptides will be released into cytosol and further degraded into amino acids. Polyubiquitination is also involved in other types of protein degradation such as autophagy and lysosome degradation (Korolchuk et al., 2010).

Ubiquitination also induces functions other than protein degradation. Polyubiquitin chains, monoubiquitination or multiubiquitination regulate enzyme activity, DNA repair, ribosomal regulation, transcription modulation and protein localization and trafficking (Watson and Irwin, 2006).

Ubiquitination plays an important role in membrane protein trafficking. Monoubiquitination alone is sufficient for some receptor internalization in yeast, such asalpha-factor receptors, permeases and transporters. Ubiquitination also regulates receptor endocytosis and sorting them to multivesicular bodies and lysosome for degradation (Acconcia et al., 2009).

1.4.3 SUMO

SUMO and ubiquitin share similar 3-D structure but only 20% similarity in amino acid sequence. SUMO proteins are about 10 kD in size and ubiquitously expressed in eukaryotic organisms. The human genome encodes four SUMO proteins: SUMO1-SUMO4. SUMO1-SUMO3 are ubiquitously expressed whereas SUMO4 mainly expressed in kidney, lymph node and spleen. The sequence identity between SUMO1 and SUMO2 is about 46%, but the mature form of SUMO2 and SUMO3 are nearly identical (Su and Li, 2002).

All SUMO proteins are expressed as an immature precursor which carries a C terminal after a Gly-Gly motif. The C terminal has to be removed to expose the double Gly motif. The mature SUMO proteins are activated by conjugating to a heterodimer (SAE1/SAE2) in an ATP dependent manner. Then SUMO is transferred to the E2 conjugating enzyme Ubc9 by forming a thioester bond between the Ubc9 and the C terminal of SUMO. Finally Ubc9 transferred SUMO to the target proteins usually with the help of E3 ligases (Figure 1.5) (Geiss-Friedlander and Melchior, 2007). In ubiquitination system, substrate specificity is determined by dozens of E2 and hundreds of E3. But for sumoylation there is only a single E2, Ubc9, and much less E3 ligases. Ubc9 deficient mice is embryonic lethal (Nowak and Hammerschmidt, 2006). SUMO proteins can be removed from the target proteins by specific enzymes like sentrin specific proteases (SENP). SENPs are also responsible for the maturation of SUMO proteins.

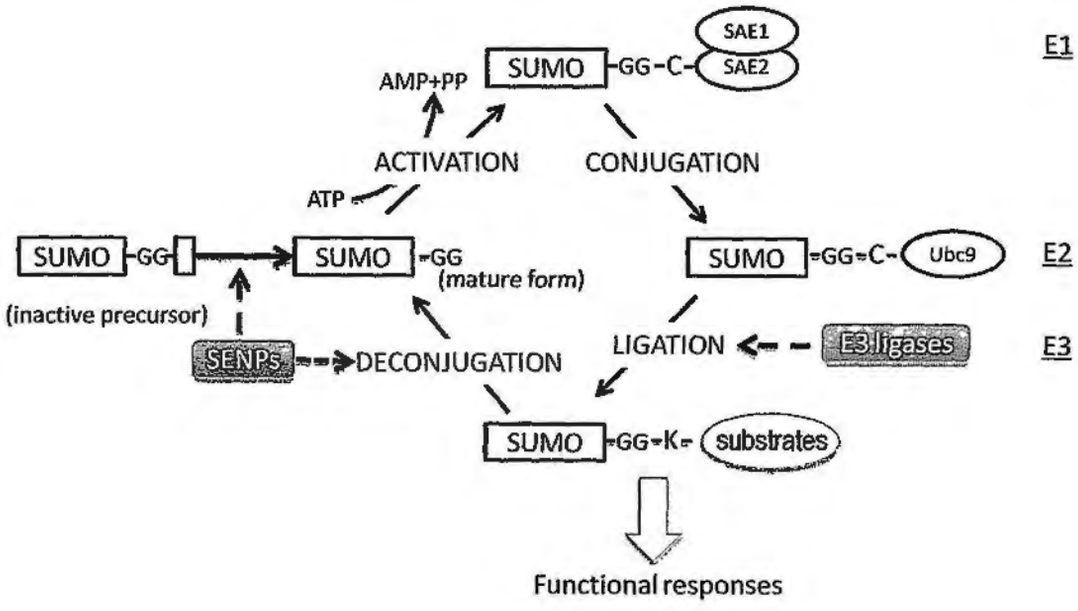

Figure 1.5 Sumoylation pathway. Sumoylation pathway consists of SUMO protein maturation, SUMO activation, conjugation to E2 ligase (Ubc9) and ligation to the target protein. Modified from Woo and Abe (2010).

A distinct feature for sumoylation is that the target lysine residues are often found in a consensus motif, ΨKXE, where Ψ is a large hydrophobic amino acid, K the modified lysine, X can be any amino acid and E is a glutamic acid residue. However not all sumoylated proteins identified contain this motif (Woo and Abe, 2010).

Hundreds of proteins have been identified to be modified by SUMO, the majority of which are nuclear proteins. In contrast to poly-ubiquitination, sumoylated proteins are often modified by a single SUMO protein on one target lysine. Monosumoylation regulates genome stability, DNA transcription and repair, and protein nuclear/cytosol transport. Poly-chains formed by SUMO2/3 have been reported lately. The function of poly-sumoylation is still poorly understood (Geiss-Friedlander and Melchior, 2007).

Sumoylation is not only restricted in nuclear. Recent data shows proteins in cytosol and cell membranes can also be sumoylated. For example, an ER related protein, protein-tyrosine phosphatase-1B (PTP1B) has been proved to be sumoylated. Sumoylation on membrane glutamate receptor 6 (mGluR6) induces endocytosis of the receptor. A GPCR Glu8 is also discovered to be sumoylated but with unknown function (Geiss-Friedlander and Melchior, 2007).

1.4.4 Interaction between sumoylation and ubiquitination

Sumoylation and ubiquitination are connected with each other. For example USP25, a deubiquitinating enzyme, could be modified by both SUMO and ubiquitin at the same lysine residue. Sumoylation on USP25 inhibits its protease activity on polyubiquitin chain which subsequently inhibits ubiquitin recycle. When USP25 is ubiquitinated, the enzyme is activated (Denuc and Marfany, 2010).

It happens quite often that sumo and ubiquitin modify the same lysine residue in one protein. The effects of the two modifications could be the same or antagonist to each other. More often, sumoylation and ubiquitination on the same lysine residue result in multiple effects. One well characterized example for this is p53. Polyubquitination on p53 leads to protein degradation in proteasome whereas monoubiquitination direct its nuclear export. SUMO1 modification on p53 increase its transcription activity (Watson and Irwin, 2006).

1.5 Aims of study

A main problem for RAS study is that the components of RAS are often expressed at low level. It is difficult to define the expression especially using antibodies with low specificity and sensitivity. This is particularly true for AT2 receptor. Whether they can be used to detect endogenously expressed AT2 receptor is still controversial (George et al., 2010). In present study, the expression and trafficking of AT2 receptor were examined. Specifically, the following three questions were addressed:

1.5.1 Does tagging affect AT2 receptor expression?

It seems that AT2 receptor behaves differently in different cell types. The results are still controversial regarding the molecular weight and signaling pathways of AT2 receptor in different cells (Lee et al., 2010). Since cell lines were used as models in present study for the trafficking and cell membrane localization of AT2 receptor, the differences of AT2 receptor expression in different cell lines should be considered.

Previous data from our lab indicated that a GFP tag attached to the C-terminus of another GPCR Mas partially affected the translocation of the receptor after agonist stimulation. It suggests that the C-terminus is important for GPCR trafficking. The C-terminus which mediates most of the functions of AT2 receptor, could also affects the receptor trafficking and localization. From sequence results of AT2 receptor in different species, most variations of amino acids are located in the N-terminal region. It suggests that the N-terminus of AT2 receptor determines the ligand binding specificity of the

receptor. The difference between C-terminal tag and N-terminal tag should also be noticed. Besides, differently tagged AT2 variants, even at the same position, could also behave differently due to the character of tags and detection methods.

To assess the influence in different cells and different tags, three different cell lines (HEK293, PC12 and CHO-K1) were used in present study and differently tagged AT2 variants were constructed. Both transient and stable expression was performed with these tagged AT2 variants in the three cell lines. The expression and subcellular localization of AT2 receptor expressed in these cells were confirmed by western blot and confocal microscopy using tag-specific antibodies. To compare the native form of AT2 receptor, mouse embryo tissue which expressed large amount of AT2 receptor was also studied with a polyclonal antibody against AT2 receptor raised in our lab years ago.

1.5.2 Whether AT2 receptor is modified by sumoylation and/or ubiquitination

Both sumoylation and ubiquitination are linked to protein transport in cells. Two putative sumoylation sites (K343, K73) were predicted by the online program SUMOplot ™, which is commonly used for sumoylation site prediction according to the consensus motif for sumoylation (Figure1.6).

SUMOplot™ Prediction

Developed by Abgent, copyright 2003-2004

Protein ID:	N/A
Defintion:	N/A
Length:	363 aa

```
  1 MKDNFSEAAT SRNITSSLPF DNLNATGINE SAFNCSHKPA DKHLEAIPVL
 51 YYMIFVIGFA VNIVVVSLFC CQKGPKKVSS IYIFNLAVAD LLLLATLPLW
101 AIYYSYRYDW LFGPVMCKVF GSFLTLNMFA SIFFITCMSV DRYQSVIYPF
151 LSQRRNPWQA SYVVPLVWCM ACLSSLPTFY FRDVRTIEYL GVNACIMAFP
201 PEKYAQWSAG IALMKNILGF IIPLIFIAIC YFGIRKHLLK TNSYGKNRIT
251 RDQVLKMAAA VVLAFIICWL PFHVLTFLDA LTWMGIINSC EVIAVIDLAL
301 PFAILLGFIN SCVNPFLYCF VGNRFQQKLR SVFRVPITWL QGKREIMSCR
351 KSSSLREMDT FVS
```

Motifs with high probability

Motifs with low probability

Overlapping Motifs

No.	Pos.	Group	Score	No.	Pos.	Group	Score
1	K343	IINLQ GKRE TMSCR	0.67	2	K73	SLFCC QKGP KKVSS	0.39

Figure 1.6 Prediction of sumoylation site on AT2 receptor. The amino acid sequence of rat AT2 receptor is analyzed on software SUMOplot ™ on the server of Abgent.

There is no such consensus motif for ubiquitination. However, there are 16 lysine residues in rat AT2 receptor, which are all conserved in mouse and human AT2 receptor. Considering the more and more recognized effects of ubiquitination on GPCR internalization and down-regulation, whether AT2 receptor is modified by ubiquitin was also investigated.

In present study, SUMO or ubiquitin was co-expressed with AT2 variants in cells. Immunoprecipitataion and western protein analysis were performed to confirm whether AT2 receptor is modified by SUMO or ubiquitin. The overall strategy is shown in Figure 1.7.

1.5.3 What affects AT2 receptor cell membrane expression?

Apart from sumoylation and ubiquitination, other factors that may affect AT2 subcellular localization were also examined in the present study.

Firstly, cell membrane expressed AT2 receptor variants were concentrated by cell surface immunoprecipitation and subcellular fractionation. Glycosylation and oligomerization on AT2 receptor were examined by studying the molecular weight of AT2 receptor in cell membrane fraction. The effects of serum starvation and ANGII stimulation were also investigated by western blot.

Furthermore mass spectrometry was performed trying to identify new interacting proteins of AT2 receptor.

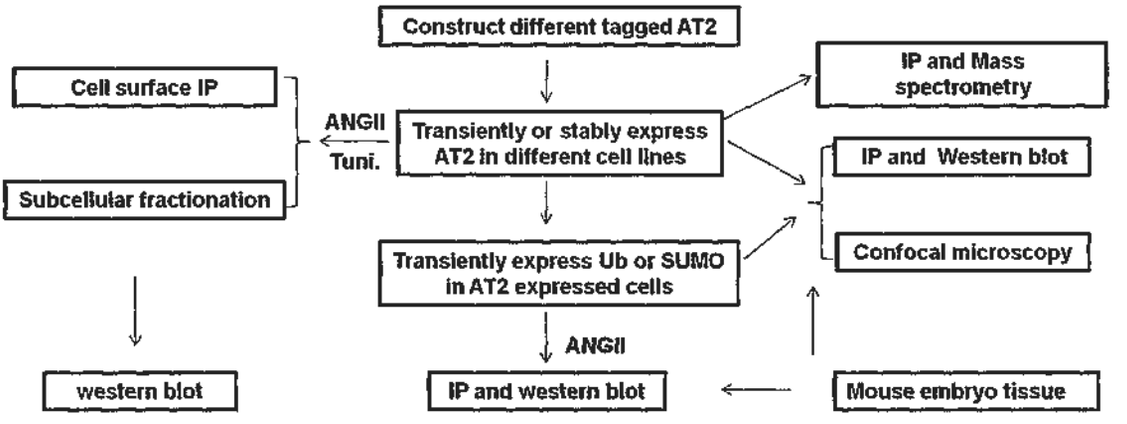

Figure 1.7 Overall strategies in present study. AT2: AT2 receptor; IP: immunoprecipitation; ANGII: angiotensin II; Ub: ubiquitin; Tuni.: tunicamycin (a deglycosylation reagent)

Chapter 2

Construction and expression of C-terminal or N-terminal tagged AT2 receptor variants

2.1 Introduction

Expressing GPCR with tags in mammalian cell lines is a common and convenient way to study localization and trafficking of GPCR in cells. One main reason for this is lacking commercially available specific antibody against GPCR. To eliminate potential effects of tags on AT2 receptor expression, various tagged AT2 receptor expression vectors were constructed. Besides, different cell types exhibited different expression pattern and signaling pathways of a same protein due to different cell content (Menard et al., 1997), so three cell lines were used in present study for both transient and stable expression.

2.1.1 Transient and stable expression

Transfection is a process introducing nucleic acid into target cell. Transfection of animal cells usually begins with opening transient "holes" in cell membrane, from where nucleic acid enters the cell. There are three common used methods for transfection: by calcium phosphate, by electroporation or by a cationic lipid (Lipofectamine 2000, in present study). Compared to calcium phosphate and electroporation, transfection by Lipofectamine2000 requires less DNA, kills fewer cells and is easy to perform.

Transfected genetic material can be expressed in target cells transiently or permanently which is referred to transient transfection or stable transfection, respectively. Transient transfection is commonly used to analyze the short term effect of expressed gene or protein. In this process transfected DNA is not integrated into the nuclear genome. Therefore gene expression is transient and usually shows a quite high expression at

24~72 hours after transfection and then the foreign DNA will be diluted by mitosis or degradation. Conversely in order to study the long term effect of an expressed gene, stable transfection is performed. Transfected material will integrate into nuclear genome in stable transfection. Selection of stably transfected cells is accomplished by introducing a selectable marker. In present study all of the expression vectors contain a neomycin resistant gene which can be selected by G418.

2.1.2 Expression constructs for tagged AT2 receptor variants

Five mammalian expression vectors were used in present study. A summary of different expression constructs for different tagged AT2 receptor variants is shown in Table 2.1. pEGFP-AT2 and pCMV-AT2-FLAG expression constructs containing a GFP tag and a FLAG tag, respectively, at the C-terminus of the rat AT2 receptor gene were constructed by a former labmate in our lab. The C-terminus is usually considered as an important region for GPCR signaling (Shirai et al., 1995) which is also true for AT2 receptor (Pulakat et al., 2002). Therefore, pCMV-Myc-AT2 and pCMV-HA-AT2 expression vectors containing a Myc tag and an HA tag, respectively, at N-terminus of AT2 gene were also constructed. To establish stable cell lines to express N-terminal tagged AT2 receptor, a pCDNA-Myc-AT2 expression vector was also constructed based on pCMV-Myc-AT2 (there is no selection gene in pCMV-Myc vector).

Table 2.1 Summary of different tagged AT2 receptor variants

AT2 receptor variants	Constructs	Empty vector
AT2-GFP	pEGFP-AT2	pEGFP-N1 (Clontech)
AT2-FLAG	pCMV-AT2-FLAG	pCMV-tag4A (Stratagene)
Myc-AT2	pCMV-Myc-AT2	pCMV-Myc (Clontech)
Myc-AT2	pDNA-Myc-AT2	pCDNA3 (Invitrogen)
HA-AT2	pCMV-HA-AT2	pCMV-HA (Clontech)

2.1.3 Cell lines used in present study

For evaluation of the effects of cellular content on tagged AT2 receptor variants expression, three cell lines were used both in transient and stable expression in present study. The three cell lines were chosen based on the species difference (human, rat and hamster) and tissue specificity (kidney, adrenals and ovary).

CHO-K1 (CHO for short) cells are Chinese hamster ovary cells, which is a stable hypodiploid line derived by spontaneous tranformation from a fibroblast culture (Tjio and Puck, 1958). CHO-K1 cells were commonly used in GPCR study, for example, regulation of β2-adrenergic receptor sequestration (Menard et al., 1997), oligomerization of C5a receptor (Klco et al., 2003), high throughput screening GPCR by stably expressed G alpha protein in CHO cells (New and Wong, 2004) and CCR5 receptor endocytosis (Longden et al., 2008). Keijiro Saku and co-workers also applied CHO-K1 cells as a model to study AT2 receptor oligomerization and constitutive activity (Miura et al., 2005). However it should be noted that hamster genome is not complete yet.

HEK293 (HEK for short) cells are human embryonic kidney cells which are adherent epithelial cells. HEK293 cells are also commonly used cell models for GPCR study, such as the endocytosis of mu-opioid receptor (MOR1) (Koch et al., 2006); glycosylation of bradykinin B2 receptor (Michineau et al., 2006); calcium response and desensitization of thyrotropin-releasing hormone (TRH) receptor (Ostasov et al., 2008); hetero-oligomerization of 5HT (1A) and 5HT (1B). Compared to CHO-K1 cells genetic background of HEK293 cells is clearly known.

PC12 cells (Adh from ATCC) are derived from a pheochromocytoma of the rat adrenal medulla. They are adherent, polygonal and neuron-like cells which will stop dividing and terminally differentiate when treated with nerve growth factor. This makes PC12 cells a useful model system for neuronal differentiation. PC12 cells are commonly used in studies of those GPCRs endogenously expressed in PC12 cells. For example PC12 cells were used to confirm heterodimerization between β-2 adrenergic receptor and bradykinin receptor (Haack et al., 2010) and ERK1/2 activation initiated by LPA, thrombin, and bradykinin receptors (Della Rocca et al., 1999). High expression of AT2 receptor was reported in adrenal medulla even in adults (Belloni et al., 1998). PC12 cells endogenously expressed AT2 receptor but only limited to earlier passages (lower than passage 17) (Webb et al., 1992). Besides ANGII stimulated cell differentiation in PC12 cells through AT2 receptor by nitric oxide-related and cyclic GMP-dependent mechanisms (Zhao et al., 2003). Compared to HEK293 cells and CHO cells, PC12 cells provide a more "native" environment for AT2 receptor expression.

2.2 Materials

2.2.1 Chemicals

F12-Nutrient power (Cat.21700-075), Dulbecco's Modified Eagle Medium power (Cat.12100-046), F-12K Nutrient mixture (Kaighn's modification, Cat.21127-022), fetal bovine serum (Cat.10270-106), penicillin/streptomycin (Cat. 15140-122), Lipofectamine 2000 (Cat. 11668-019), all primers, dNTP, 1kb/1kb plus DNA marker, electrophoresis grade agarose were purchased from Invitrogen (Carlsbad, CA, USA). G418 sulfate was from Chemsonic (Germany). Nitrocellulose transfer membrane was from Whatman (Hahnestrabe 3, Dassel, Germany). Amersham ECL™ Western Blotting Detection reagents were from G.E Healthcare (UK). Medical X-ray film was from FUJI (Japan). Precision Plus Protein Standards were from Bio-Rad (Berkeley, CA, USA). Yeast extract; Bacto Tryptone and agar Nobel were from B.D (Sparks, MD, USA). All other chemicals and reagents were from Sigma-Aldrich (St.Louis, MO, USA). Protein A agarose and Protease inhibitor cocktail tablets were from Roche (Roche Diagnostics Corporation, IN.USA)

2.2.2 Enzymes

Pfu DNA polymerase was from Promega (Madison, WI, USA). All restriction enzyme was from New England Biolabs (Beverley, MA, USA). T4 ligase was from Invitrogen (Carlsbad, CA, USA).

2.2.3 Kits and Instruments

Gel extraction kit was from G.E Healthcare (UK). Plasmid DNA purification kit was from INtRon (Korea). Elmer Gene Amp 9700 PCR was from Applied Bio systems. Bicinchoninic Acid (BCA) protein assay kit was from Thermo (HK). 37 °C humidified cell culture incubators was form Thermo (HK). TCS SP5 confocal microscope was from Leica (German). Quant microplate reader was from Bio-Tek Instruments Inc (Winnoski, VT, USA)

2.2.4 Antibodies

Mouse monoclonal (Cat.632381) and rabbit polyclonal anti-GFP antibody (Cat.632460) were from Clontech (Mountain View, CA, USA). Rabbit polyclonal anti-AT2 antibody (Cat. sc-9040); mouse monoclonal anti-Myc antibody (Cat. sc-40), mouse monoclonal anti-HA antibody (sc-7392) were from Santa Cruz Biotechnology (CA,USA). Mouse monoclonal anti-FLAG M2 antibody (Cat. F3165) and polyclonal anti-FLAG (Cat. F7425) was from Sigma-Aldrich (St.Louis, MO, USA).

2.3 Methods

2.3.1 Construction of pCMV-Myc-AT2 and pCMV-HA-AT2

2.3.1.1 Amplify AT2 fragment by PCR

The full-length of AT2 receptor cDNA was amplified from pCMV-AT2-FLAG vector with forward primer F1496 (5' CCG GAA TTC AGC GGA TGA AGG ACA ACT TCA GT 3') and reverse primer F1497 (5' CCG CTC GAG TTA AGA CAC AAA GGT GTC CAT 3'). The underlined nucleotides sequence in the primer pair were EcoR I and Xho I restriction cutting sites. The PCR reaction was performed in a system containing 10× Pfu buffer (2.5 µl), 10 mM dNTP (1 µl), 10 µM primer (1 µl for each primer), pCMV-AT2-FLAG plasmid (10 ng) as template, 1 µl Pfu DNA polymerase (2.5 U/µl) and nano pure water to a final volume of 25 µl. Applied Biosystems Elmer Gene Amp 9700 PCR machine was used to initiate the reaction. After denaturing at 94 °C for 5 minutes, PCR reaction was running for 30 cycles with a denature temperature at 94 °C for 30 seconds, an annealing temperature at 60°C for 30 seconds, and an extension temperature at 72 °C for 70 seconds, followed by an extended incubation at 72 °C for 7 minutes.

2.3.1.2 Agarose gel electrophoresis

PCR products of AT2 fragments were mixed with 6× orange loading dye and loaded into 1% agarose gel [agarose (w)/1×TAE buffer (v)] containing 0.5 µl/ml Ethidium Bromide (EB). Electrophoresis was performed at 120 V constant voltage until loading dye run to 2/3 of the gel.

2.3.1.3 Gel extraction of PCR product

PCR products were extracted with the Gel Extraction kit according to manufactures' instruction. DNA band was visualized by UV light and cut with a clean blade. Capture buffer type 2 (500 µl) was added to the gel slices and heated at 65 °C for 5 minutes. Sample mixture was centrifuged shortly and loaded to the assembled GFX Microspin column and collection tube. Samples were spun down at 16000 g for 30 seconds. The flow was discarded and the column was washed by 500 µl of Wash buffer type1. After centrifuge at 16000 × g for 30 seconds, 50 µl of nano pure water was added to the centre of the membrane in the assembled GFX Microspin column. After incubating at room temperature for 1 minute, DNA was spun down at 16000 × g for 1 minute.

2.3.1.4 Quantification of DNA or RNA

Given that DNA solution at a concentration of 50 µg/ml will have absorbance at 260 nm (OD260) equal to 1, DNA concentration (µg/ml) of sample= OD260 × dilution factor × 50 µg/ml.

Given that RNA solution at a concentration of 40 µg/ml will have absorbance at 260 nm (OD260) equal to 1, RNA concentration (µg/ml) of sample= OD260 × dilution factor × 40 µg/ml.

Moreover, the absorbance ratio of OD260/OD280 reflects the purity of DNA or RNA.

2.3.1.5 Restriction enzyme digestion

Purified AT2 fragment (~50 μg) was digested in a mixture containing 10 μl of 10× NEB EcoR I buffer, 1 μl of BSA, 2 μl of EcoR I (20 U/ μl), 2 μl of Xho I (20 U/ μl) in a final volume of 100 μl. The digestion was carried out at 37 °C overnight and confirmed by agarose gel electrophoresis. PCMV-Myc and pCMV-HA plasmid (~50 μg) was digested by the same step as described above.

2.3.1.6 Ligation of AT2 fragment into pCMV-Myc and pCMV-HA vector

The EcoR I –Xho I digested pCMV-Myc (or pCMV-HA) vector and AT2 fragment was ligated at 1:3 (mol/mol) ratio. The size of pCMV-Myc (or PCMV-HA) vector and AT2 fragment were 3.8 kb and 1kb, respectively. The ligation system consisted of 5× ligation buffer 4 μl , T4 ligase 1 μl (1U/ μl) and 1:3 ratio mixed up pCMV-Myc (or pCMV-HA) vector and AT2 fragment. The ligation was performed at 16°C water bath overnight. The vector map of pCMV-Myc-AT2 and pCMV-HA-AT2 are shown in Figure 2.1 and Figure 2.2, respectively.

2.3.1.7 Preparation of competent cells

DH5α E.coli were thawed from -80 °C stock and streaked on a LB (Luria-Bartani) agar plate. Following incubation at 37 °C for 14 hours, single colonies were picked and amplified in 2 ml of LB medium at 37 °C overnight, shaking at 250 rpm. The next day, 1ml of bacteria was put into 100 ml of LB medium, continue cultured until OD_{600} reached 0.4~0.6. After centrifuged at 3000 g for 10 minutes at 4 °C, the bacteria pellet was resuspended in 25 ml of 0.1 M ice-cold $CaCl_2$, incubated on ice for 15 minutes. The cells were pelleted by centrifuge at 3000 g for 10 minutes and then resuspended in 5 ml

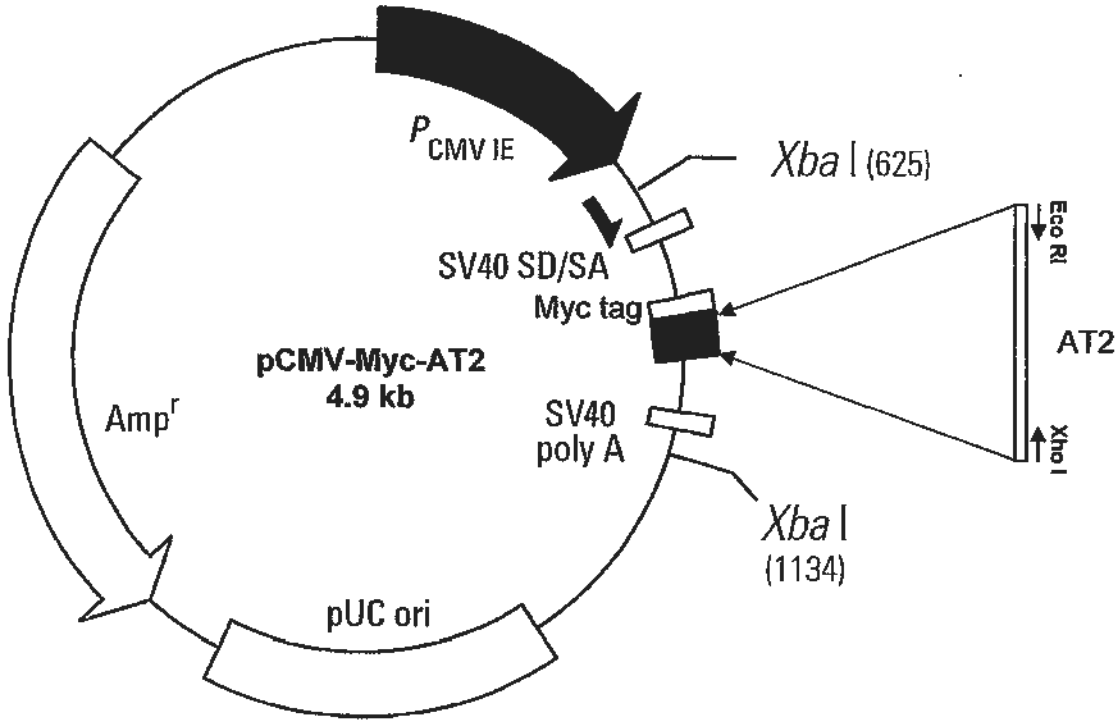

Figure 2.1 Vector map of pCMV-Myc-AT2. The full length of rat AT2 gene was amplified by PCR and inserted into EcoR I and Xho I restriction cutting sites in pCMV-Myc vector. AT2 receptor expression was controlled by a pCMV early promoter. The expression vector encoded ampicillin for selection in bacteria hosts. The vector map was modified form the vector map of pCMV-Myc from Clontech.

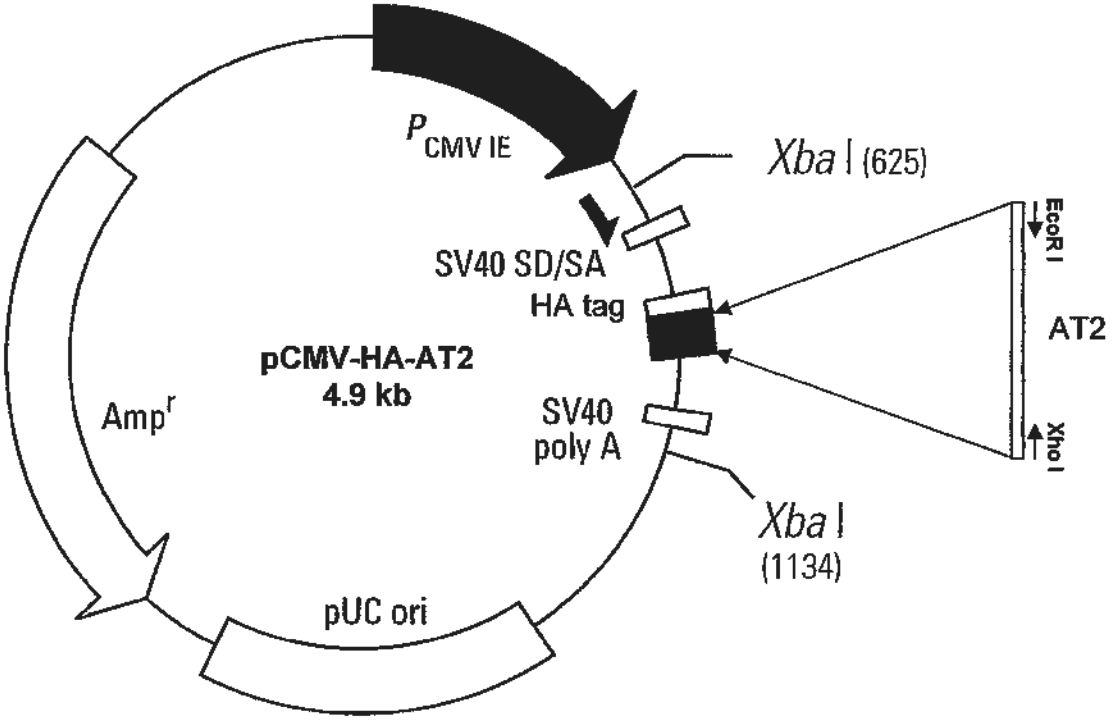

Figure 2.2 Vector map of pCMV-HA-AT2. The full length of rat AT2 gene was amplified by PCR and inserted into EcoR I and Xho I restriction cutting sites in pCMV-HA vector. AT2 receptor expression was controlled by a pCMV early promoter. The expression vector encoded ampicillin for selection in bacteria hosts. The vector map was modified form the vector map of pCMV-HA from Clontech.

of 0.1 M ice-cold $CaCl_2$ with 10% glycerol. All competent cells were aliquot and stored at -80 °C.

2.3.1.8 Bacteria transformation

The competent cells were thawed from -80°C stock. Ligation products (10 µl) was added to 50 µl of competent cells, mixed by pipetting up and down, followed by a 30 minutes incubation on ice. The 1.5 ml tube containing the competent cells and DNA was put into 42 °C water bath for 90 seconds and then incubated on ice for 2 minutes. LB medium (800 µl) was added to the tube. After shaking at 37 °C for 1 hour, cells were spun down and resuspended in 100 µl of LB medium. The bacteria culture was spread onto a 100 mm LB agar plate with ampicillin (100 µg/ml) and grown at 37°C overnight.

2.3.1.9 Minipreparation of plasmid

INtRon plasmid DNA purification kit was used for minipreparation of plasmid. A single colony from a freshly streaked bacteria plate was picked and put into 3ml of LB medium with appropriate antibiotic. After culture at 37°C overnight the bacteria was harvested by centrifugation at 17949 g for 30 seconds and lysed in 250 µl of resuspension buffer (with 100 mg/ml RNase A). Lysis buffer (250 µl) and neutralization buffer (350 ul) were added in order and mixed gently by inverting the tube several times. After centrifugation at 17949 g for 10 minutes at 4°C, the supernatant was transferred to a spin column. After centrifugation at 17949 g for 60 seconds, DNA bound to the column was washed once by 700 µl of washing buffer B. The filter membrane in the column was dried by another centrifugation at 17949 g for 60 seconds. Then 50 µl of nano pure water was added to

the centre of membrane and incubated for 1 minute at room temperature. DNA was collected by centrifugation at 17949 g for 60 seconds.

2.3.1.10 DNA sequencing

The purified plasmid DNA was sequenced by Beijing Genomics Institute-Hong Kong (BGI-HK).

2.3.2 Construction of pCDNA-Myc-AT2

2.3.2.1 Restriction enzyme digestion

Mini-prepared plasmid of pCMV-Myc-AT2 (~50 μg) or pCDNA3 (~50 μg) was digested in a 100 μl volume mixture containing 10 μl of 10× NEB buffer 4, 1 μl of BSA, 2 μl of Xba I (20 U/ μl). The digestion was carried out at 37 °C overnight and confirmed by agarose gel electrophoresis.

2.3.2.2 Ligation of Myc-AT2 fragment into pCDNA3 vector

Digested vector of pCDNA3 and digested fragment of Myc-AT2 (from pCMV-Myc-AT2) were purified with gel purification kit as described in section 2.3.1.3 and ligated at 1:3 (mol/mol) ratio. The size of digested pCDNA3 and digested Myc-AT2 were 5.4 kb and 1.6 kb, respectively. The ligation system with a final volume of 20 μl, consisted of 5 × ligation buffer 4 μl, T4 ligase 1 μl (1U/ μl), mixed digested pCDNA3 vectors and digested fragment of Myc-AT2 at a ratio of 1:3. The ligation was performed at 16°C water bath overnight. The vector map of pCDNA-Myc-AT2 is shown in Figure 2.3.

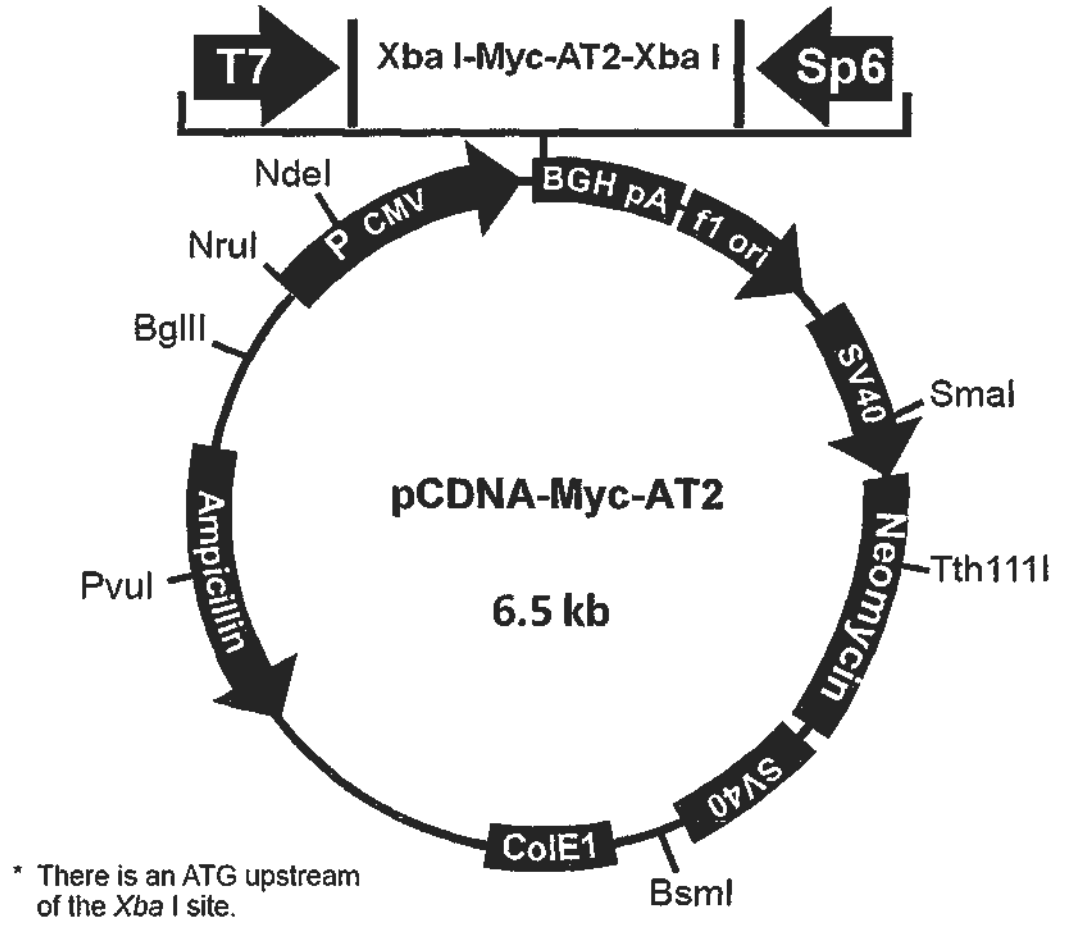

Figure 2.3 Vector map of pCDNA3-Myc-AT2. The full length of rat AT2 gene with a Myc tag was digested from pCMV-Myc-AT2 with Xba I restriction enzyme and ligated into the Xba I restriction enzyme cutting site in pCDNA3 vector. AT2 receptor expression was controlled by a pCMV promoter. The expression vector encoded ampicillin and neomycin resistant gene for selection in bacteria or mammalian hosts. The vector map was modified from the vector map of pCDNA3 from Invitrogen.

2.3.2.3 Transformation and DNA sequencing

Bacteria transformation and DNA sequencing were performed as described in section 2.3.1.8 and 2.3.1.10.

2.3.3 Transient transfection by Lipofectamine 2000

2.3.3.1 Large scale plasmid preparation

A single colony was picked and cultured in 2 ml of LB medium for 8 hours. The bacteria culture (1 ml) was added to 100 ml of LB medium and cultured for another 12~16 hours. Bacteria were collected by centrifugation at 3000 g for 10 min at room temperature. Cell pellet was resuspended in 5 ml of solution I (50 mM glucose, 25 mM Tris pH8.0, 10 mM EDTA), 10 ml of solution II (0.2 m NaOH, 1% SDS) and 6 ml of ice cold solution III (3 M potassium acetate and 11.5% acetic acid) sequentially. The mixture was incubated on ice for 10 minutes and centrifuged at 27216 g for 15 minutes. Supernatant was transferred to a new tube and centrifuged again at 27216 g for 15 minutes. After centrifugation, 12.6 ml of isopropanol was mixed with the supernatant and kept in room temperature for 15 minutes. DNA was recovered by centrifugation at 1811 g for 20 minutes. Pellet was air-dried and dissolved in 3 ml of TE buffer (10 mM Tris, 1 mM EDTA, pH 8.0). Equal volume (3 ml) of autoclaved 5 M LiCl was mixed with the DNA solution and spun down at 10000 g for 10 minutes at 4°C. Supernatant was transferred to a new tube and mixed with equal volume of ice cold isopropanol and left at -20°C for 20 minutes. Precipitated nucleic acids were recovered by centrifuging at 1811 g for 20 minutes. Pellet after centrifugation was resuspendend in 0.5 ml of TE buffer containing 20 μg/ml RNAse (DNase free) and incubated at 37°C for 30 minutes. An equal volume of phenol was mixed with the DNA solution and vortex for about 20 seconds before

centrifuging at 12000 g for 5 minutes. This phenol extraction step was repeat twice. Supernatant was transferred to a new tube and precipitated with 1/10 volume of 3 M sodium acetate and 2 volume of 100% ethanol. The solution was incubated at room temperature for more than 10 minutes and spun down at 12000 g for 5 minutes. Pellet was washed by 75% ethanol (v/v) and resuspended in 0.5~1 ml of nano pure water.

2.3.3.2 Routine cell culture

CHO-K1 cells were cultured in F12 medium containing 10% fetal bovine serum and 1% penicillin/streptomycin; HEK293 cells were cultured in DMEM medium containing 10% fetal bovine serum and 1% penicillin/streptomycin; PC12 cells were cultured in F12-K medium containing 15% horse serum, 2.5% fetal bovine serum and 1% penicillin/streptomycin. Cells were subcultured every 4~5 days. During subculture, cells were rinsed by PBS once and incubated with 0.25 % Trypsin/EDTA (1 ml for a 100 mm dish) for 3~5 minutes. After cells detached, fresh medium were added to the dish. Cells were spun down and 1/10 of the cells were transferred to another dish with fresh medium for next passage.

2.3.3.3 Transient transfection by Lipofectamine 2000

Transient transfection was performed according to the manual of Liopofectamine2000. The following procedure was used to transfect DNA into mammalian cells in 6-well format. One day before transfection, (1~5) $\times 10^5$ cells were seeded in 1 ml of culture medium without antibiotics. On the day of transfection, 1 μg DNA and 2 μl Lipofectomine2000 were separately diluted into 125 μl DMEM medium (free of fetal bovine serum and antibiotics). After incubation at room temperature for 5 minutes the

diluted DNA was combined with the diluted Lipofectamine2000 and kept at room temperature for 20 minutes. The mixture was added to one well containing cells and medium, mixed gently and kept cultured at 37 °C in a humidified 5% CO_2 incubator for 4 hours. The transfection medium was discarded and changed to fresh culture medium. Cells were cultured for 24~48 hours prior to testing for transgene expression.

2.3.4 Stable cell lines establishment

2.3.4.1 Dosage curve of G418 for different cell lines

Three different concentrations of cells (10^2/well, 10^3/well, and 10^4/well) were seeded in 6-well plate. Cells of each concentration were incubated with medium containing 4 different concentrations of G418 (0 mg/ml, 0.5 mg/ml, 1 mg/ml, and 2 mg/ml) for up to 2 weeks. The minimum concentration of G418 in which no viable cells were detected was the optimized condition for selection.

2.3.4.2 Preparation of linearized vectors

PEGFP-N1 and pEFGP-AT2 was linearized by digesting with DraIII. Briefly, plasmid (50 μg) was incubated overnight at 37°C with 5 μl of DraIII (5 units/μl), 10 μl of 1×NEB buffer 3, 3 μl of 1mg/ml BSA with sterile water to a final volume of 100 μl.

PCMV-tag4A and pCMV-AT2-FLAG were linearized by digesting with ApaL I. Briefly, plasmid (50 μg) was incubated overnight at 37°C with 5 μl of ApaLI (10 units/μl), 10 μl of 1×NEB buffer 4, 3 μl of 1 mg/ml BSA with sterile water to a final volume of 100 μl.

PCDNA-Myc-AT2 and pCDNA3 were linearized by digesting with PVUI. Briefly, plasmid (20 μg) was incubated overnight at 37°C with 5 μl of PVUI (750 units/ml), 10 μl of 1×NEB buffer 3, 3 μl of 1 mg/ml BSA with sterile water to a final volume of 100 μl.

After digestion, DNA was purified by Gel extraction kit as described in section 2.3.1.3.

2.3.4.3 Screening for stably transfected cells

DNA was delivered into cells by Lipofectamine 2000 as described in section 2.3.3.3. After 48 hours culture, cells were trypsinized and resuspended in 500 μl of culture medium. Aliquot (20 μl) of the cell suspension were taken from each well for cell counting with a hemocytometer. Cells (1×10^2) were seeded in a new well of a 6-well plate and incubated with 2 ml of selection medium (culture medium with appropriate concentration of G418). Selection medium was changed every 3 days to remove floating dead cells and cell debris. After two weeks, colonies were observed. Well-isolated colonies were picked with a 10 μl pipette tip through physical scrubbing and put into a well of 96-well plate containing 50 μl of Trypsin /EDTA solution. After digestion at 37 °C for 3 minutes the cells were collected by pipetting up and down several times and transferred to a new well in 24-well plate which contained 1 ml of selection medium and continue cultured for two weeks . In the next subculture, the same clone was seeded into two wells in a 6-well plate. One was for subculture; the other was for confocal microscopy. Positive colonies were trypsinized and counted with a hemocytometer. After counting, cells were diluted to a final concentration of 1 cell/ml with selection medium. Cell suspension of 100 μl was added into each well of a 96-well plate and

cultured for another two weeks. Colonies derived from single cell in 96-well plate were subcultured consecutively in 24-well plate, 6-well plate and 100 mm dish.

2.3.5 Determination of AT2 receptor mRNA expression in stable cell lines by RT-PCR

2.3.5.1 Isolation of total RNA by TRI_{ZOL} reagent

Cells of a 60 mm dish were rinsed by 2 ml of PBS and lysed in 1 ml of Tri_{ZOL} reagent. Cell lysate was passed through a 1 ml syringe several times and transferred to a 1.5 ml eppendorf. Cell lysate was incubated at room temperature for 5 minutes and mixed with 0.3 ml of chloroform with vigorous shaking. After incubation at room temperature for 2 minutes, the cell lysate was centrifuged at 12000 g for 15 minutes at 4°C. The aqueous phase was transferred to a fresh tube and mixed with 0.5 ml of isopropanol. After incubating at room temperature for 10 minutes, the mixture was centrifuged at 12000 g for 10 minutes at 4°C. The RNA pellet was washed with 1 ml of 75% ethanol (v/v diluted by DEPC treated water) and centrifuged at 7500 g for 5 minutes at 4°C. RNA pellet was air-dried and dissolved in 50 µl of DEPC treated water. RNA concentration was quantified as described in section 2.3.1.4.

2.3.5.2 Reverse transcription of total RNA into cDNA

A reaction mixture containing 1 µl of 0.5 µg/µl oligo dT, 5 µg of extracted RNA and 1 µl of 10 mM dNTP in a final volume of 13 µl was heated at 65°C for 5 minutes and quickly chilled on ice. First strand buffer (5 ×, 4 µl) and 0.1 M DTT (2 µl) were added to the reaction mixture. The mixture was incubated at 42°C for 2 minutes. At the end 1

μl superscript reverse transcriptase was added to the mixture. The mixture was incubated at 42°C for another 50 minutes and heated at 70°C for 15 minutes.

2.3.5.3 Analysis of AT2 receptor mRNA expression in stable cell lines by PCR

AT2 receptor expression in the stable cell lines was analyzed by polymerase chain reaction (PCR) in a solution of 25 μl containing 2.5 μl of 10 × PCR buffer, 1.5 μl of 25 mM $MgCl_2$, 1 μl of 10 mM dNTP, 1 μl of 10 mM forward and reverse primers each, 1 μl of RT product and 1 μl of Taq DNA polymerase (5U/μl). The PCR primers F1060 (5'TCT CAG AGA AGG AAT CCC TGG CAA GCA 3') and R1347 (5' GGA ATT CTT AAG ACA CAA AGG TGT CCA 3') were designed based on a 3'-end 600 bp fragment of rat AT2 mRNA.

2.3.6 Confocal microscopy to detect AT2 receptor expression in stable cell lines

2.3.6.1 Indirected immunofluorescence

Coverslips (size: 25 mm) were sterilized by 75 % ethanol, pretreated with 0.01% poly-D-Lysine [(w/v) in autoclaved water] for 10 minutes at room temperature, then put into a well of 6-well plate. Cells (2×10^5) were seeded onto the coated coverslip and cultured in a 37 °C humidified incubator for 24 ~48 hours. Medium was discarded and the coverslips were rinsed by PBS once. Fixation was performed by incubation with 1 ml of methanol for 10 minutes at -20°C (for PC12-Myc-AT2 and HEK-AT2-FLAG) or with 4 % paraformaldehyde (v/v in PBS) for 15 minutes at room temperature (for other stable cell lines). After fixation, the coverslips were washed by Tris buffer (50 mM Tris, pH 7.4) for 15 minutes (5 minutes × 3 times). Non-specific binding sites were blocked by incubation with blocking buffer (Tris buffer containing 0.5% Triton X-100 and 10%

goat serum) at room temperature for 30 minutes. Coverslips were then washed by Tris/Triton buffer (Tris buffer containing 0.1% Triton X-100) for 15 minutes (5 minutes × 3 times). Primary antibody was 1:200 diluted with antibody dilution buffer (Tris/Triton buffer containing 10% goat serum). Diluted primary antibody solutions (100 µl) were incubated with each 25 mm coverslip in a humidified air-tight box at 4°C overnight. Washing step (5 minutes × 3 times with Tris/Triton buffer) was repeated again. Fluorescent-conjugated secondary antibody (such as FITC conjugated goat anti-mouse antibody) was 1:200 diluted with antibody dilution buffer and incubated with the coverslips in a humidified air-tight box for 1 hour at room temperature. The washing step was repeated again. The coverslips were air dried, mounted with anti-fade mounting medium (0.1 M Tris-HCl, pH 8.0, 90% glycerol, 0.02% sodium azide, 2.3% 1, 4-diazabicyclo-[2, 2, 2]-octane) and sealed with nail polish.

2.3.6.2 Confocal microscopy

Live cells on 25 mm coverslips (cell lines stably expressed AT2-GFP or EGFP) or coverslips prepared from indirected immunofluorescence as described in section 2.3.6.1 were examined with a Leica TCS SP5 confocal microscope. GFP and FITC were excited at 488 nm by an Ar/Kr laser and fluorescence signal was detected at wavelength of 525±50.

2.3.7 Immunoprecipitation

Cells from a confluent 100 mm dish were collected by a scraper. After washing with PBS once, cells were lysed in 1 ml of RIPA buffer [0.1 M Tris pH 7.4, 150 mM NaCl, 1% sodium deoxycholate, 1% Triton X-100, 5 mM EDTA, 40 µl/ml of protease inhibitor

cocktail (1 tablet in 2 ml of nano pure water as store solution)]. Cell lysate was pipetted up and down for several times and kept on ice for 15 minutes. Sonication at power 5 for 30 seconds was performed for completely solubilization. The cell lysate was centrifuged at 10621 g for 10 minutes. The supernatant was transferred to a new 1.5 ml tube. For protein concentration determination 10 µl of supernatant was taken out and measured by bicinchoninic Acid (BCA) protein assay kit. Firstly, serial concentration of BSA (2 mg/ml, 1 mg/ml, 0.5 mg/ml, 0.25 mg/ml, 0.125 mg/ml, and 0.0625 mg/ml) was used for protein standards. Then 10 µl of cell lysate or protein standards were added to a well in 96-well plate. Solution A and B were mixed at a ratio of 50:1. The solution mixture of A and B (80 µl) were added to each well containing cell lysate or BSA standards. After incubation at room temperature for 5 minutes, the plate was read in a Quant microplate reader (Bio-Tek Instruments Inc, Winnoski, VT, USA) at 562 nm. Data was analyzed with KC junior software (Bio-Tek Instruments Inc, Winnoski, VT, USA). After concentration determination, 2 µl of antibody and 50 µl of protein A agarose beads were added to the cell lysate of equal amount of protein. The mixture was rocked at 4°C overnight. The agarose bead was spun down at 1000 g for 1 minute and washed by RIPA buffer for 40 minutes (10 minutes × 4 times). Then 80 µl of a sample buffer (2% SDS, 10% glycerol, 40 µl/ml β-mercaptoethanol and 0.01% bromphenol blue in 50 mM Tris-HCl, pH6.8) was added to the pelleted agarose at the end of washing step. The sample was boiled in boiling water for 10 minutes and spun down. Supernatant with denatured protein was analyzed by western blot.

2.3.8 Western blot

For mini gel, gel set of Mighty Small II for 8 × 9 cm gel (GE Health care, USA) was used for SDS-PAGE. Protein sample (30~50 μl) was loaded to each well and separated on 10% SDS-PAGE in a running buffer (25 mM Tris, 192 mM glycine and 0.1% SDS) at constant voltage (80V for stacking gel, 120V for separating gel) until the loading dye reached the bottom of the gel. Proteins were transferred to nitrocellulose membranes in a transferring buffer (25 mM Tris, 192 mM glycine and 10% methanol) at a constant voltage of 70 V for 1 hour in a mini gel tank (Bio-Rad). For protein gel of large format, the HOEFER SE 600 series vertical slab gel unit (14 cm × 16 cm) was used for SDS-PAGE. Protein sample (80~100 μl) was loaded to each well and separated on 10% SDS-PAGE in the running buffer at constant voltage (80V for stacking gel, 60V overnight for separating gel) until the loading dye reached the bottom of the gel. Proteins were transferred to nitrocellulose in the transferring buffer at a constant voltage of 70 V for 3 hours.

Non-specific binding sites on the nitrocellulose membrane were blocked by incubation with an immunobloting buffer (25 mM Tris pH 7.4, 1 mM $CaCl_2$, 40 mM NaCl, 0.1 % NP40, 5 % non-fat milk) for 30 minutes at room temperature. Primary antibody diluted in the immunobloting buffer (anti-GFP monoclonal antibody 1:5000; anti-Myc monoclonal antibody 1:1000; anti-HA monoclonal antibody 1:1000) was incubated with the membrane at 4°C overnight by gentle shaking. The next day the membrane was washed with a washing buffer (25 mM Tris pH 7.4, 1 mM $CaCl_2$, 40 mM NaCl, 0.1 % NP40) for 40 minutes (10 minutes × 4 times). For ECL detection system, HRP-conjugated secondary antibody (1:2000 diluted in the immunobloting buffer) was incubated with the membrane for 70 minutes at room temperature. Unbound antibody

was washed in a washing buffer for 40 minutes (10 minutes × 4 times). Proteins bands were visualized by incubating with the Amersham ECL™ Western Blotting Detection reagents (GE Healthcare, UK) and chemoluminescent signal was detected with FUJI medical X-ray film. For colorimetry detection, AP-conjugated secondary antibody (1:2000 diluted in immunobloting buffer) was incubated with the membrane for 70 minutes at room temperature. Unbound antibody was washed in the washing buffer for 40 minutes (10 minutes × 4 times). Proteins bands were visualized by incubation with a mixture solution of NBT/BCIP (10 ml solution containing 50 µl of NBT and 37.5 µl of BCIP).

2.3.9 Preparation of membrane fraction from mouse embryo

All animal procedure was approved by HEEC. Female BALB/C mice (obtained from the university's animal house) were mated with males of the same age. If spermatozoa were found in vaginal smears in the morning after mating, the mouse was termed as day 0.5 of pregnancy. Two pregnant mice on day 19 were collected. The mice were killed by cervical dislocation and embryos were quickly removed. Brain, viscera and body were isolated from embryo and stored in minus 80 °C before homogenization. Tissues was homogenized in a TE buffer (50 mM Tris, Ph 7.4, 5 mM EDTA) using a tissue-tearer. Homogenate was centrifuged at 1000 g for 10 minutes to remove cell debris. The supernatant was transferred to another tube and centrifuged at 15000 g for one hour. The pellet was used as cell membrane fraction. The membrane pellet was dissolved in the RIPA buffer (containing protease inhibitor cocktail) and rocked at 4 °C for one hour. The membrane lysis was centrifuged at 10621 g for 10 minutes. Supernatant was

transferred to a new tube and used in immunoprecipitation assay as described in section 2.3.7.

2.3.10 Immunohistochemistry

A 12 μm cryo-section of adrenal gland was prepared by a former labmate. The slides were warmed at 49°C for 30 minutes and then deparaffinized with xylene for 20 minutes (10 minutes ×twice) and dehydrated through 100% ethanol for 10 minutes (5 minutes × twice), 70% ethanol 5 minute once and PBS for 15 minutes (5 minutes ×three times). After incubation in 3% H_2O_2 (prepared in PBS) for 10 minutes, the sections were washed with PBS for 15 minutes (5 minutes ×three times) and then blocked with blocking solution (3% BSA in PBS) for 1 hour at room temperature. After incubated with normal goat serum to block non-specific binding sites, the sections were incubated with blocking solution containing diluted primary antibody (anti-AT2 antibody raised in our lab 1:500 diluted; anti-AT2 antibody from Santa Cruz 1:100 diluted) at 4 °C overnight. The sections then were washed by a Tris buffer (20 mM Tris Ph 7.4) for 10 minutes (5 minutes × twice) and then washed by Tris/Triton (0.1% Trition in Tris buffer). FITC conjugated anti-rabbit antibody was 1:2000 diluted in blocking solution and incubated with the sections for 2 hours at room temperature. The sections were washed by Tris/Triton buffer for 10 minutes (5 minutes × twice) and PBS for 5 minutes once. The sections were air dried and sealed with mounting medium and nail polish.

2.4 Results

2.4.1 Preparation of pCMV-HA-AT2, pCMV-Myc-AT2, pCDNA-Myc-AT2

After transformation, one or two positive clones were selected and sent for sequencing. The sequencing results were aligned with rat AT2 sequence using online software ClustalW2 (European Molecular Biological Laboratory). The nucleotide sequence of Myc-AT2 and HA-AT2 was identical to the rat AT2 receptor and respective tag (Figure 2.4 A, B). DNA sequence was translated into amino acid sequence via online software of ExPASy (Swiss Institute of bioinformatics). The amino acid sequence proved that both AT2 and respective tag were in correct reading frame (Figure 2.4 C, D).

Figure 2.4 DNA sequence alignment and amino acid sequence of Myc-AT2 and HA-AT2.

A). Multiple sequence alignment of DNA sequence of Myc-AT2 (pCMV-Myc-AT2 and pCDNA-Myc-AT2) with rat AT2 gene. The sequence results of pCMV-Myc-AT2 and pCDNA-Myc-AT2 were identical to the rat AT2 sequence and the Myc tag sequence which is shown with red box. The start codon and stop codon are shown with black box. Between Myc tag and AT2 sequence is multiple cloning sites.

B). Multiple sequence alignment of DNA sequence of HA-AT2. The sequence result of pCMV-HA-AT2 was identical to the rat AT2 sequence and the HA tag sequence which is shown with red box. The start codon and stop codon are shown with black box. Between HA tag and AT2 sequence was multiple cloning sites.

C). Amino acid sequence of Myc-AT2. Blue color represents the amino acid sequence of Myc tag while green color represents the sequence of rat AT2 protein. AT2 has 363 amino acids and Myc tag has 13 amino acids. Between the two proteins are 10 additional amino acids (color in black) resulted from multiple cloning sites. The fusion protein contains totally 387 amino acids with an predicted MW of 44 kDa using Compute pI/Mw on ExPASy (http://au.expasy.org/tools/pi_tool.html).

D). Amino acid sequence of HA-AT2. Blue color represents the amino acid sequence of HA tag while green color represents the sequence of rat AT2 protein. AT2 has 363 amino acids and HA tag has 10 amino acids. Between the two proteins are 10 additional amino acids (color in black) resulted from multiple cloning sites. The fusion protein contains totally 384 amino acids with a predicted MW of 43.7 kDa using Compute pI/Mw on ExPASy (http://au.expasy.org/tools/pi_tool.html).

A

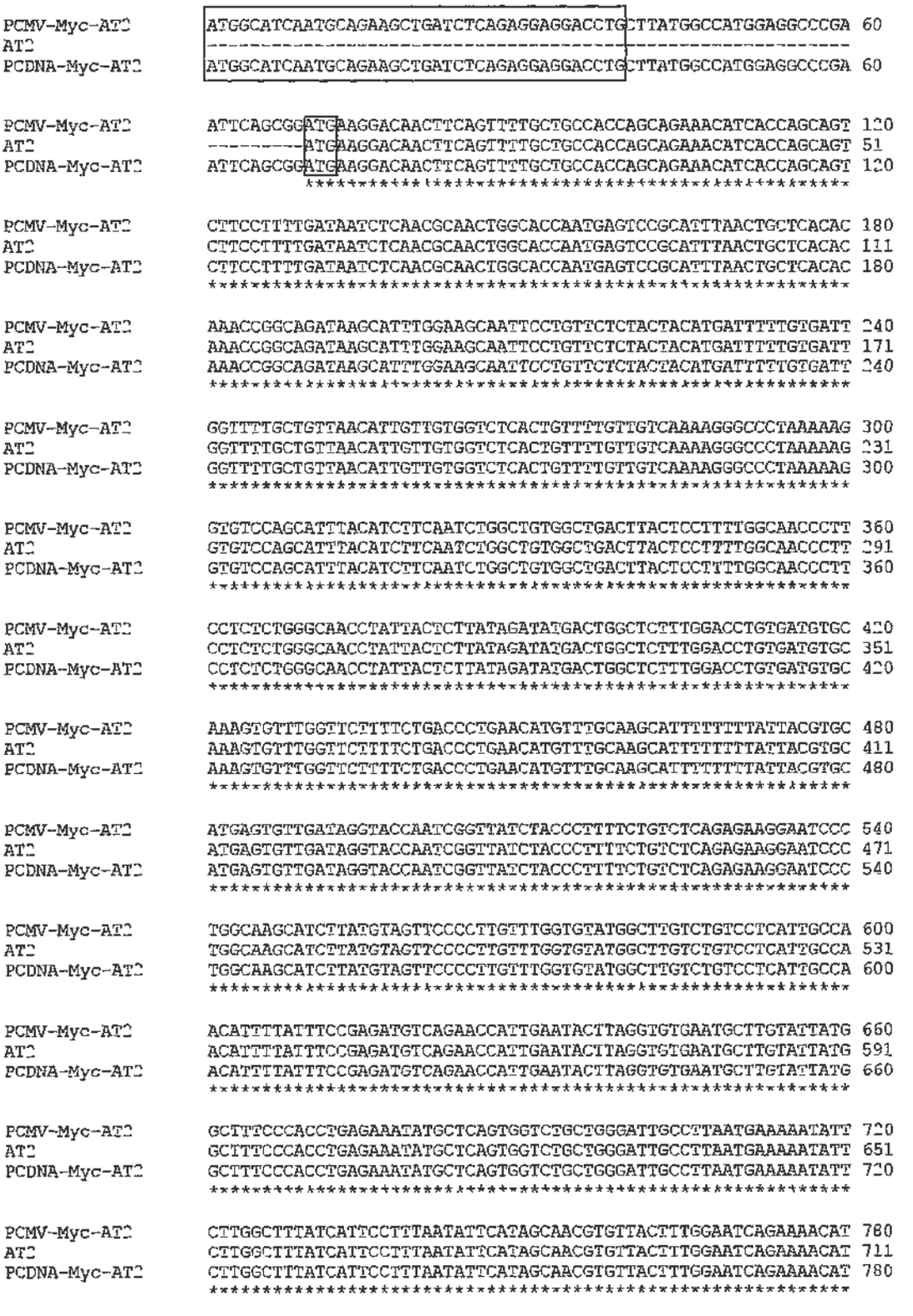
PCMV-Myc-AT2 ATGGCATCAATGCAGAAGCTGATCTCAGAGGAGGACCTGCTTATGGCCATGGAGGCCCGA 60
AT2 ---------- 0
PCDNA-Myc-AT2 ATGGCATCAATGCAGAAGCTGATCTCAGAGGAGGACCTGCTTATGGCCATGGAGGCCCGA 60
PCMV-Myc-AT2 ATTCAGCGGATGAAGGACAACTTCAGTTTTGCTGCCACCAGCAGAAACATCACCAGCAGT 120
AT2 ---------ATGAAGGACAACTTCAGTTTTGCTGCCACCAGCAGAAACATCACCAGCAGT 51
PCDNA-Myc-AT2 ATTCAGCGGATGAAGGACAACTTCAGTTTTGCTGCCACCAGCAGAAACATCACCAGCAGT 120
PCMV-Myc-AT2 CTTCCTTTTGATAATCTCAACGCAACTGGCACCAATGAGTCCGCATTTAACTGCTCACAC 180
AT2 CTTCCTTTTGATAATCTCAACGCAACTGGCACCAATGAGTCCGCATTTAACTGCTCACAC 111
PCDNA-Myc-AT2 CTTCCTTTTGATAATCTCAACGCAACTGGCACCAATGAGTCCGCATTTAACTGCTCACAC 180
PCMV-Myc-AT2 AAACCGGCAGATAAGCATTTGGAAGCAATTCCTGTTCTCTACTACATGATTTTTGTGATT 240
AT2 AAACCGGCAGATAAGCATTTGGAAGCAATTCCTGTTCTCTACTACATGATTTTTGTGATT 171
PCDNA-Myc-AT2 AAACCGGCAGATAAGCATTTGGAAGCAATTCCTGTTCTCTACTACATGATTTTTGTGATT 240
PCMV-Myc-AT2 GGTTTTGCTGTTAACATTGTTGTGGTCTCACTGTTTTGTTGTCAAAAGGGCCCTAAAAAG 300
AT2 GGTTTTGCTGTTAACATTGTTGTGGTCTCACTGTTTTGTTGTCAAAAGGGCCCTAAAAAG 231
PCDNA-Myc-AT2 GGTTTTGCTGTTAACATTGTTGTGGTCTCACTGTTTTGTTGTCAAAAGGGCCCTAAAAAG 300
PCMV-Myc-AT2 GTGTCCAGCATTTACATCTTCAATCTGGCTGTGGCTGACTTACTCCTTTTGGCAACCCTT 360
AT2 GTGTCCAGCATTTACATCTTCAATCTGGCTGTGGCTGACTTACTCCTTTTGGCAACCCTT 291
PCDNA-Myc-AT2 GTGTCCAGCATTTACATCTTCAATCTGGCTGTGGCTGACTTACTCCTTTTGGCAACCCTT 360
PCMV-Myc-AT2 CCTCTCTGGGCAACCTATTACTCTTATAGATATGACTGGCTCTTTGGACCTGTGATGTGC 420
AT2 CCTCTCTGGGCAACCTATTACTCTTATAGATATGACTGGCTCTTTGGACCTGTGATGTGC 351
PCDNA-Myc-AT2 CCTCTCTGGGCAACCTATTACTCTTATAGATATGACTGGCTCTTTGGACCTGTGATGTGC 420
PCMV-Myc-AT2 AAAGTGTTTGGTTCTTTTCTGACCCTGAACATGTTTGCAAGCATTTTTTTTATTACGTGC 480
AT2 AAAGTGTTTGGTTCTTTTCTGACCCTGAACATGTTTGCAAGCATTTTTTTTATTACGTGC 411
PCDNA-Myc-AT2 AAAGTGTTTGGTTCTTTTCTGACCCTGAACATGTTTGCAAGCATTTTTTTTATTACGTGC 480
PCMV-Myc-AT2 ATGAGTGTTGATAGGTACCAATCGGTTATCTACCCTTTTCTGTCTCAGAGAAGGAATCCC 540
AT2 ATGAGTGTTGATAGGTACCAATCGGTTATCTACCCTTTTCTGTCTCAGAGAAGGAATCCC 471
PCDNA-Myc-AT2 ATGAGTGTTGATAGGTACCAATCGGTTATCTACCCTTTTCTGTCTCAGAGAAGGAATCCC 540
PCMV-Myc-AT2 TGGCAAGCATCTTATGTAGTTCCCCTTGTTTGGTGTATGGCTTGTCTGTCCTCATTGCCA 600
AT2 TGGCAAGCATCTTATGTAGTTCCCCTTGTTTGGTGTATGGCTTGTCTGTCCTCATTGCCA 531
PCDNA-Myc-AT2 TGGCAAGCATCTTATGTAGTTCCCCTTGTTTGGTGTATGGCTTGTCTGTCCTCATTGCCA 600
PCMV-Myc-AT2 ACATTTTATTTCCGAGATGTCAGAACCATTGAATACTTAGGTGTGAATGCTTGTATTATG 660
AT2 ACATTTTATTTCCGAGATGTCAGAACCATTGAATACTTAGGTGTGAATGCTTGTATTATG 591
PCDNA-Myc-AT2 ACATTTTATTTCCGAGATGTCAGAACCATTGAATACTTAGGTGTGAATGCTTGTATTATG 660
PCMV-Myc-AT2 GCTTTCCCACCTGAGAAATATGCTCAGTGGTCTGCTGGGATTGCCTTAATGAAAAATATT 720
AT2 GCTTTCCCACCTGAGAAATATGCTCAGTGGTCTGCTGGGATTGCCTTAATGAAAAATATT 651
PCDNA-Myc-AT2 GCTTTCCCACCTGAGAAATATGCTCAGTGGTCTGCTGGGATTGCCTTAATGAAAAATATT 720
PCMV-Myc-AT2 CTTGGCTTTATCATTCCTTTAATATTCATAGCAACGTGTTACTTTGGAATCAGAAAACAT 780
AT2 CTTGGCTTTATCATTCCTTTAATATTCATAGCAACGTGTTACTTTGGAATCAGAAAACAT 711
PCDNA-Myc-AT2 CTTGGCTTTATCATTCCTTTAATATTCATAGCAACGTGTTACTTTGGAATCAGAAAACAT 780

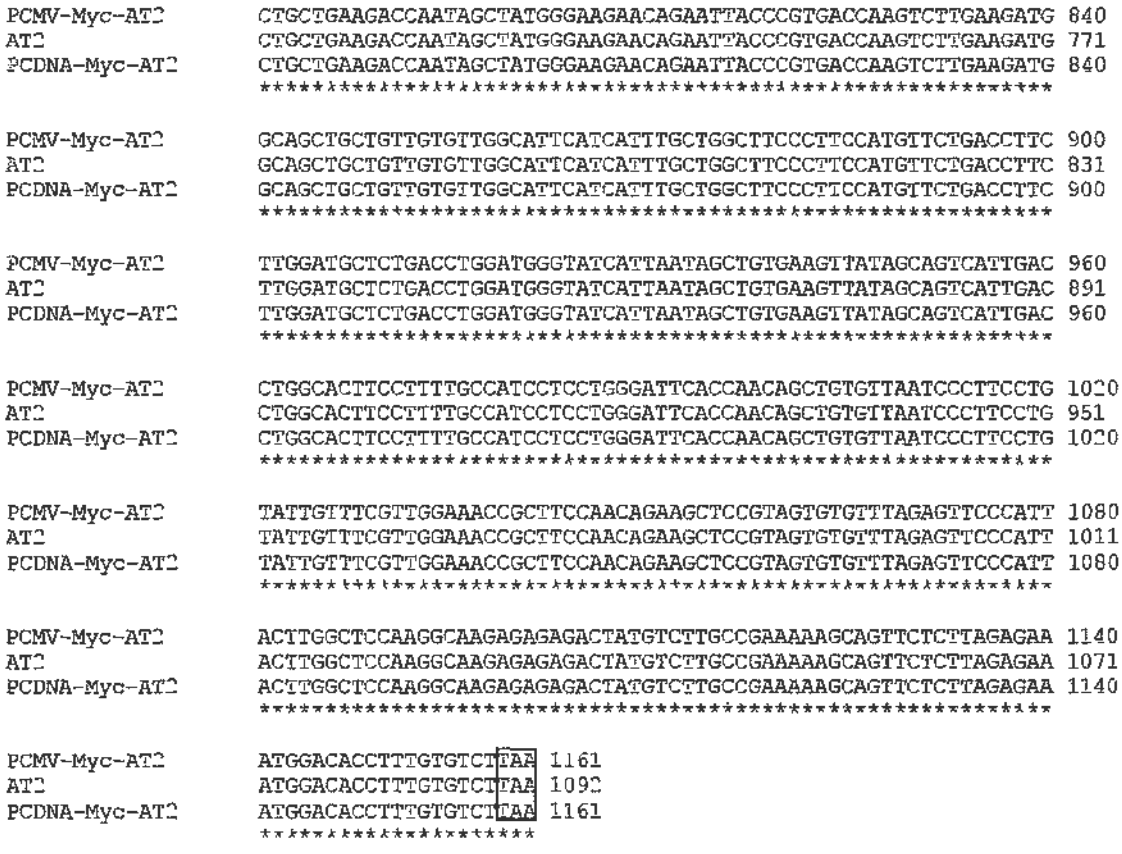
PCMV-Myc-AT2 CTGCTGAAGACCAATAGCTATGGGAAGAACAGAATTACCCGTGACCAAGTCTTGAAGATG 840
AT2 CTGCTGAAGACCAATAGCTATGGGAAGAACAGAATTACCCGTGACCAAGTCTTGAAGATG 771
PCDNA-Myc-AT2 CTGCTGAAGACCAATAGCTATGGGAAGAACAGAATTACCCGTGACCAAGTCTTGAAGATG 840
PCMV-Myc-AT2 GCAGCTGCTGTTGTGTTGGCATTCATCATTTGCTGGCTTCCCTTCCATGTTCTGACCTTC 900
AT2 GCAGCTGCTGTTGTGTTGGCATTCATCATTTGCTGGCTTCCCTTCCATGTTCTGACCTTC 831
PCDNA-Myc-AT2 GCAGCTGCTGTTGTGTTGGCATTCATCATTTGCTGGCTTCCCTTCCATGTTCTGACCTTC 900
PCMV-Myc-AT2 TTGGATGCTCTGACCTGGATGGGTATCATTAATAGCTGTGAAGTTATAGCAGTCATTGAC 960
AT2 TTGGATGCTCTGACCTGGATGGGTATCATTAATAGCTGTGAAGTTATAGCAGTCATTGAC 891
PCDNA-Myc-AT2 TTGGATGCTCTGACCTGGATGGGTATCATTAATAGCTGTGAAGTTATAGCAGTCATTGAC 960
PCMV-Myc-AT2 CTGGCACTTCCTTTTGCCATCCTCCTGGGATTCACCAACAGCTGTGTTAATCCCTTCCTG 1020
AT2 CTGGCACTTCCTTTTGCCATCCTCCTGGGATTCACCAACAGCTGTGTTAATCCCTTCCTG 951
PCDNA-Myc-AT2 CTGGCACTTCCTTTTGCCATCCTCCTGGGATTCACCAACAGCTGTGTTAATCCCTTCCTG 1020
PCMV-Myc-AT2 TATTGTTTCGTTGGAAACCGCTTCCAACAGAAGCTCCGTAGTGTGTTTAGAGTTCCCATT 1080
AT2 TATTGTTTCGTTGGAAACCGCTTCCAACAGAAGCTCCGTAGTGTGTTTAGAGTTCCCATT 1011
PCDNA-Myc-AT2 TATTGTTTCGTTGGAAACCGCTTCCAACAGAAGCTCCGTAGTGTGTTTAGAGTTCCCATT 1080
PCMV-Myc-AT2 ACTTGGCTCCAAGGCAAGAGAGAGACTATGTCTTGCCGAAAAAGCAGTTCTCTTAGAGAA 1140
AT2 ACTTGGCTCCAAGGCAAGAGAGAGACTATGTCTTGCCGAAAAAGCAGTTCTCTTAGAGAA 1071
PCDNA-Myc-AT2 ACTTGGCTCCAAGGCAAGAGAGAGACTATGTCTTGCCGAAAAAGCAGTTCTCTTAGAGAA 1140
PCMV-Myc-AT2 ATGGACACCTTTGTGTCTTAA 1161
AT2 ATGGACACCTTTGTGTCTTAA 1092
PCDNA-Myc-AT2 ATGGACACCTTTGTGTCTTAA 1161

B

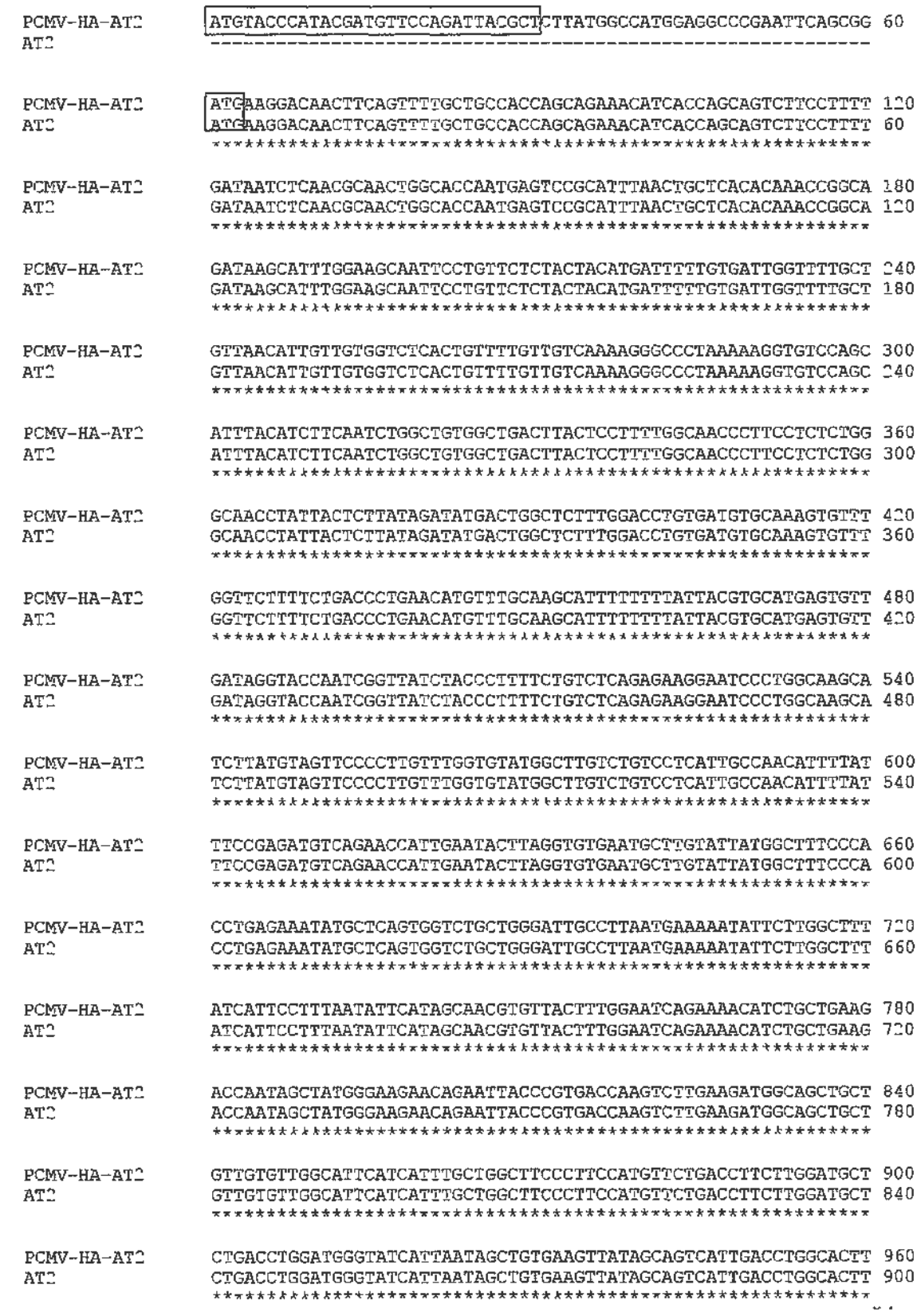
PCMV-HA-AT2 ATGTACCCATACGATGTTCCAGATTACGCTCTTATGGCCATGGAGGCCCGAATTCAGCGG 60
AT2 --
PCMV-HA-AT2 ATGAAGGACAACTTCAGTTTTGCTGCCACCAGCAGAAACATCACCAGCAGTCTTCCTTTT 120
AT2 ATGAAGGACAACTTCAGTTTTGCTGCCACCAGCAGAAACATCACCAGCAGTCTTCCTTTT 60
PCMV-HA-AT2 GATAATCTCAACGCAACTGGCACCAATGAGTCCGCATTTAACTGCTCACACAAACCGGCA 180
AT2 GATAATCTCAACGCAACTGGCACCAATGAGTCCGCATTTAACTGCTCACACAAACCGGCA 120
PCMV-HA-AT2 GATAAGCATTTGGAAGCAATTCCTGTTCTCTACTACATGATTTTTGTGATTGGTTTTGCT 240
AT2 GATAAGCATTTGGAAGCAATTCCTGTTCTCTACTACATGATTTTTGTGATTGGTTTTGCT 180
PCMV-HA-AT2 GTTAACATTGTTGTGGTCTCACTGTTTTGTTGTCAAAAGGGCCCTAAAAAGGTGTCCAGC 300
AT2 GTTAACATTGTTGTGGTCTCACTGTTTTGTTGTCAAAAGGGCCCTAAAAAGGTGTCCAGC 240
PCMV-HA-AT2 ATTTACATCTTCAATCTGGCTGTGGCTGACTTACTCCTTTTGGCAACCCTTCCTCTCTGG 360
AT2 ATTTACATCTTCAATCTGGCTGTGGCTGACTTACTCCTTTTGGCAACCCTTCCTCTCTGG 300
PCMV-HA-AT2 GCAACCTATTACTCTTATAGATATGACTGGCTCTTTGGACCTGTGATGTGCAAAGTGTTT 420
AT2 GCAACCTATTACTCTTATAGATATGACTGGCTCTTTGGACCTGTGATGTGCAAAGTGTTT 360
PCMV-HA-AT2 GGTTCTTTTCTGACCCTGAACATGTTTGCAAGCATTTTTTTTATTACGTGCATGAGTGTT 480
AT2 GGTTCTTTTCTGACCCTGAACATGTTTGCAAGCATTTTTTTTATTACGTGCATGAGTGTT 420
PCMV-HA-AT2 GATAGGTACCAATCGGTTATCTACCCTTTTCTGTCTCAGAGAAGGAATCCCTGGCAAGCA 540
AT2 GATAGGTACCAATCGGTTATCTACCCTTTTCTGTCTCAGAGAAGGAATCCCTGGCAAGCA 480
PCMV-HA-AT2 TCTTATGTAGTTCCCCTTGTTTGGTGTATGGCTTGTCTGTCCTCATTGCCAACATTTTAT 600
AT2 TCTTATGTAGTTCCCCTTGTTTGGTGTATGGCTTGTCTGTCCTCATTGCCAACATTTTAT 540
PCMV-HA-AT2 TTCCGAGATGTCAGAACCATTGAATACTTAGGTGTGAATGCTTGTATTATGGCTTTCCCA 660
AT2 TTCCGAGATGTCAGAACCATTGAATACTTAGGTGTGAATGCTTGTATTATGGCTTTCCCA 600
PCMV-HA-AT2 CCTGAGAAATATGCTCAGTGGTCTGCTGGGATTGCCTTAATGAAAAATATTCTTGGCTTT 720
AT2 CCTGAGAAATATGCTCAGTGGTCTGCTGGGATTGCCTTAATGAAAAATATTCTTGGCTTT 660
PCMV-HA-AT2 ATCATTCCTTTAATATTCATAGCAACGTGTTACTTTGGAATCAGAAAACATCTGCTGAAG 780
AT2 ATCATTCCTTTAATATTCATAGCAACGTGTTACTTTGGAATCAGAAAACATCTGCTGAAG 720
PCMV-HA-AT2 ACCAATAGCTATGGGAAGAACAGAATTACCCGTGACCAAGTCTTGAAGATGGCAGCTGCT 840
AT2 ACCAATAGCTATGGGAAGAACAGAATTACCCGTGACCAAGTCTTGAAGATGGCAGCTGCT 780
PCMV-HA-AT2 GTTGTGTTGGCATTCATCATTTGCTGGCTTCCCTTCCATGTTCTGACCTTCTTGGATGCT 900
AT2 GTTGTGTTGGCATTCATCATTTGCTGGCTTCCCTTCCATGTTCTGACCTTCTTGGATGCT 840
PCMV-HA-AT2 CTGACCTGGATGGGTATCATTAATAGCTGTGAAGTTATAGCAGTCATTGACCTGGCACTT 960
AT2 CTGACCTGGATGGGTATCATTAATAGCTGTGAAGTTATAGCAGTCATTGACCTGGCACTT 900

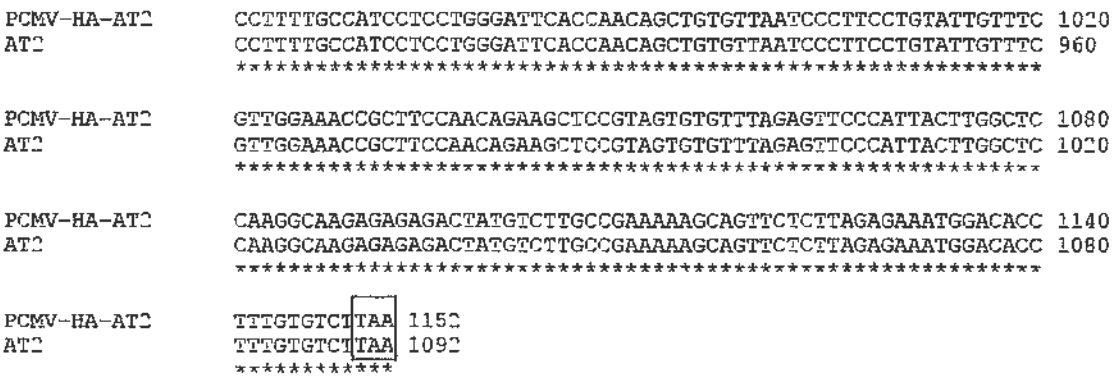
PCMV-HA-AT2 CCTTTTGCCATCCTCCTGGGATTCACCAACAGCTGTGTTAATCCCTTCCTGTATTGTTTC 1020
AT2 CCTTTTGCCATCCTCCTGGGATTCACCAACAGCTGTGTTAATCCCTTCCTGTATTGTTTC 960
PCMV-HA-AT2 GTTGGAAACCGCTTCCAACAGAAGCTCCGTAGTGTGTTTAGAGTTCCCATTACTTGGCTC 1080
AT2 GTTGGAAACCGCTTCCAACAGAAGCTCCGTAGTGTGTTTAGAGTTCCCATTACTTGGCTC 1020
PCMV-HA-AT2 CAAGGCAAGAGAGAGACTATGTCTTGCCGAAAAAGCAGTTCTCTTAGAGAAATGGACACC 1140
AT2 CAAGGCAAGAGAGAGACTATGTCTTGCCGAAAAAGCAGTTCTCTTAGAGAAATGGACACC 1080
PCMV-HA-AT2 TTTGTGTCTTAA 1152
AT2 TTTGTGTCTTAA 1092

C

```
1   MASMQKLISE EDLLMAMEAR IQRMKDNFSF AATSRNITSS LPFDNLNATG TNESAFNCSH
61  KPADKHLEAI PVLYYMIFVI GFAVNIVVVS LFCCQKGPKK VSSIYIFNLA VADLLLLATL
121 PLWATYYSYR YDWLFGPVMC KVFGSFLTLN MFASIFFITC MSVDRYQSVI YPFLSQRRNP
181 WQASYVVPLV WCMACLSSLP TFYFRDVRTI EYLGVNACIM AFPPEKYAQW SAGIALMKNI
241 LGFIIPLIFI ATCYFGIRKH LLKTNSYGKN RITRDQVLKM AAAVVLAFII CWLPFHVLTF
301 LDALTWMGII NSCEVIAVID LALPFAILLG FTNSCVNPFL YCFVGNRFQQ KLRSVFRVPI
361 TWLQGKRETM SCRKSSSLRE MDTFVS-
```

D

```
1   MYPYDVPDYA LMAMEARIQR MKDNFSFAAT SRNITSSLPF DNLNATGTNE SAFNCSHKPA
61  DKHLEAIPVL YYMIFVIGFA VNIVVVSLFC CQKGPKKVSS IYIFNLAVAD LLLLATLPLW
121 ATYYSYRYDW LFGPVMCKVF GSFLTLNMFA SIFFITCMSV DRYQSVIYPF LSQRRNPWQA
181 SYVVPLVWCM ACLSSLPTFY FRDVRTIEYL GVNACIMAFP PEKYAQWSAG IALMKNILGF
241 IIPLIFIATC YFGIRKHLLK TNSYGKNRIT RDQVLKMAAA VVLAFIICWL PFHVLTFLDA
301 LTWMGIINSC EVIAVIDLAL PFAILLGFTN SCVNPFLYCF VGNRFQQKLR SVFRVPITWL
361 QGKRETMSCR KSSSLREMDT FVS-
```

2.4.2 Transient expression of tagged AT2 receptor variants in different cell lines

2.4.2.1 Transient expression detected by confocal microscopy

Initially, the subcellular localization of transiently expressed AT2 receptor variants in different cell lines were examined by confocal microscopy. Expression constructs including pEGFP-AT2, pCMV-HA-AT2, pCMV-Myc-AT2 were transiently transfected into CHO-K1 cells, HEK293 cells and PC12 cells. PCMV-AT2-FLAG and pCDNA-Myc-AT2 were only transfected into HEK293 cells. Transfection condition was optimized to 1 μg plasmid combined with 2 μl Lipofectamine 2000 for each well in a 6-well plate. For pEGFP-AT2 or pEGFP transfected cells, live cells were examined with confocal microscope. For pCMV-HA-AT2, pCMV-Myc-AT2, pCMV-AT2-FLAG, pCDNA-Myc-AT2 and respective vector control transfected cells, specific anti-tag antibody was used in immunofluorescence assay. FITC conjugated secondary antibody was used to visualize the primary antibody staining.

Among all three cell lines, transfection efficiency (number of transfected cells/total cells in a random view under microscope) in HEK293 cells was highest, while the lowest was that in PC12 cells. With pCMV-Myc-AT2 as an example, under the same transfection condition about 30%~50% (data from three transfection experiments) of HEK293 cells were transfected; in CHO cells about 5% cells were transfected; in PC12 cells less than 0.5% cells were transfected. Therefore in the following study, HEK293 cells were used in transient transfection to determine protein-protein interactions in Chapter 4.

In the same cell line, transfection efficiency of pCMV-Myc-AT2 was highest. As mentioned, about 30%~50% of HEK293 cells were transfected with pCMV-Myc-AT2. About 5% of HEK293 cells were transfeceted with pEGFP-AT2 and pCMV-HA-AT2 (which shares the same promoter as pCMV-Myc-AT2). Only about 1% cells were transfected with pCMV-AT2-FLAG constructs. Therefore in the following study, pCMV-Myc-AT2 was used in transient transfection to determine protein-protein interactions in Chapter 4.

In HEK293 cells all tagged AT2 receptor variants displayed clear cell membrane expression. AT2 variants were also detected in cytosol in HEK293 cells. In CHO cells and PC12 cells most tagged AT2 receptor variants expressed in cytosol while membrane expression was not as clear as that in HEK293 cells (Figure 2.5).

Figure 2.5 Transient expression of AT2 receptor variants detected by confocal microscopy. HEK293 cells (5×10^5), CHO-K1 cells (1×10^5) and PC12 cells (2×10^5) were seeded on 25 mm coverslips in a 6-well plate. Plasmid (1 μg) combined with Lipofectamine 2000 (2 μl) was delivered into cells as described in Methods. pEGFP-AT2 transfected cells (a, b, c) were directly examined by live cell imaging; pEGFP transfected CHO cells (d) was used as a control. Immunofluorescenct confocal microscopy were performed on pCMV-Myc-AT2 (e, f, g), pCMV-HA-AT2 (i, j, k), pCMV-AT2-FLAG (m) and pCDNA-Myc-AT2 (o) transfected cells. HEK 293 cells transiently transfected with pCMV-Myc (h), pCMV-HA (l), pCMV-4A (n) and pCDNA3 (p) empty vectors were used as controls. The fluorescent images are shown. Scale bar is 10 μm.

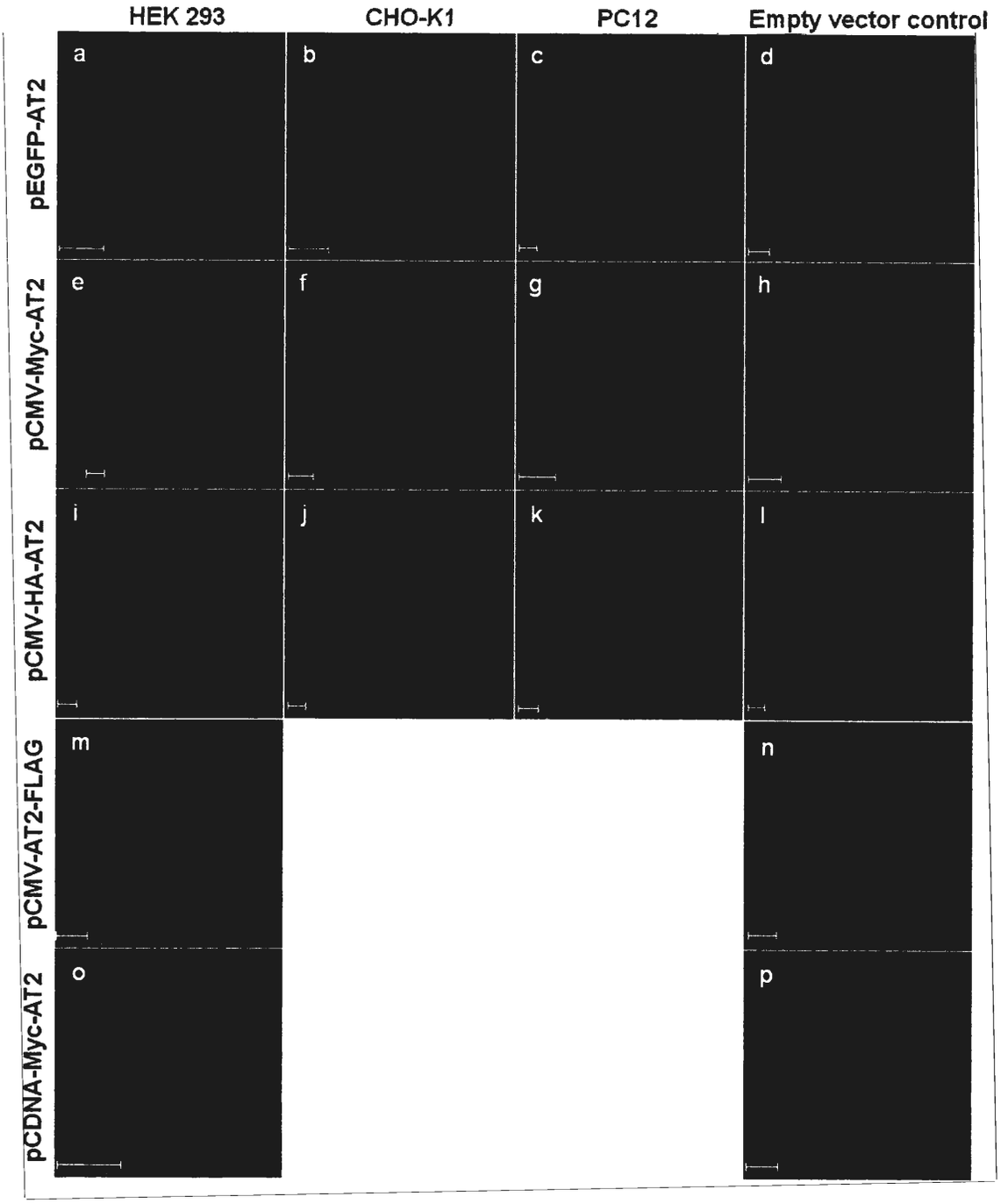
HEK 293
CHO-K1
PC12
Empty vector control
pEGFP-AT2
pCMV-Myc-AT2
pCMV-HA-AT2
pCMV-AT2-FLAG
pCDNA-Myc-AT2
a
b
c
d
e
f
g
h
i
j
k
l
m
n
o
p

2.4.2.2 Gene dosage effect on AT2 receptor expression

In transient transfection, increasing DNA amount would increase protein expression (Nikcevic et al., 2003). The gene dosage effect on AT2 receptor expression was also studied using confocal microscopy. Two dosage (0.5 μg /2 μg) of DNA was transfected into cells cultured in 6-well plate and DNA/Lipofectamine2000 ratio was kept at (1:2). Difference in the expression levels were demonstrated with pCMV-Myc-AT2 constructs (Figure 2.6).

In CHO cells, Myc-AT2 located mainly on cell membrane when 0.5μg DNA was transfected. However, when DNA amount was increased to 2 μg, green fluorescence aggregated to dots near nuclear region which may caused by protein over expression in Golgi body.

In PC12 cells, Myc-AT2 expressed in the whole cytosol in both lower amount and higher amount of DNA transfection. Fluorescence was brighter when 2 μg DNA was used which indicated higher expression level.

In HEK293 cells, Myc-AT2 also located on cell membrane when 0.5 μg DNA was used in transient transfection; when DNA amount was increased to 2 μg, many cells displayed shrieked cell body which indicates that AT2 over expression cause cell toxicity.

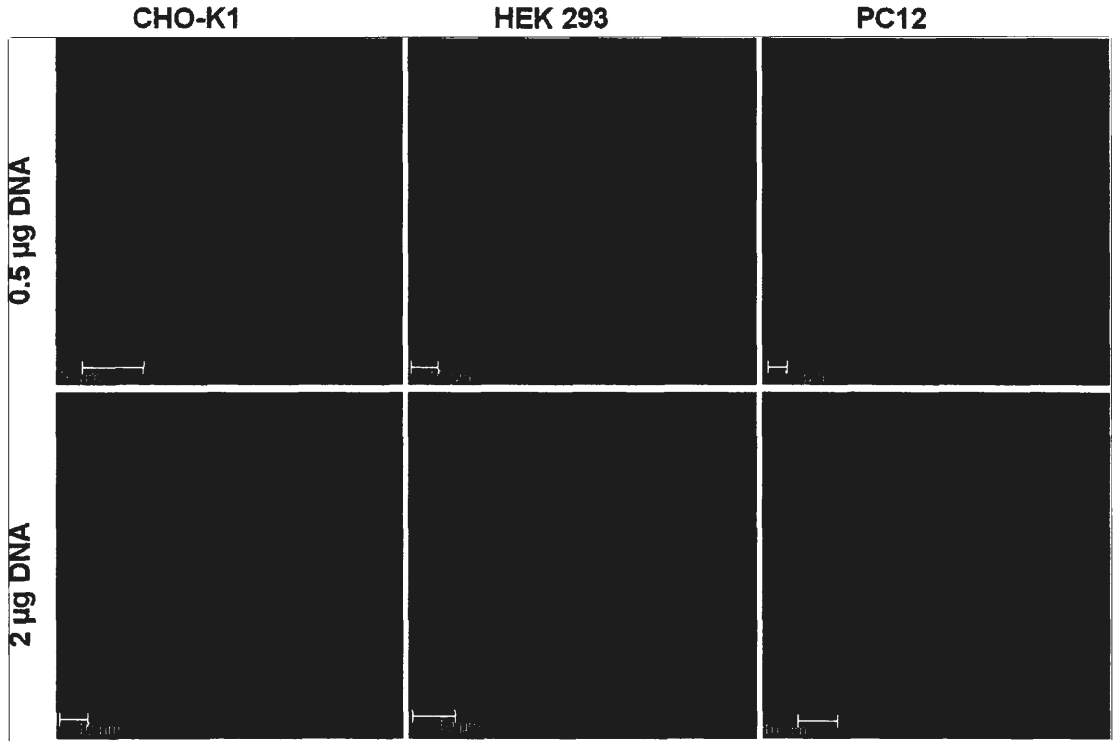

Figure 2.6 Gene dosage effect on Myc-AT2 expression. HEK293 cells (5×10^5), CHO-K1 cells (1×10^5) and PC12 cells (2×10^5) were seeded on 25 mm coverslips in a 6-well plate. PCMV-Myc-AT2 plasmid (0.5 or 2 µg) was transiently transfected into cells using Lipofectamine 2000. Immunofluorescent confocal microscopy were performed as described in Methods. The fluorescent image was shown. Scale bar is 10 µm.

2.4.2.3 Western protein analysis of transiently-expressed tagged AT2 receptor variants

The transient expression of AT2 was also studied by western protein analysis. For various tagged AT2 receptor constructs, the highest transfection efficiency was shown in transiently-tranfected HEK293 cells. Therefore, pEGFP-AT2, pCMV-AT2-FLAG and pCMV-Myc-AT2 were transiently transfected into HEK cells. The expressed AT2 receptor was concentrated by immunoprecipitation and detected in western blot using specific anti-GFP, anti-FLAG and anti-Myc antibody, respectively.

However due to low transfection efficiency, only Myc-AT2 was detected in western blot. Compared to vector control, Myc-AT2 was detected as monomer (45 kDa, the predicted MW of Myc-AT2) as well as ladder of high MW bands in HEK293 cells, suggesting a posttranslational modification of newly synthesized AT2 receptor (Figure 2.7).

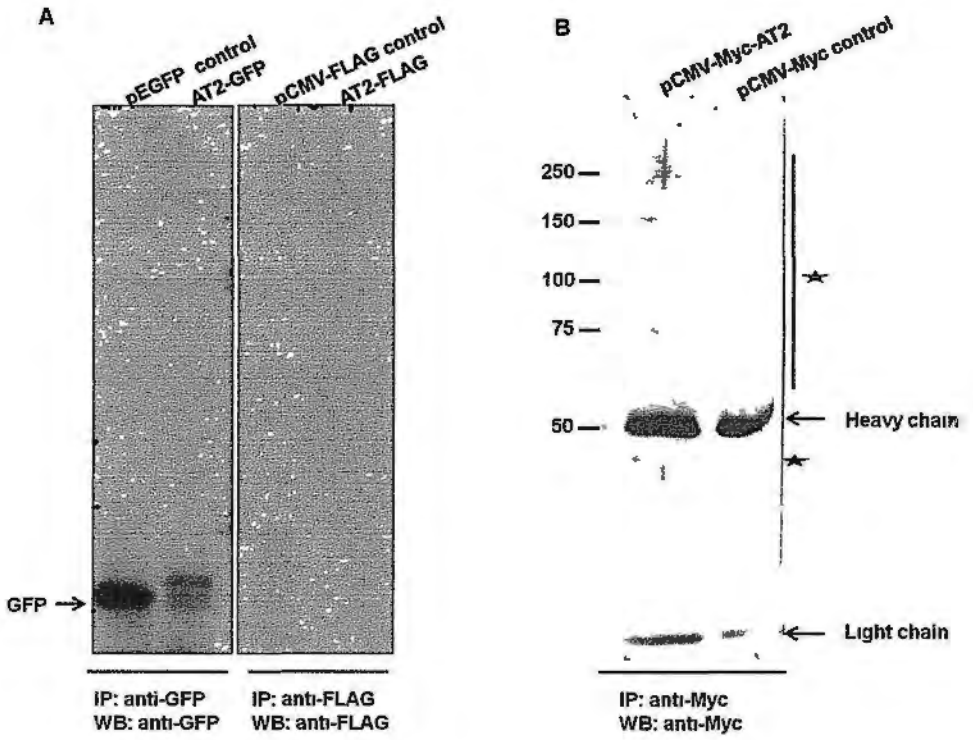

Figure 2.7 Transient expression of AT2 receptor variants detected by western blot. HEK293 cells (2×10^6) were seeded on 100 mm dish and cultured until 85%~90% confluence. Plasmid (5 μg) of pEGFP-AT2, pCMV-AT2-FLAG, pCMV-Myc-AT2 and respective vector controls were transiently transfected into the cells using Lipofectamine2000. Polyclonal anti-GFP antibody, polyclonal anti-FLAG antibody and monoclonal anti-Myc antibody were employed in immunoprecipitation. Precipitated samples were separated on 10% SDS-PAGE. AT2 receptor variants expression was detected by monoclonal anti-GFP antibody, monoclonal anti-FLAG antibody (A) and monoclonal anti-Myc antibody (B).

2.4.3 Stable expression of different tagged AT2 receptor variants in three different cell lines

2.4.3.1 Stable cell lines establishment

For stable cell line establishment, plasmids expressing AT2 receptor and respective empty vector controls were linearized first, which prevented cutting in the transgene during construct integration. Linearized expression vectors were transfected into different cells using Lipofecomine 2000 as described in transient transfection. Transfected cells were selected against G418 as described in 2.3.4.1. Concentration of G418 for selection was tested by series dilution: in CHO-K1 cells and PC12 cells was 1 mg/ml; in HEK293 cells was 2 mg/ml. Stable cell lines expressing tagged AT2 receptor variants and respective controls were summarized in Table 2.2. At least two clones of each cell lines were established (clone No. listed in the table) and expression level was determined using immunofluorescent confocal microscopy. The clones with highest expression were used for further study (clone No. in red).

2.4.3.2 AT2 receptor mRNA expression in stable cell lines detected by RT-PCR

AT2 receptor mRNA expression in stable cell lines was first detected by RT-PCR. Total RNA of stable cell lines was extracted with Tri_{ZOL} reagent. AT2 receptor expression was detected with specific primer (F1060/R1347) targeting a 600 bp fragment at the 3'-end of rat AT2 mRNA. Compared to empty vector controls, a clear band of 600 bp was seen in all AT2 expressing stable cell lines (Figure 2.8).

cell line	AT2-GFP	GFP	AT2-FLAG	PCMV-FLAG	PCDNA-myc-AT2	PCDNA3
CHO	**CHO-AT2-GFP C5 , C6**	**CHO-GFP C11**			**CHO-Myc-AT2 C2, C4**	**CHO-PCDNA C1, C2**
HEK 293	**HEK-AT2-GFP C1, C5**	**HEK-GFP C6**	**HEK-AT2-FLAG C1, C4**	**HEK-FLAG C2, C4**	**HEK-Myc-AT2 C2, C3, C5**	**HEK-PCDNA C5**
PC12					**PC12-Myc-AT2 C2, C9, C12**	**PC12-PCDNA C1,C2,C3**

Table 2.2 Summary of AT2 receptor stably expressing cell lines

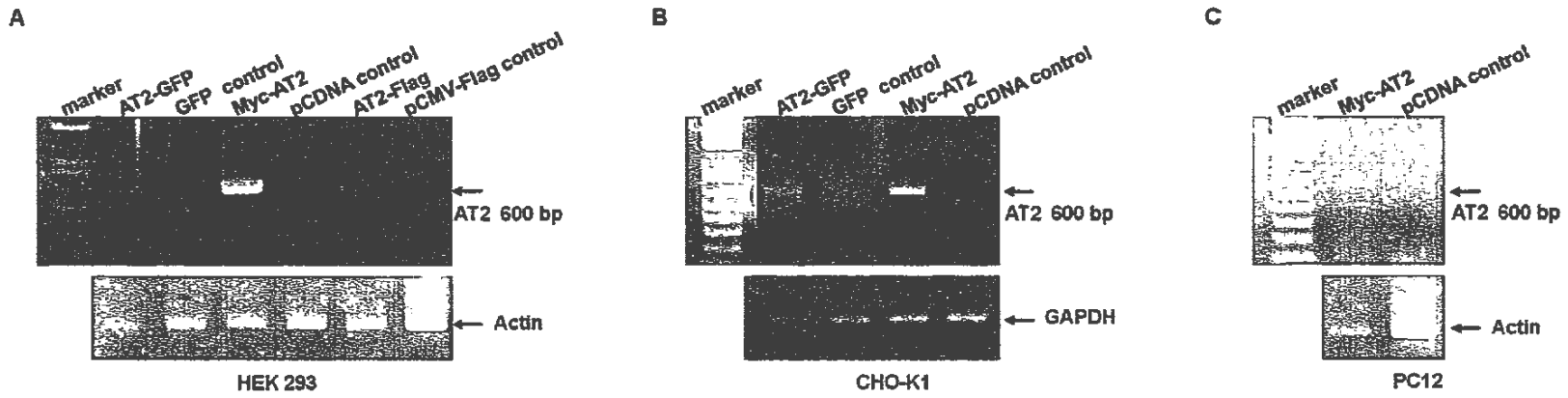

Figure 2.8 Stable expression of AT2 receptor variants detected by RT-PCR. Stable cell lines of HEK293 cells (A), CHO cells (B) and PC12 cells (C) were seeded on 60 mm dish and cultured until confluence. Total RNA was extracted by Tri_{zol} reagent. cDNA was obtained from reverse transcription of total RNA. AT2 expression was detected by PCR with specific primer (F1060/R1347) targeting 3'-end of rat AT2 mRNA.

2.4.3.3 AT2 receptor variants expression in stable cell lines analyzed by confocal microscopy

To analyze the subcellular localization of tagged AT2 receptor variants, stable cell lines were examined by confocal imaging.

AT2-GFP: In both CHO and HEK293 cells, AT2-GFP displayed clear cell membrane expression with some dots like expression at perinuclear region, while GFP expressed evenly in the whole cell (Figure 2.9A).

Myc-AT2: Clear cell membrane expression was observed in HEK293 cells and PC12 cells. However expression level in PC12 was much lower than that in HEK293 cells and CHO cells. In CHO cells, Myc-tagged AT2 receptor variants distributed in cytosol and also aggregated to dots like expression like AT2-GFP in CHO cells (Figure 2.9B).

AT2-FLAG: AT2-FLAG expressed on cell membrane and expression level was quite low compared with AT2-GFP and Myc-AT2 (Figure 2.9 B).

Figure 2.9 Stable expression of AT2 receptor variants detected by confocal microscopy. AT2 receptor stably transfected HEK293 cells (5×10^5), CHO-K1 cells (1×10^5) and PC12 cells (2×10^5) were seeded on 25 mm coverslips in a 6-well plate and cultured for 24 hours. For AT2-GFP and GFP controls, fluorescent images were taken with live cells. For Myc-AT2, AT2-FLAG, immunofluorescence assays were performed before confocal microscopy. Fluorescent images images were shown. Scale bar is 10 μm.

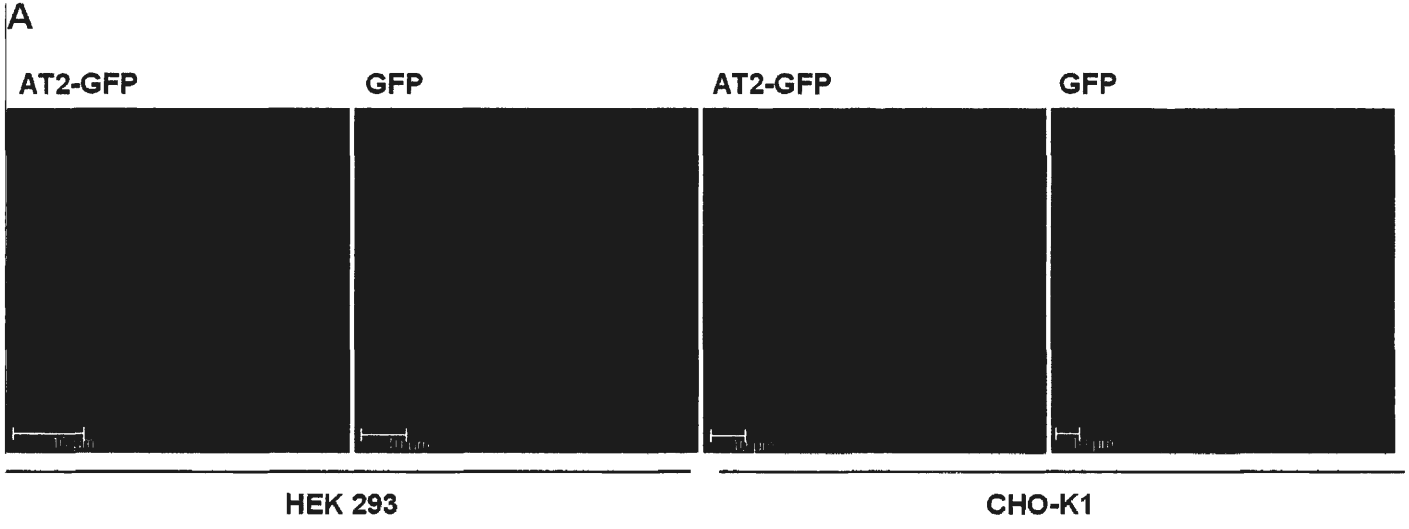
A
AT2-GFP
GFP
AT2-GFP
GFP
HEK 293
CHO-K1

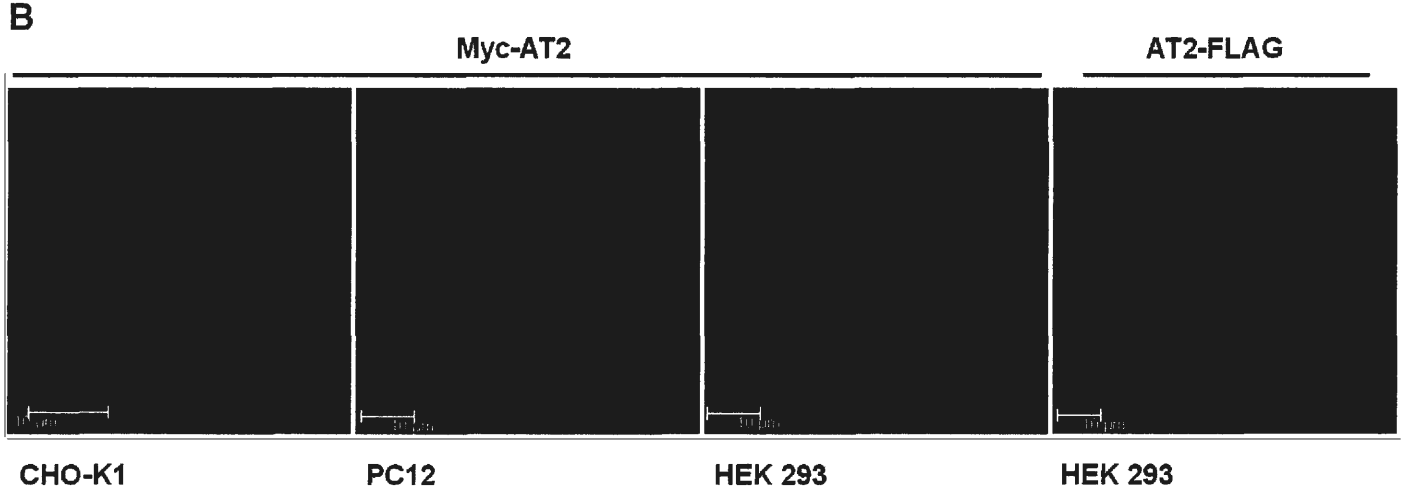
B
Myc-AT2
AT2-FLAG
CHO-K1
PC12
HEK 293
HEK 293

2.4.3.4 AT2 receptor expression in stable cell lines analyzed by western blot

Tagged AT2 receptor variants from cells cultured on 100 mm dish were immunoprecipitated with anti-GFP, anti-Myc and anti-FLAG antibodies. Precipitated protein was analyzed on western blot with respective tag-specific antibodies.

AT2-GFP (Figure 2.10 A): GFP was detected at 25 kDa in both CHO-K1 and HEK293 cells. A clear immuno-reactive band with size of approximately 67 kDa was observed in the AT2 stably expressing cell lines. The molecular weight was close to the sum of AT2 and GFP. However, the majority of AT2-GFP expression was detected as two bands at higher molecular weight region. One immuno-reactive band was between 100 kDa~150 kDa, the other one was above 250 kDa. This could be due to oligomerization or posttranslational modification of AT2-GFP.

AT2-FLAG (Figure 2.10 A): compared to vector control cells only a very high molecular weight band was observed in AT2-FLAG expressed cells. Confocal images indicated that AT2-FLAG expression was quite low in HEK-AT2-FLAG cells. The lack of low MW bands could be due to the low expression. The specificity of anti-FLAG antibody was determined by a cytosolic expressed protein (data not shown here), suggesting that poor detection of AT2-FLAG was not due to the antibody specificity.

Myc-AT2 (Figure 2.10 B, C): Empty control cell lines only showed staining of heavy chain and light chain in western blot. Compared to control cells, an immuno-reactive band with molecular weight of about 45 kDa was detected in HEK293 cells. The

molecular weight was close to the predicted molecular weight of Myc-AT2. Another band detected by anti-Myc antibody in HEK293 cells was at a higher MW region at about 75 kDa~ 110 kDa. The expression of Myc-AT2 in CHO cells and PC12 cells were almost undetectable in normal condition (Figure 2.10 B). Serum starvation was reported to increase AT2 receptor expression in R3T3 cells, a cell line endogenously expressing AT2 receptor (Dudley and Summerfelt, 1993). Serum-free culture also increased Myc-AT2 expression in present study (Figure 2.10 C). After serum-free culture, the expression pattern of Myc-AT2 in PC12 and CHO cells were similar to that of HEK 293 cells.

Figure 2.10 Stable expression of AT2 receptor variants analyzed by immunoprecipitation and western blot. Stably transfected cells were seeded in 100 mm dish and cultured until confluence. Cells were lysed in RIPA buffer and precipitated with polyclonal anti-FLAG, polyclonal anti-GFP and monoclonal anti-Myc antibody Precipitated proteins were separated on 10% SDS-PAGE. Protein bands were detected with monoclonal anti-FLAG, monoclonal anti-GFP antibody (A) and monoclonal anti-Myc antibody (B, C) in western blot. The cells shown in panel C were cultured in serum-free medium for 24 hours before cell lysis. The stars show the specific staining compared to control cells.

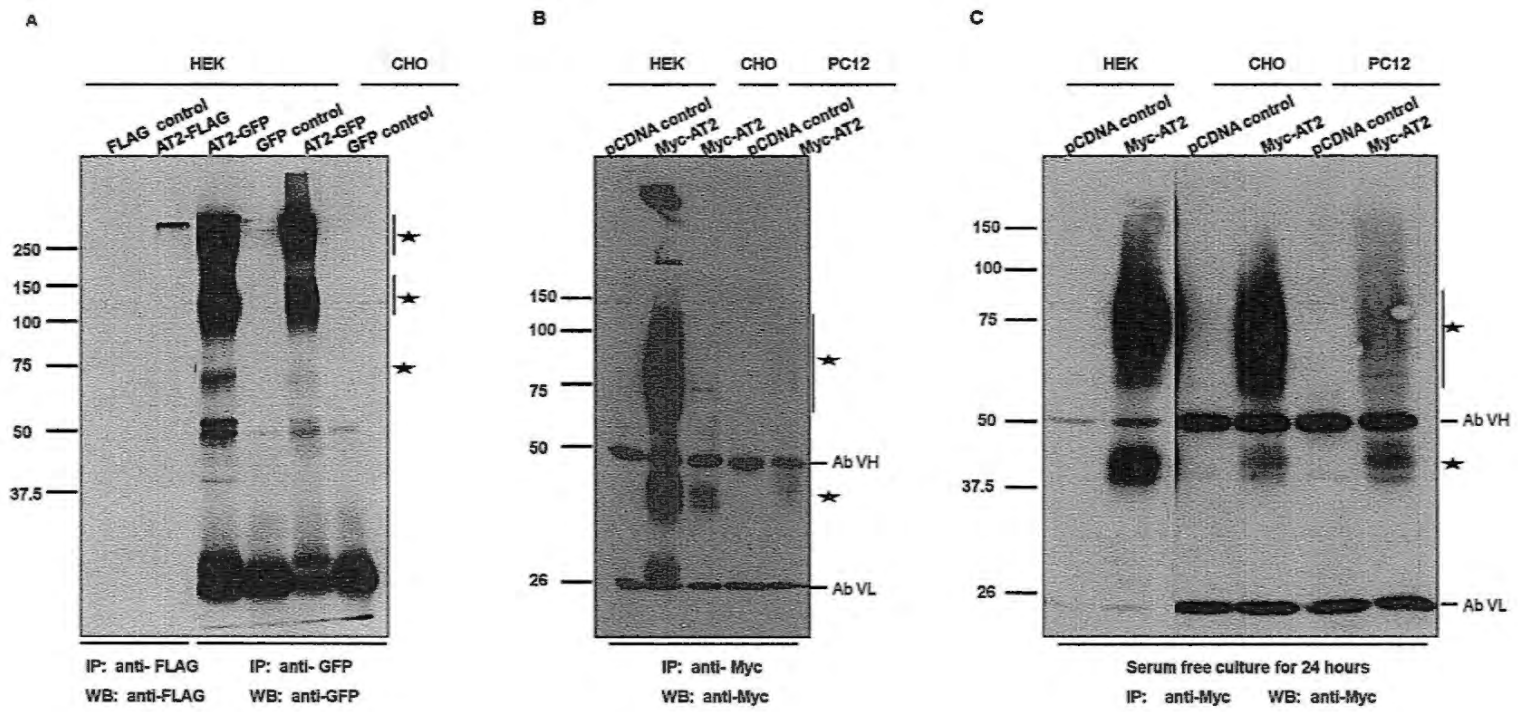
A
HEK
CHO
FLAG control
AT2-FLAG
AT2-GFP
GFP control
AT2-GFP
GFP control
250
150
100
75
50
37.5
IP: anti- FLAG
WB: anti-FLAG
IP: anti- GFP
WB: anti-GFP
B
HEK
CHO
PC12
pCDNA control
Myc-AT2
Myc-AT2
pCDNA control
Myc-AT2
150
100
75
50
26
Ab VH
Ab VL
IP: anti- Myc
WB: anti-Myc
C
HEK
CHO
PC12
pCDNA control
Myc-AT2
pCDNA control
Myc-AT2
pCDNA control
Myc-AT2
150
100
75
50
37.5
26
Ab VH
Ab VL
Serum free culture for 24 hours
IP: anti-Myc
WB: anti-Myc

2.4.3.5 AT2 receptor expression in stable cell lines detected by anti-AT2 antibodies

2.4.3.5.1 Anti-AT2 antibodies in immunofluorescence

There are two anti-AT2 antibodies in our lab: one was raised by our lab in rabbit against a C terminal peptide (GKRETMSCRK) equivalent to amino acids 342-352 of rat AT2 receptor; the other one was purchased from Santa Cruz which was raised against amino acids 221-363 of human AT2 receptor. In immunohistochemical staining, anti-AT2 raised in our lab but not anti-AT2 from Santa Cruz, showed specific staining in rat adrenal section as reported (Wong et al., 2004). Both of the two antibodies failed to recognize Myc-AT2 transiently expressed in CHO cells. Anti-AT2 from our lab also failed to recognized Myc-AT2 stably expressed in CHO and PC12 cells (Figure 2.11)

2.4.3.5.2 Anti-AT2 antibodies in western blot

Both anti-AT2 antibodies were used for immunoprecipitation of mouse embryo tissue lysate. Compared to control serum, no specific protein bands but heavy chains were detected with anti-AT2 antibody from Santa Cruz. Some high MW bands were detected in the precipitated samples with anti-AT2 raised in our lab (Figure 2.12). Polyclonal anti-GFP antibody also raised in rabbit in our lab was used in immunoprecipitation as a negative control.

In western protein analysis of stable cell lines, neither of the two antibodies recognized AT2-GFP and Myc-AT2 expressed in HEK cells (Figure 2.13 A). However anti-AT2 antibody from our lab, but not the one from Santa Cruz, recognized the 45 kDa band and some higher MW bands around 100 kDa in PC12-Myc-AT2 cell lines. However, the MW was bigger than the one in Figure 2.10 C.

Figure 2.11 Anti-AT2 antibody staining in confocal microscopy. Rat adrenal sections, CHO cells transiently transfected with pCMV-Myc-AT2 and CHO-Myc-AT2, PC12-Myc-AT2 stable cells were prepared for confocal microscopy as described in Methods. FITC was excited at 488 nm and green fluorescence was collected at wavelength of 525±50.

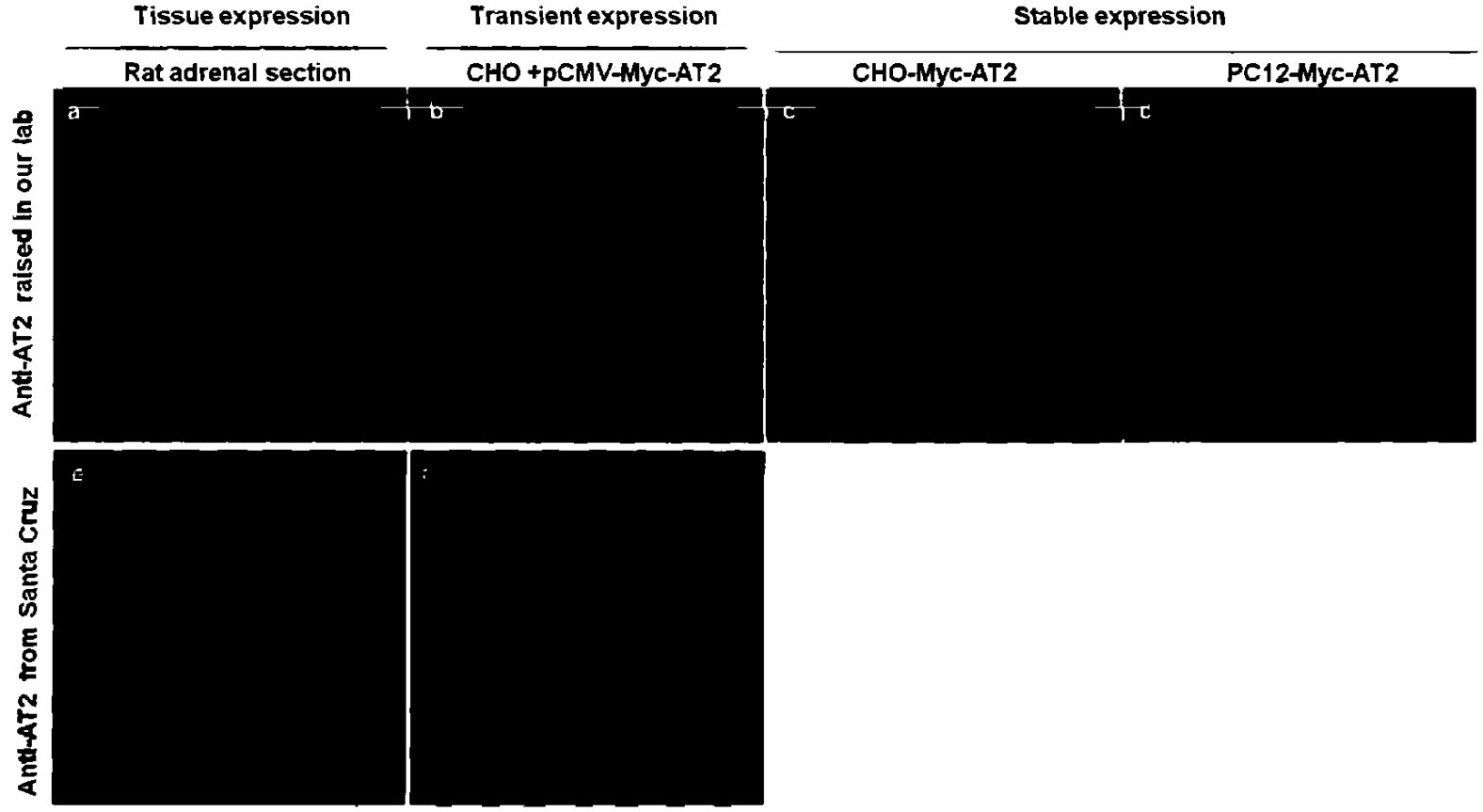
Tissue expression
Transient expression
Stable expression
Rat adrenal section
CHO +pCMV-Myc-AT2
CHO-Myc-AT2
PC12-Myc-AT2
Anti-AT2 raised in our lab
Anti-AT2 from Santa Cruz
a
b
c
d
e
f

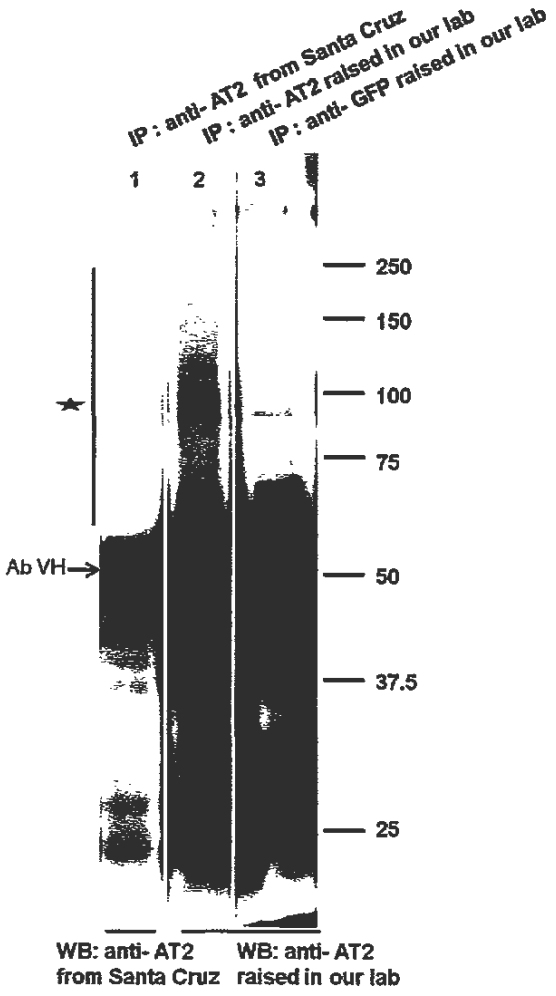

Figure 2.12 Immunoprecipitation of mouse embryonic proteins by anti-AT2 antibodies.

Membrane of mouse embryo viscera was lysed and immunoprecipitated as described in Methods. Tissue lysate was precipitated with anti-AT2 antibody from Santa Cruz and detected with the same antibody in western blot (lane 1); Tissue lysate was immunoprecipitated with anti-AT2 antibody raised in our lab and detected with the same antibody in western blot (lane 2); Tissue lysate was immunoprecipitated with anti-GFP antibody raised in our lab and detected with anti-AT2 antibody raised in our lab (lane 3).

Figure 2.13 Western protein analysis of immunoprecipitated AT2 receptor variants with anti-AT2 antibodies. Stably transfected HEK293, CHO and PC12 cells were seeded on 100 mm dish and cultured until confluence. Cells were lysed in RIPA buffer and precipitated as described in Methods.

A). AT2-GFP stably expressed in HEK and CHO cells were precipitated with polyclonal anti-GFP antibody; Myc-AT2 stably expressed in HEK cells were precipitated with monoclonal anti-Myc antibody. The membrane was detected with a mixture of anti-AT2 raised in our lab and anti-AT2 from Santa Cruz.

B). Myc-AT2 stably expressed in PC12 cells were precipitated with monoclonal anti-Myc antibody and detected with anti-Myc antibody, anti-AT2 raised in our lab and anti-AT2 antibody from Santa Cruz.

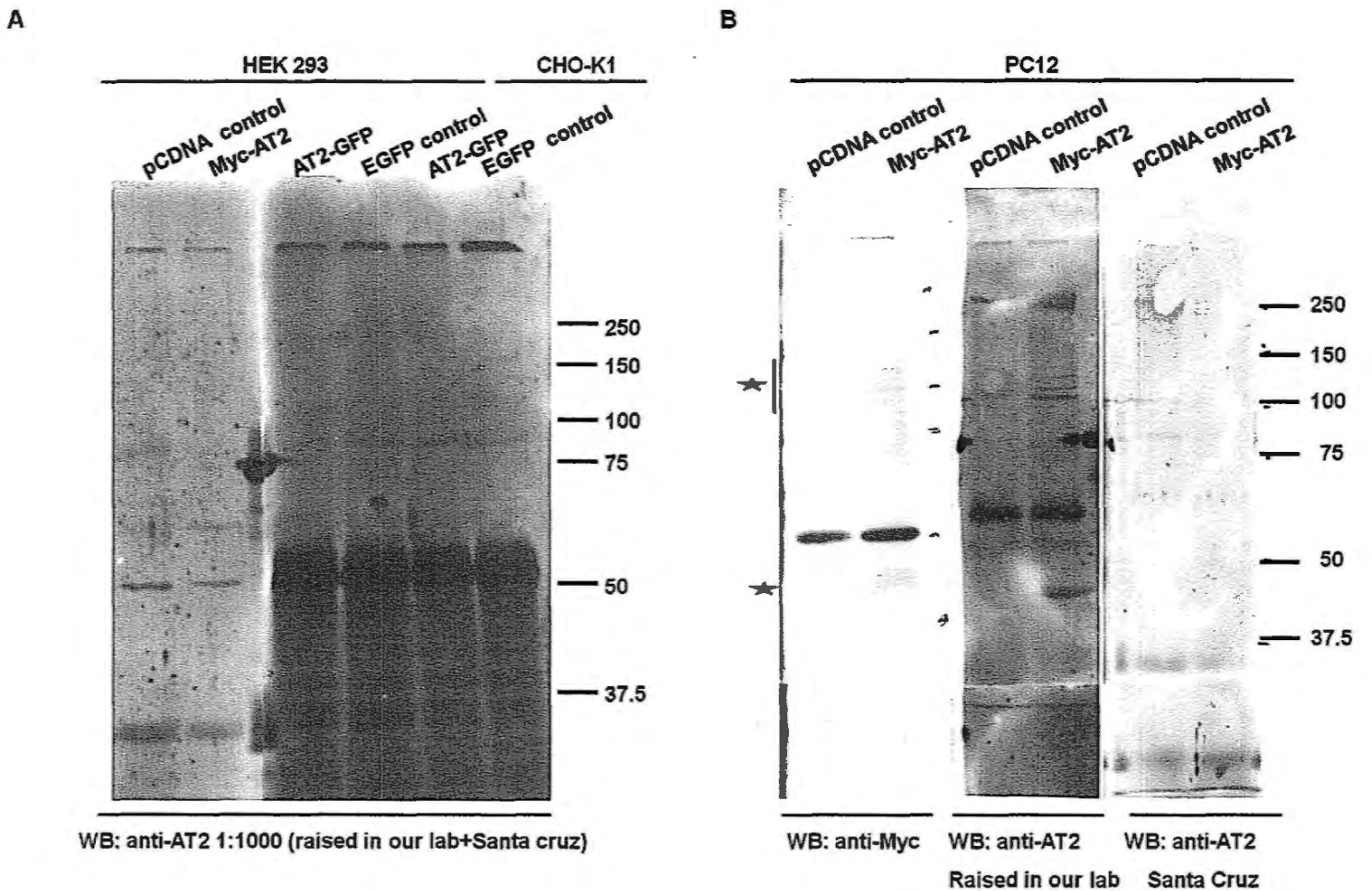
A
HEK 293
CHO-K1
pCDNA control
Myc-AT2
AT2-GFP
EGFP control
AT2-GFP
EGFP control
250
150
100
75
50
37.5
WB: anti-AT2 1:1000 (raised in our lab+Santa cruz)
B
PC12
pCDNA control
Myc-AT2
pCDNA control
Myc-AT2
pCDNA control
Myc-AT2
250
150
100
75
50
37.5
WB: anti-Myc
WB: anti-AT2
Raised in our lab
WB: anti-AT2
Santa Cruz

2.5 Discussion

AT2 receptor was discovered in 1989 (Steckelings et al., 2005), but the function and signaling pathway of AT2 receptor are still not well understood. One important reason for this is the AT2 receptor is not easy to "find". AT2 receptor expresses widely in fetus, but in adult AT2 receptor only expresses in certain tissue like brain, adrenal, renal and cardiac structure. For *in vitro* assays only limited numbers of cells express AT2 receptor such as R3T3 (a mouse fibroblast cell line) and PC12W cells (a rat pheochromocytoma cell line). However even in these cell lines the expression of AT2 receptor was restricted by cell culture condition and cell cultured passage (Dudley and Summerfelt, 1993). Primary cultures are often needed. These cell lines and primary cultured cells were often applied in studies in the physiological and pathological role of AT2 receptor, but for studies on receptor cell membrane expression they are not suitable models (Miura and Karnik, 2000).

Trafficking of even the same GPCR in different cells is different (Gray et al., 2001), so in present study three different cell lines were used to study the subcellular localization and expression of AT2 receptor. CHO-K1 and HEK293 have been used for AT2 receptor expression in others' reports (Feng et al., 2005; Miura and Karnik, 2000). Besides, one aim of present study was to examine whether AT2 receptor was modified by SUMO. Using HEK293 cells and CHO-K1 cells to study sumoylation on target protein had been reported before, which indicated that HEK293 cells and CHO cells had the whole system for sumoylation. For example, HEK cells was used to confirm

sumoylation on an ion channel Kv2.1 (Dai et al., 2009); CHO cells was used to illustrate sumoylation on Ku70 (Yurchenko et al., 2008) and estrogen receptor (Zhu and Zhou, 2008).

To my knowledge, PC12 cells have not been used for AT2 receptor over-expression before. PC12 cells less than 17 passages are known to exclusively express AT2 receptor (Zhao et al., 2003) which made them an endogenous expression model (Wolf et al., 2004). In our untransfected PC12 cells, AT2 expression was barely detected by RT-PCR. It might be because the passage number was too high. However, PC12 was derived from adrenal medulla, a region endogenously expressed AT2 receptor even in adults, which could supply a "native" environment for AT2 receptor expression. Data in present study also confirmed this hypothesis. Only in PC12-Myc-AT2 cells, AT2 receptor variant was detected by anti-AT2 antibody raised in our lab, although the MW was still different from that of embryo tissue.

AT2 receptor expression in fetus tissue or pathological condition was commonly detected by RT-PCR or isotope-labeled ligand binding assays (Grady et al., 1991; Millan et al., 1991). These methods are highly sensitive but do not display the trafficking and subcellular localization of the receptor. Another reason for detection with these methods might be lacking of efficient anti-AT2 antibody. In the present study, to study posttranslational modification of AT2 receptor, specific anti-tag antibodies were used to detect AT2 receptor expression in both immunofluorescence and western blot. All tag-antibodies showed high specificity in our experiments.

2.5.1 AT2 receptor expression detected by fluorescent confocal microscopy

Immunofluorescence and confocal microscopy directly told the localization and expression level of target protein. In present study, the expression level and membrane localization mainly depends on cell type. A summary for confocal microscopy data is shown in Table 2.3 and plus represents the expression level. HEK293 cells provided the best membrane expression and highest expression level for all tagged AT2 receptor variants in both transient and stable expression (Figure 2.5 and 2.9). In the following study HEK293 cells were used as a model to study interaction between AT2 receptor and other modifier. However when larger amount (2μg for a well in 6-well plate) of AT2 expressing construct was transiently expressed in HEK293 cells, it caused cell toxicity (Figure 2.6). Whether those unhealthy cells underwent apoptosis or autophagy needs further study, however so far no reports mentioned that transient expression of AT2 gene alone caused apoptosis or necrosis. Although expression of AT2 receptor in PC12 cells was detected by anti-AT2 antibody (Figure 2.13), the transfection efficiency in PC12 was too low to perform co-expression and co-immunoprecipitation assays. Nuclear AT2 was reported in kidneys (Gwathmey et al., 2009), however, in our cell system tagged AT2 receptor only showed cell membrane expression, distribution in the cytosol and perinuclear enrichment like other GPCRs (Lu et al., 1998).

There was one technical problem in immunofluorescence assay. In the beginning, Myc-AT2 stably expressed in PC12 cells and AT2-FLAG stably expressed in HEK293 cells could not be detected in immunofluorescence. The problem did not exist in transient transfection. It was finally found that the fixation method mattered in sample preparation

		HEK293	PC12	CHO-K1
Transient	**Cell surface**	++++	–	+
	Cytosol	+	+++++	++++
Stable	**Cell surface**	++++	+++	++
	Cytosol	+	++	+++

Table 2.3 Summary of Confocal Microscopy

for immunofluorescence. In stably transfected PC12-Myc-AT2 and HEK-AT2-FLAG cells, no fluorescence was detected when cells were fixed with 4% paraformaldehyde (PFA); but expression was detected as shown in Figure 2.9 when cells were fixed in ice cold methanol. Both fixation methods were commonly used in immunofluorescence and there was no such difference in other stable cell lines. Compared to PFA fixation, methanol could precipitate or extract some cytosolic protein and distorts cell structure. However methanol could reserve the antigenity of proteins compared to PFA. PFA fixation has little extraction and preserve morphology of cells (Leong et al., 1979). The difference between different fixation methods in the two cell lines might be due to the low expression level of AT2 receptor in these two cell lines. Methanol reserve antigenity of antigens better than PFA but destroy the cytoskeleton structure of cells (Smith-Clerc and Hinz, 2010) which made AT2 expression easily detected.

2.5.2 AT2 receptor expression detected by western blot

Using immunoprecipitation to concentrate the target protein and detecting it with specific antibody in western blot are commonly used to study protein posttranslational modification by comparing the MW change of proteins. In present study, the molecular weight of AT2 receptor mainly depended on the tags attached to AT2. A summary for western protein analysis is shown in Table 2.4. AT2-GFP expressed at 67 kDa, 100 kDa~150 kDa, and over 250 kDa in both stably transfected CHO and HEK293 lines (Figure 2.10). After serum starvation, Myc-AT2 was also detected at similar region: 45 kDa and 75 kDa~110 kDa in western blot in all three kinds of cells (Figure 2.10). The MW mainly depended on the amino acid composition and modification of protein. It

	AT2-GFP	Myc-AT2	AT2-Flag
Transient		**Series of bands**	
Stable	**67, 100-150, >250 kD**	**45, 70-110 kD**	**>250 kD**
Mouse embryo	**Series of bands**		

Table 2.4 Summary of western protein analysis

suggested that even in different cells the posttranslational modification of the same tagged AT2 receptor was similar.

Due to the low expression level, AT2-GFP and AT2-FLAG in transiently transfected cells were not detected in western blot (Figure 2.7). Interestingly, AT2-GFP and AT2-FLAG, the two C-terminal tagged AT2 receptor, expressed in stable cell lines were both detected at very high region in western blot (Figure 2.10). One possible explanation for this is that C-terminal tag affected AT2 receptor interaction with other cytosolic proteins and resulted in homo-dimer or oligomer of AT2 receptor. Myc-AT2 transiently expressed in HEK cells showed series of bands (Figure 2.7). In stably expressing cells, Myc-AT2 expressed at specific region: 45kDa and 75kDa~110kDa on western blot. The reasons for difference between transient and stable expression are unknown (Figure 2.10).

The molecular weight of AT2 receptor reported was different literature to literature. In earlier studies, I^{125} labeled agonist or antagonist was used to concentrate AT2 receptor. The samples were separated on SDS-PAGE and detected by autoradiogram. In this way, AT2 receptor was reported as 70 kDa (Ouali et al., 1993) and 113 ± 12 kDa (Servant et al., 1994) in PC12 cells; 108 kDa in AR42J cells (Chappell et al., 1995) ; 91 ± 7.3 kDa in R3T3 cells (Servant et al., 1994); 66 kDa, 120 kDa and 200 kDa in human myometrium (Lazard et al., 1994).

Later polyclonal serum was raised against AT2 receptor in different labs. Using these serum, AT2 receptor was detected as 45 kDa in transiently transfected COS7 cells, 65

kDa in stable cell lines of CHO cells and 65kDa in extracts of smooth muscle cells (Zahradka et al., 1998); 47 ± 6.5 kDa in rat kidney (Wehbi et al., 2001); 40 kDa in cremaster and soleus muscle (Nora et al., 1998); 66 kDa and 110 kDa in N1E-115 cells (Yee et al., 1994).With anti-AT2 antibody raised in our lab immunoreactive bands of 56, 68, and 78 kDa was detected in total cell lysis of adrenal, kidney, liver, salivary glands, and pancreas (Wong et al., 2004).

In recent years anti-AT2 antibody was commercially available. Using these antibodies AT2 receptor was recognized as 50 kDa in adrenal glands and in HA-AT2 transfected HEK293 cells (Harada et al., 2010); 42 kDa in kidney (Hakam et al., 2006); 62.4 kDa in Neuro-2a cells which endogenously expresses AT2 receptor (Hoffmann and Cool, 2003)

Although the molecular weight of AT2 receptor reported ranged from 40ka to 200 kDa they can be divided into two groups: 40~70 kDa and multiple of (40~70 kDa). All the results were based on denaturing SDS-PAGE as performed in present study. The reasons to explain the molecular weight range in all the literatures mentioned above was single: glycosylation.

Besides the tag antibodies, anti-AT2 antibodies available in our lab were also used in the present study. Polyclonal anti-GFP antibody also raised in rabbit was used as a control in precipitation to exclude the non-specific binding to rabbit immunoglobulin. In mouse embryo tissue a series of protein bands were detected in high molecular weight region by our anti-AT2 antibody. This antibody also worked well in immunohistochemistry in rat adrenal section. However it failed to detect AT2 receptor expressed in our cell lines

in immunofluorescence. AT2 receptor stably expressed in PC12 cells was detected by our anti-AT2 antibody in western blot. It seemed that this antibody was good at recognizing adrenal expressed AT2 receptor. Anti-AT2 from Santa Cuz against a peptide of human AT2 receptor, which also claimed to recognize rat AT2 receptor, failed in both western blot and immunofluorescence.

Chapter 3

Functional characterization of AT2 receptor variants in stable cell lines

3.1 Introduction

In Chapter 2, different tagged AT2 receptor variants were stably expressed in CHO-K1, HEK293 and PC12 cells. Whether the AT2 receptor variants expressed in these stable cell lines were functional or not will be discussed in this chapter.

ANGII is not only a potent vasoactive peptide but also an important regulator of cellular proliferation. ANGII-activated AT1 receptors promote cell growth and migration (Chung et al., 1999). In contrast, lines of evidences demonstrate that ANGII-activated AT2 receptors inhibit cell proliferation and induce apoptosis (Horiuchi et al., 1999).

AT2 receptor also displays ANGII independent activities, the so called constitutive activities. In 2000, Miura and co-workers reported that AT2 receptor induced ligand-independent apoptosis after serum starvation and the apoptosis was mediated by p38 MAPK (Miura and Karnik, 2000a). Later, AT2 receptor was reported to inhibit cell growth and cell cycle progression from G1 to S phase in AT2 receptor stably transfected rat fibroblast cells (Gingras et al., 2003).

In the present study the constitutive activities of AT2 receptor were examined. The experiment design was shown in figure 3.1 . Whether AT2 receptor expression could induce apoptosis or proliferation inhibition were determined firstly. If the AT2 receptor

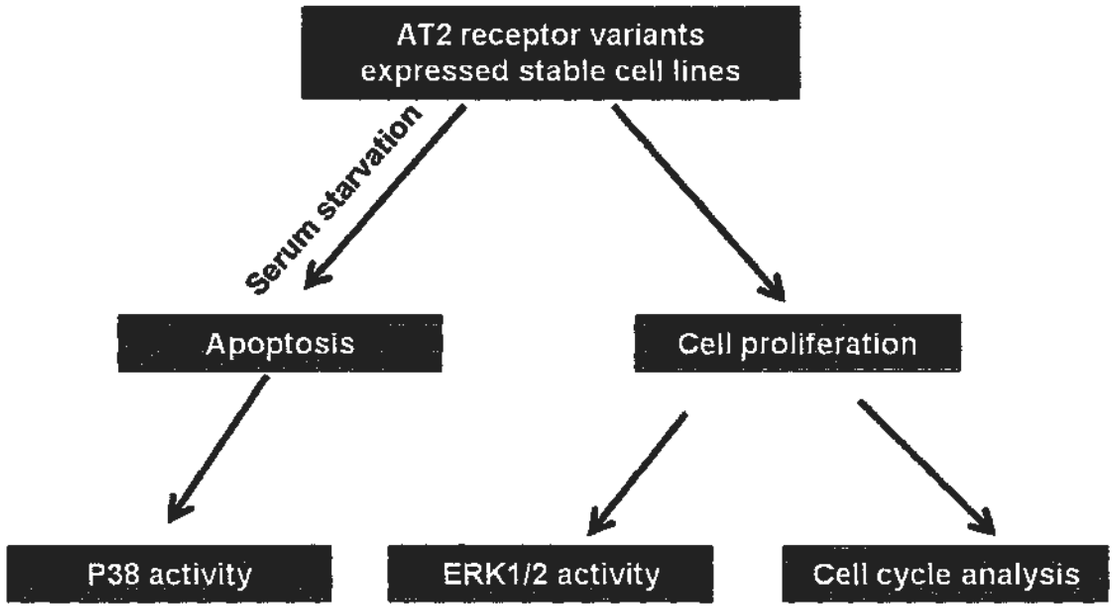

Figure 3.1 Experimental design of the constitutive activity of AT2

variants were constitutively active, cell cycle analysis and MAPK activities determination were performed to explain the underlying mechanisms.

Apoptosis, also called programmed cell death, is cell suicide. The progress of apoptosis is controlled by a diverse range of cell signals from extracellular or intracellular. Extracellular signals including hormones, growth factors, cytokines, toxins have to cross the membrane or transmit the signal through the membrane bound receptor. A series of cell stresses including radiation, heat, nutrient deprivation, hypoxia and viral infection, release the intracellular apoptotic signals. Apoptosis leads to cell morphology changes and eventually causes cell death. The morphological changes including membrane blebbing, nuclear chromatin condensation and DNA fragmentation are most commonly used criteria to characterize apoptosis (Wyllie, 2010). Proliferation of cells can be measured by BrdU incorporation, ^{3}H thymidine incorporation and cell counting. The former two methods reflect the rate of DNA synthesis while the last one directly reflects cell number change.

Mitogen-activated protein kinase (MAPK) are serine/threonine protein kinases which are activated through a sequential phosphorylation cascade and transduces signals from the cell membrane to the nucleus. They promote a large diversity of cellular fuctions in many cell types. Three major mammalian MAPK subfamilies have been described: the extracellular signal-regulated kinases 1 and 2 (ERK1/2), the c-Jun NH2-terminal kinases (JNK) and the p38 kinases. Generally speaking, JNK and p38 mediate cell death and

ERK1/2 promotes cell growth (Subramaniam and Unsicker, 2010). However the effects of MAPK could be quite different denpendent on the stimuli type, stimulation duration and cell types (Cagnol and Chambard, 2010).

The cell cycle is an ordered set of events in which a cell is duplicated and divided into two daughter cells. The cell cycle can be divided into two periods: interphase and mitosis (M phase). During interphase cell grows, synthesizes proteins and duplicates its DNA. In mitosis, both nuclear and cytoplasm division occur and a cell is divided into two distinct cells (Smith and Martin, 1973). The interphase is further divided into 3 phases: G1, S, and G2. The notable feature for G1 phase is synthesis of various enzymes required in S phase, mainly those needed for DNA duplication. In S phase DNA synthesis occurs and in the end all the chromosomes will be replicated. However during S phase protein synthesis is slowed down (Nelson et al., 2002). Then the cell enters G2 phase in which protein synthesis accelerates again, mainly for the proteins required in mitosis. There is also a quiescent phase called G0, in which cells leave the cell cycle and stop dividing. Regulation of cell cycle directly regulates cell proliferation (Maiato, 2010).

3.2 Materials

3.2.1 Chemicals

F12-Nutrient power (Cat.21700-075), Dulbecco's Modified Eagle Medium power (Cat.12100-046), F-12K Nutrient mixture (Kaighn's modification, Cat.21127-022), fetal bovine serum (Cat.10270-106), penicillin/streptomycin (Cat. 15140-122), 100 bp DNA marker, electrophoresis grade agarose were purchased from Invitrogen (Carlsbad, CA, USA). G418 sulfate was from Chemsonic (Germany). Nitrocellulose transfer membrane was from Whatman (Hahnestrabe 3, Dassel, Germany). Amersham ECL^{TM} Western Blotting Detection reagents were from G.E (Healthcare, UK). Medical X-ray film was from FUJI (Japan). Precision plus Protein Standards were from Bio-Rad (Berkeley, CA, USA). Yeast extract; Bacto Tryptone and agar Nobel were from B.D (Sparks, MD, USA). Protein A agarose, NBT/BCIP and Protease inhibitor cocktail tablets were from Roche (Roche Diagnostics Corporation, IN.USA). All other chemicals and reagents were from Sigma-Aldrich (St.Louis, MO, USA).

3.2.2 Enzymes

RNase was from Roche (Roche Diagnostics Corporation, IN.USA), proteinase K was purchased from Invitrogen (Carlsbad, CA, USA).

3.2.3 Kits and Instruments

Bicinchoninic Acid (BCA) protein assay kit was from Thermo (HK). Humidified cell culture incubator was from Thermo (HK). Quant microplate reader was from Bio-Tek

Instruments Inc (Winnoski, VT, USA). Vi-cell^{TM}XR viability analyzer was from Beckman coulter (Brea, CA USA). Flow cytometor was from B.D (Sparks, MD, USA).

3.2.4 Antibodies

Rabbit anti phospho-P38 antibody (Cat no. 9211), rabbit anti phospho-ERK1/2 (Cat no. 4370s) and rabbit anti ERK1/2 antibody (Cat no.4695) were from Cell Signaling Technology (Danvers, MA, USA).

3.3 Methods

3.3.1 DNA fragmentation

Stably transfected CHO cells (5×10^5 cells), PC12 cells (5×10^5 cells), HEK293 cells (1×10^6 cells) were seeded in a 60 mm dish and cultured at 37 °C in a humidified 5% CO_2 incubator for 3 days. Cell culture medium was replaced by serum-free medium (supplemented with 1% penicillin/streptomycin) and incubated with cells for another 72 hours. Cells were trypsinized and collected into a 15 ml falcon tube. After washed once with PBS solution, cells were lysed in a DNA lysis buffer (200 mM Tris, pH 8.3, 100 mM EDTA and 1% SDS) supplemented with 10 µl of proteinase K (10 mg/ml). Cell lysate was incubated in 50°C water bath for 2 hours and then mixed with 150 µl of 5 M NaCl. Cell lysate was shaken vigorously for 1 minute and centrifuged at 6500 g for 15 minutes. Supernatant was saved and mixed with 1 ml of ice cold absolute ethanol. The mixture was centrifuged at 15000 g for 20 minutes. DNA pellet was washed with 1 ml of ice cold 75% ethanol and centrifuged at 7000 g for a further 5 minutes. Supernatant was discarded and DNA pellet was air dried. Finally the pellet was dissolved in 60 µl of RNase A solution (0.2 mg/ml) and incubated in 37 °C water bath for 90 minutes. DNA fragmentation was shown on a 2% TAE agarose gel.

3.3.2 Phospho-p38 detection by western blot

Stably transfected CHO cells (1×10^5 cells), PC12 cells (2×10^5 cells), HEK293 cells (5×10^5 cells) were seeded in a well of 6-well plate and cultured at 37 °C in a humidified 5% CO_2 incubator for 3 days. Cell culture medium was replaced by serum-free medium

(supplemented with 1% penicillin/streptomycin) and incubated with cells for another 72 hours. Cells were trypsinized and collected into a 15 ml falcon tube. After washed with PBS solution once, the cells were lysed in 300 µl of RIPA buffer [0.1 M Tris pH 7.4, 150 mM NaCl, 1% sodium deoxycholate, 1% Triton X-100, 5 mM EDTA, 40 µl/ml of protease inhibitor cocktail (1 tablet in 2 ml of nano pure water as store solution), 2 mM PMSF and 1 mM Na_3VO_4]. Cell lysate were kept on ice for 15 minutes and centrifuged at 10621 g for 10 minutes. Supernatant was saved and protein concentration was determined by BCA assay as described in section 2.3.7. Sample buffer (4 ×, 30 µl) was added to 90 µl of supernatant and heated in boiling water for 10 minutes. Proteins were separated on 12% SDS-PAGE (14 cm ×16 cm). Western blot was performed as described in section 2.3.8. The immunoreative bands in western blots were digitalized using a flat-bed scanner (EPSON GT9500) and were quantified using UN-SCAN-IT software (Silk Scientific, Utah, USA). Band intensity was displayed as pixel values. Area with no immunoreactive bands was used as background control. Band intensity was calculated as (pixel target - pixel background). The differences of band intensities in each lane were analyzed with GraphPad Prism software (GraphPad Software, Inc, San Diego, CA, USA).

3.3.3 Cell proliferation determined by cell counting

Stably transfected CHO cells (1×10^5 cells), PC12 cells (5×10^5 cells), HEK293 cells (5×10^5 cells) were seeded in 60 mm dish and kept at 37 °C in a humidified 5% CO_2 incubator for up to 5 days. The day when cells were seeded was recorded as Day 0. On Day 5, cells were trypsinized and resuspended in respective culture medium. Then 500

μl of cell suspension were taken from each plate for counting using Beckman coulter Vi-cell^{TM}XR viability analyzer. Total cell number was calculated as cell concentration (reading) × cell suspension volume. Growth rate was calculated by dividing total cell number Day 5 by the number seeded on Day 0 (N_5/N_0). The difference of growth rate in different cell line was analyzed with GraphPad Prism software (GraphPad Software, Inc, San Diego, CA, USA).

3.3.4 Cell cycle analysis

Stably transfected PC12 cells (5×10^5 cells), HEK293 cells (1×10^6 cells) were seeded in 60 mm dish and cultured at 37 °C in a humidified 5% CO_2 incubator for 2 days. Cells were resuspended in 300 μl of PBS solution. Then 700 μl of ice-cold absolute ethanol was added to cell solution drop by drop and vortexes for several times. The mixture was kept at 4 °C for less than 7 days. After washed with PBS once, the cells were resuspended in 1 ml of PBS solution containing 8 μg/ml RNaseA and 40 μg/ml PI. The cell solution was incubated in 37 °C water bath for 20 minutes and kept in dark before analysis. FCS (voltage: 80) and SSC (voltage: 220) were recorded in log scale. PI A (voltage: 420) and PI W were recorded in liner scale. Data was analyzed with Graph Prism software (GraphPad Software, Inc, San Diego, CA, USA).

3.3.5 Phospho-ERK1/2 detection by western blot

Stably transfected PC12 cells (5×10^5 cells), HEK293 cells (5×10^5 cells) were seeded in a 60 mm dish and cultured at 37 °C in a humidified 5% CO_2 incubator for 3 days. Cells

were lysed and analyzed by western blot as described in section 3.3.2. Rabbit monoclonal anti phospho-ERK1/2 (1:2000 diluted) was incubated with the membrane at 4 °C overnight. Immunoreactive bands were detected with ECL detection system as described in section 2.3.8.

After phospho-ERK1/2 detection, the membrane was stripped by washing with a stripping buffer (14.35 ml acetic acid, 14.61g NaCl, added water to a final volume of 500 ml) for 30 minutes (10 minutes × 3 times). The membrane was then washed with water for 30 minutes (10 minutes × 3 times). After stripping, the membrane was incubated with rabbit monoclonal anti-ERK (1:1000 diluted) at 4 °C overnight. Other procedures were performed as described in section 2.3.8.

The immunoreative bands in western blots were digitalized using a flat-bed scanner (EPSON GT9500) and were quantified using UN-SCAN-IT software (Silk Scientific, Utah, USA). Band intensity was displayed as pixel values. Area with no immunoreative bands was used as background control. Band intensity was calculated as (pixel target-pixel background). Normalized ERK1/2 activity was calculated as (Band intensity of phospho-ERK1/2 divided by Band intensity of total ERK1/2). The differences of ERK1/2 phosphorylation in each cell line were analyzed with GraphPad Prism software (GraphPad Software, Inc, San Diego, CA, USA).

3.4 Results

3.4.1 AT2 receptor variants expression induced apoptosis

AT2 receptor displayed ligand independent apoptosis after serum starvation in AT2 receptor transfected cell lines, including CHO-K1 cells (Miura and Karnik, 2000a). In present study, apoptosis after serum starvation was determined by DNA fragmentation. Consistent to the report, DNA fragmentation exhibited in AT2 receptor variants stably expressing CHO cells (CHO-AT2-GFP and CHO-Myc-AT2) after 3 days serum-free culture but not in the respective empty vector control CHO cells. However, in PC12-Myc-AT2 cells and all AT2 receptor variants stably expressing HEK293 cells, no DNA fragmentation was seen (Figure 3.2). In PC12 and HEK293 cells, AT2 receptor-expressing cells were similar to the vector control cells in morphology and no DNA fragmentation was shown even cultured for 4~5 days in serum-free medium (data not shown).

In AT2 receptor-expressing cell lines, phospho-p38 MAPK was elevated and p38 inhibitor blocked AT2 receptor-induced apoptosis (Miura and Karnik, 2000a). P38 MAPK is a class of MAPK. Four isoforms of p38 MAPK has been identified: α, β, γ and δ. Once activated, p38 are phosphorylated at Thr180 and Tyr182. Expression of phospho-p38 was determined by western blot in present study. The antibody used here only detected the phosphorylated p38. Consistent with DNA fragmentation results, only in AT2 receptor-expressing CHO cells, phospho-p38 was increased (Figure 3.3).

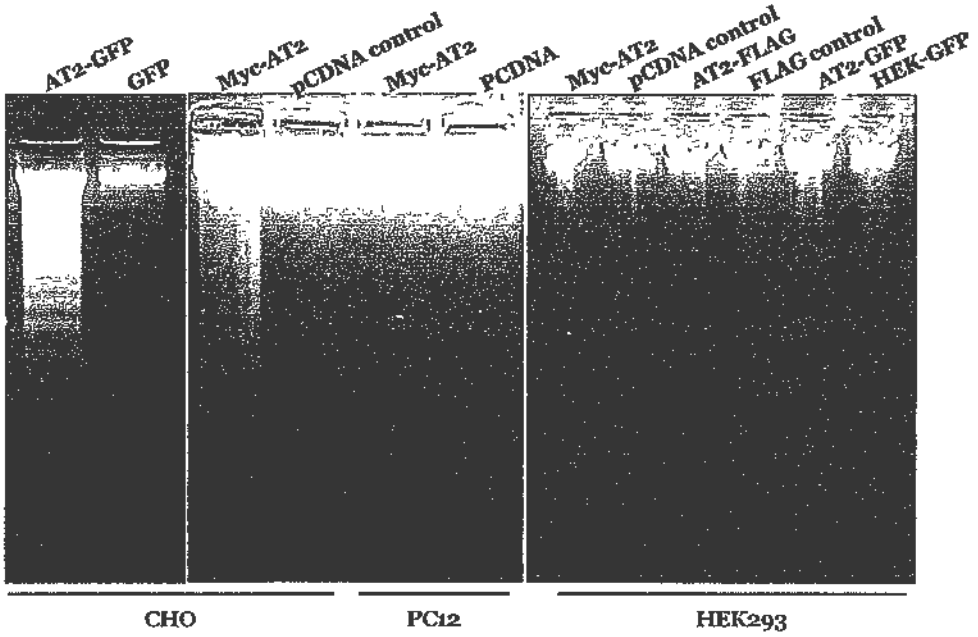

Figure 3.2 DNA fragmentation after serum starvation. AT2 receptor stably-expressing CHO cells (5×10^5), PC12 cells (5×10^5), HEK cells (1×10^6) and respective control cells were seeded on 60 mm dish and cultured for 72 hours. Then the cells were changed into serum-free medium and cultured for another 72 hours. Genomic DNA was extracted and analyzed on 2% TAE agarose gel. A, DNA of CHO and PC12 cells; B, DNA of HEK cells.

Figure 3.3 Phospho-p38 detection by western blot.

A, Stable cell lines of CHO cells (1×10^5), PC12 cells (2×10^5) and HEK293 cells (5×10^5) were seeded in 6-well plate and cultured for 3 days. Then the cells were cultured in serum-free medium for another 72 hours. Cells were lysed in RIPA buffer and protein concentration was quantified by BCA assay. Equal amount of proteins were analyzed on 12% SDS-PAGE and detected with an anti-phospho-p38 antibody.

B, The immunoreactive bands in western blots were digitalized using a flat-bed scanner and the UN-SCAN-IT$_{TM}$ software. Band intensity was calculated as described in Methods. Graph was created in GraphPad Prism software. Each symbol represented an individual cell line; each dot represented an individual experiment.

A

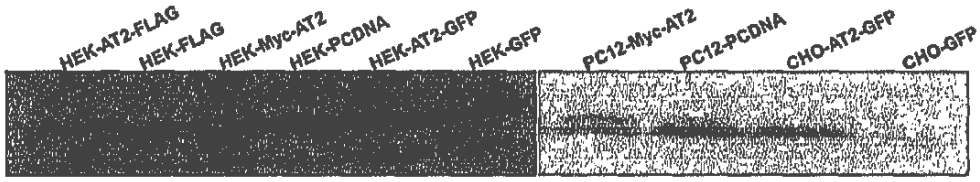
HEK-AT2-FLAG
HEK-FLAG
HEK-Myc-AT2
HEK-PCDNA
HEK-AT2-GFP
HEK-GFP
PC12-Myc-AT2
PC12-PCDNA
CHO-AT2-GFP
CHO-GFP

B

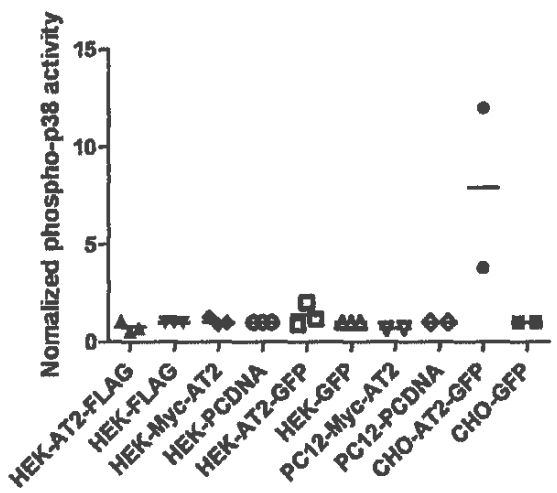
Nomalized phospho-p38 activity
15
10
5
0
HEK-AT2-FLAG
HEK-FLAG
HEK-Myc-AT2
HEK-PCDNA
HEK-AT2-GFP
HEK-GFP
PC12-Myc-AT2
PC12-PCDNA
CHO-AT2-GFP
CHO-GFP

3.4.2 AT2 receptor variants expression induced cell proliferation inhibition

3.4.2.1 Cell proliferation rate of AT2 receptor variants-expressing stable cell lines

Cell proliferation was determined by direct cell counting. The same type of cells were seeded on 60 mm dishes with the same cell number and cultured under the same condition (No ANGII in medium). Cells were counted on the Day5 using Beckman coulter Vi-cell TM XR cell viability analyzer. Cell proliferation rate was recorded as fold change of cell number.

Proliferation rate of HEK-AT2-GFP was significantly lower than that of HEK-GFP. In contrast there was no significant difference between CHO-AT2-GFP and CHO-GFP cells (Figure 3.4A). The proliferation rate of PC12-Myc-AT2, HEK-Myc-AT2 was also significant lower than that of respective vector control cells. However, there is no significant difference in proliferation between CHO-Myc-AT2 and CHO-PCDNA cells (Figure 3.4A). This indicated that AT2 receptor alone could induce cell proliferation inhibition in PC12 and CHO-K1 cells.

The growth inhibition was not reversed by PD123319, a common used AT2 antagonist, in HEK-Myc-AT2 cells (Figure 3.4 B). Besides no growth inhibition was observed in AT2 receptor-expressing CHO cells after ANGII treatment (Figure 3.4 B). It implied that the growth inhibition effect was not due to the cell endogenously-produced ANGII.

Figure 3.4 Cell proliferation of stably-transfected cell lines. Stably transfected CHO cells (1×10^5 cells), PC12 cells (5×10^5 cells) and HEK293 cells (5×10^5 cells) were seeded on 60 mm dish and cultured for up to 5 days. Cell number was counted using Beckman coulter Vi-cell TM XR cell viability analyzer. The original cell number was recorded as N0; cell number on day 5 was recorded as N5. Cell proliferation rate was recorded as fold change of N5/N0. Data was shown as mean ± SEM from 5 independent experiments. For comparison, T-test was used.

A, Stably transfected HEK293, CHO-K1 and PC12 stable cell lines were cultured for 5 days. * represents $p<0.05$

B, Stably transfected HEK293 cells were cultured for 5 days with 10 μM PD 123319 in medium; Stably transfected CHO-K1 were cultured for 5 days with 1 μM ANGII in medium. * represents $p<0.05$

A

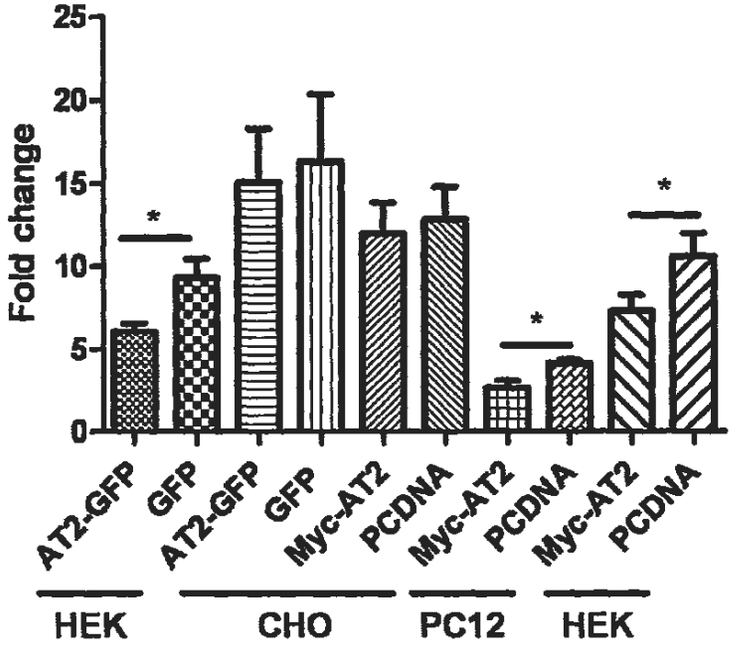
Fold change
25
20
15
10
5
0
*
*
*
AT2-GFP
GFP
AT2-GFP
GFP
Myc-AT2
PCDNA
Myc-AT2
PCDNA
Myc-AT2
PCDNA
HEK
CHO
PC12
HEK

B

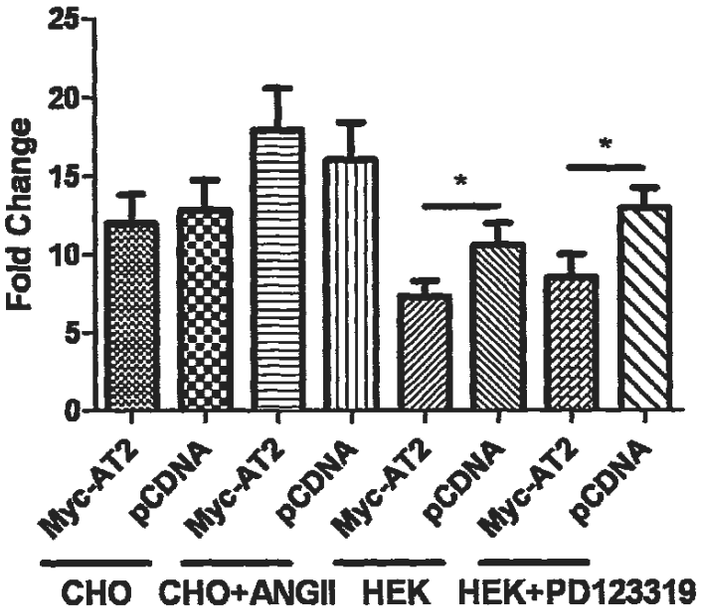
Fold Change
25
20
15
10
5
0
*
*
Myc-AT2
pCDNA
Myc-AT2
pCDNA
Myc-AT2
pCDNA
Myc-AT2
pCDNA
CHO
CHO+ANGII
HEK
HEK+PD123319

3.4.2.2 Cell cycle analysis of AT2 expressed cell lines

There are two possible reasons for proliferation inhibition: the cells grew slower or died more. Data from the Beckman coulter Vi-cell TM XR cell viability analyzer showed that the percentage of dead cells was similar between all AT2 receptor-expressing cells and respective control cells (data not shown). Besides, AT2 receptor-expressing HEK293 and PC12 cells did not undergo apoptosis even after serum starvation (Figure 3.2). Therefore the inhibition of proliferation In the present study was not due to cell death.

AT2 receptor expression inhibited cell growth and delayed cell cycle progression from G1 to S phase in AT2 receptor transfected rat fibroblast cells (Gingras et al., 2003). To figure out why AT2 receptor variants expressing HEK293 and PC12 cells grew slowly, cell cycle analysis was performed. Cells in exponential phase of proliferation were prepared as described in Methods. As shown in Figure 3.5, more AT2 receptor stably expressing HEK293 cells were found in G1 phase compared to empty vector control cells (Figure 3.5 A, B, C), which was consistent to that in transfected rat fibroblast cells. In contrast more AT2 receptor-stably transfected PC12 cells were found in S phase compared to vector control cells (Figure 3.5 D).

Figure 3.5 Cell cycle analyses. Stably transfected HEK cells (1×10^6) and PC12 cells (5×10^5) were seeded in 60 mm dish. After 2 days, cells were collected and fixed in ice cold ethanol. After RNase treatment and PI staining, the samples were subjected to flow cytometry analysis. Representative cell analysis graph of HEK-AT2-FLAG and respective control cells (A), HEK-AT2-GFP and GFP control cells (C), HEK-Myc-AT2 and respective control cells (E) and PC12-Myc-AT2 and respective control cells (G) were shown. In comparison with respective control cells, the percentages of each population was shown in panel B, D, F. Data was shown as mean±SEM from at least 4 independent experiments. * represents $p<0.05$; ** represents $p<0.01$; *** represents $p<0.001$.

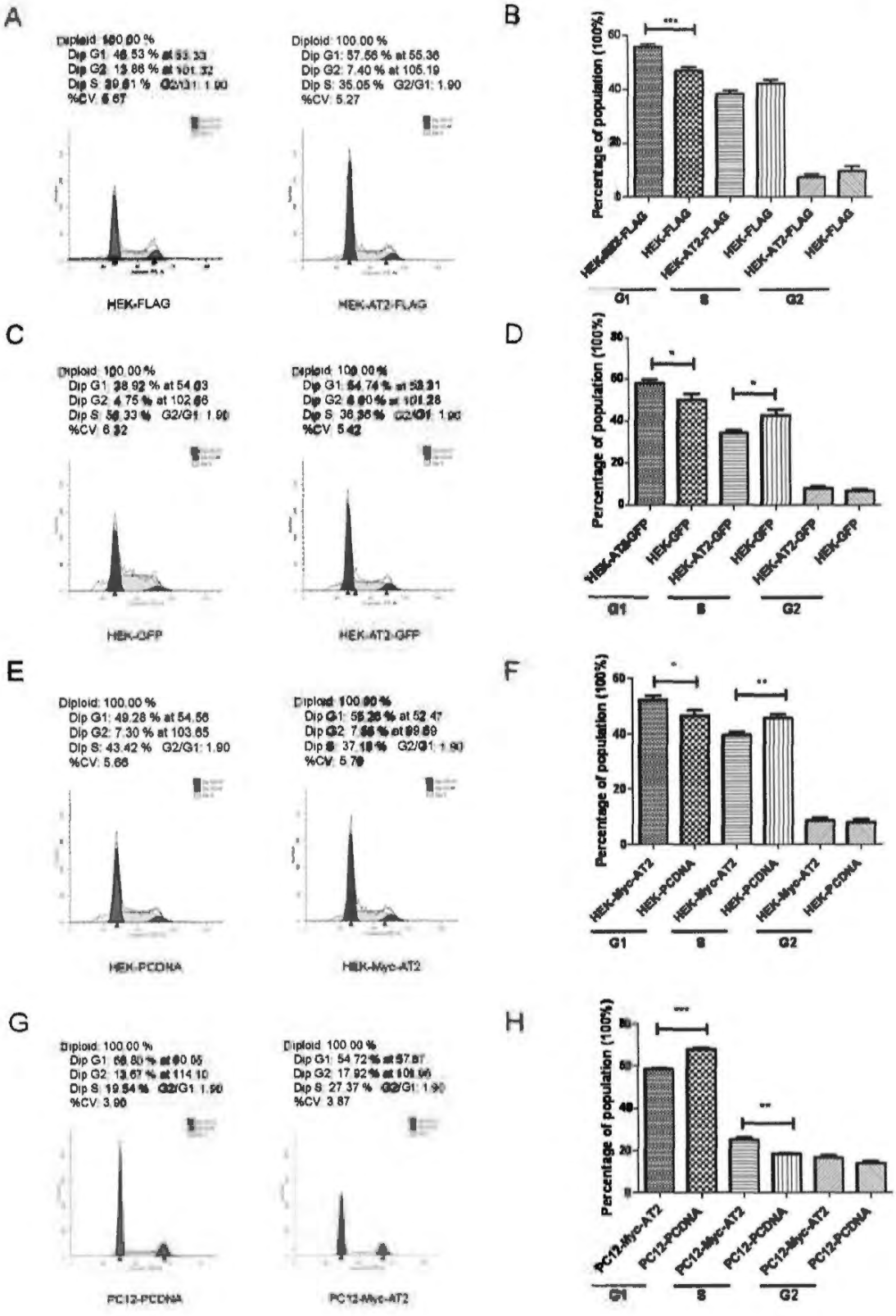
A
Diploid: 100.00 %
Dip G1: 57.56 % at 55.36
Dip G2: 7.40 % at 105.19
Dip S: 35.05 % G2/G1: 1.90
%CV: 5.27
HEK-FLAG
HEK-AT2-FLAG
B
Percentage of population (100%)
HEK-FLAG
HEK-AT2-FLAG
HEK-FLAG
HEK-AT2-FLAG
HEK-FLAG
G1
S
G2
C
Diploid: 100.00 %
Dip G1: 38.92 % at 54.03
Dip G2: 4.75 % at 102.66
Dip S: 56.33 % G2/G1: 1.90
%CV: 6.32
HEK-GFP
HEK-AT2-GFP
D
Percentage of population (100%)
HEK-GFP
HEK-AT2-GFP
HEK-GFP
G1
S
G2
E
Diploid: 100.00 %
Dip G1: 49.28 % at 54.56
Dip G2: 7.30 % at 103.65
Dip S: 43.42 % G2/G1: 1.90
%CV: 5.66
HEK-PCDNA
HEK-Myc-AT2
F
Percentage of population (100%)
HEK-Myc-AT2
HEK-PCDNA
HEK-Myc-AT2
HEK-PCDNA
G1
S
G2
G
Diploid: 100.00 %
Dip G1: 68.80 % at 90.05
Dip G2: 13.67 % at 114.10
Dip S: 19.54 % G2/G1: 1.90
%CV: 3.90
PC12-PCDNA
PC12-Myc-AT2
H
Percentage of population (100%)
PC12-Myc-AT2
PC12-PCDNA
PC12-Myc-AT2
PC12-PCDNA
G1
S
G2

3.4.2.3 Activity of ERK1/2 MAPK in AT2 receptor expressed cell lines

ERK1/2 (also known as p42/p44 MAPK) is the first elucidated member of MAPK. ERK1 is a 44 kDa protein while ERK2 is 42 kDa. The ERK cascade can be activated by various stimuli and regulates proliferation, differentiation, survival and apoptosis (Shaul and Seger, 2007). ERK1/2 activity is commonly analyzed by determining phosphorylated ERK1/2 with western blot. Although ERK1/2 was not involved in AT2 receptor mediated ligand independent apoptosis in CHO cells (Miura and Karnik, 2000a), down regulation of ERK1/2 in several types of cells contributed to the anti-growth effect of AT2 receptor (Cui et al., 2001).

To study the proliferation inhibition effect of AT2 receptor, ERK1/2 activity was determined in stable cell lines. In basal state, the level of phospho-ERK1/2 in HEK-Myc-AT2 and HEK-AT2-FLAG cells was similar to that of respective control cells. However, the level of phospho-ERK1/2 in HEK-AT2-GFP cells was higher than that in HEK-GFP cells. By contrast, the level of phospho-ERK1/2 was lower in PC12-Myc-AT2 compared to PC12-pCDNA control cells. There was no clue why the phosphorylation level of ERK1/2 was different in different cell lines (Figure 3.6).

Figure 3.6 ERK1/2 activity in stably-transfected cells. Stably transfected HEK293 cells (5×10^5 cells) and PC12 cells (5×10^5 cells) were seeded in a 60 mm dish and cultured for 3 days. The cells were lysed in RIPA buffer and protein concentration was measured by BCA kit.

A). Total cell lysate were analyzed on 10% SDS-PAGE and detected with anti-phospho-ERK1/2 antibody. Then the membrane was stipped and reprobed with anti-total-ERK antibody to confirm equal loading.

B). The immunoreactive bands in western blots were digitalized using a flat-bed scanner and the UN-SCAN-IT$_{TM}$ software. Normalized ERK1/2 activity was calculated as described in Methods. Graph was created in GraphPad Prism software. Each symbol represented an individual cell line; each dot represented an individual experiment.

A

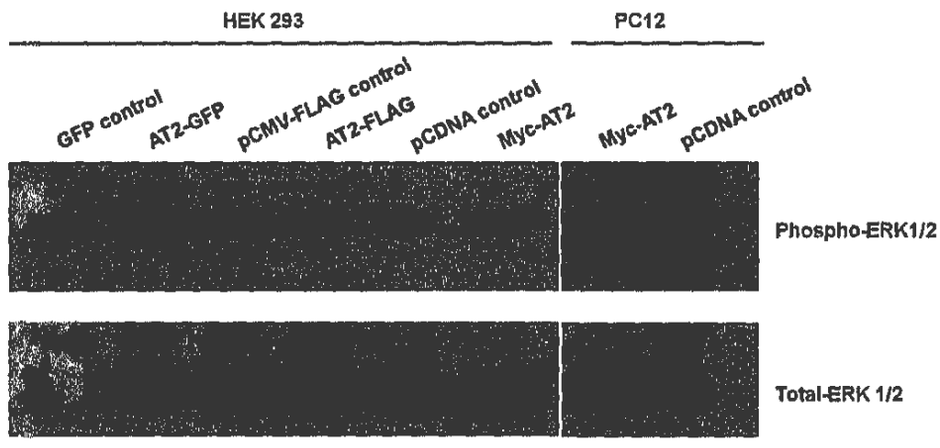
HEK 293
PC12
GFP control
AT2-GFP
pCMV-FLAG control
AT2-FLAG
pCDNA control
Myc-AT2
Myc-AT2
pCDNA control
Phospho-ERK1/2
Total-ERK 1/2

B

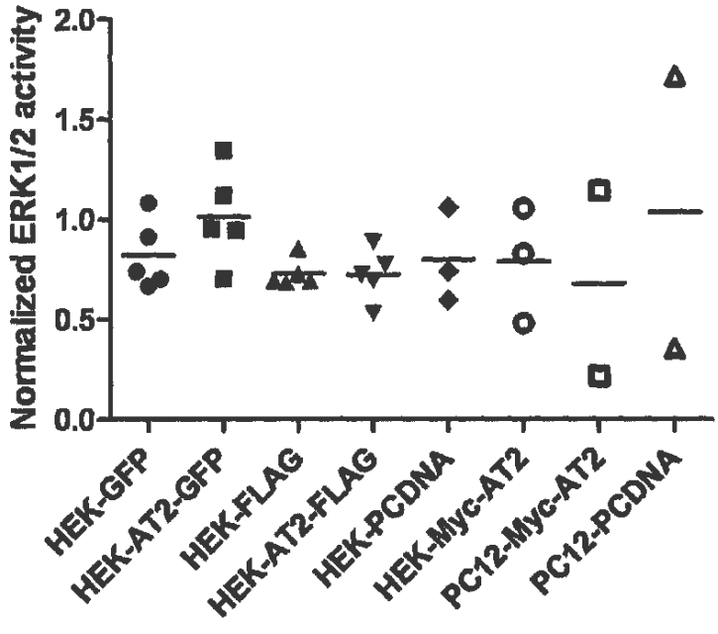
Normalized ERK1/2 activity
2.0
1.5
1.0
0.5
0.0
HEK-GFP
HEK-AT2-GFP
HEK-FLAG
HEK-AT2-FLAG
HEK-PCDNA
HEK-Myc-AT2
PC12-Myc-AT2
PC12-PCDNA

3.5 Discussion

It is commonly believed that AT2 receptor mediates anti-growth and pro-apoptotic effects (Lee et al., 2010b). However, the activities of AT2 receptor could be different depending on cell type and experimental condition. For example, in human coronary endothelial cells and human renal proximal tubule epithelial cells AT2 receptors mediated ANGII-induced apoptosis (Stoll et al., 1995; Weidekamm et al., 2002). In contrast, there is a very rare case that in cardiomyocytes AT2 receptor constitutive activation was shown to mediate proliferation (D'Amore et al., 2005). In immortalized cell lines, activities of AT2 receptors differed in different experiments depending on cell culture condition, such as serum and density of cultured cells (Horiuchi et al., 1999). For example ANGII/AT2 receptor has been proved to mediate either apoptosis or growth inhibition in PC12 cells in two independent reports (Meffert et al., 1996a; Yamada et al., 1996). In the present study AT2 receptor variants expressed in stable cell lines were constitutive active and the activities were also cell type dependent.

3.5.1 AT2 receptor-mediated apoptosis after serum starvation is cell type specific

ANGII/AT2 receptor-induced apoptosis has been reported in AT2 receptor endogenously expressed cell lines such as PC12W cells and R3T3 cells (Yamada et al., 1996), in AT2 receptor-transfected cells such as transfected vascular smooth muscle cells (Yamada et al., 1998) and in primary cultured cells from fetal tissue such as fetal vascular smooth muscle cells (Cui et al., 2001). It should be noted that in these experiments, cells were all serum starved before ANGII treatment. The possible reasons

for this could be: 1) serum starvation brings cells into quiescence which mimics the physiological condition in tissues; 2) serum starvation reduces interference of other hormones in serum; 3) as mentioned in the introduction, nutrient deprivation itself could introduce apoptosis. Combining with serum starvation, apoptotic effects of ANGII could be easier detected. For example, in presence of serum, it is almost impossible to detect the apoptosis in PC12W cells, R3T3 cells and transfected vascular smooth muscle cells (Yamada et al., 1998; Yamada et al., 1996). However, ANGII only is sufficient to induce apoptosis in primary cultured endothelial cells (Dimmeler et al., 1997; Lee et al., 2010a).

AT2 receptor also induced ANGII-independent apoptosis after serum starvation in R3T3 cells, AT2-EYFP transfected CHO-K1 cells and AT2-EYFP transfected A7r5 cells. In these cell lines serum deprivation triggered AT2 receptor to induce apoptosis and ANGII did not enhance the apoptosis (Miura and Karnik, 2000a). In present study, apoptosis after serum starvation was detected by DNA fragmentation. Consistent to the report, AT2 receptor variants stably-expressing CHO cells underwent ANGII independent apoptosis after serum starvation. In PC12 and HEK293 stable cell lines, no apoptosis was observed, even after a longer time of serum starvation. It indicated that the apoptosis effect was only dependent on cell type but not on the tag attached to the receptor.

The three cell lines used in previous literature report are all fibroblast cells: R3T3 are mouse fibroblast cell lines which endogenously express AT2 receptor (Servant et al.,

1994); CHO-K1 cells are derived from Chinese hamster ovary fibroblast cells; A7r5 cells are rat thoracic aorta-derived smooth muscle cells. In contrast PC12 cells are rat polygonal cells of adrenal gland while HEK 293 cells were human epithelial cells of embryo kidney. Whether AT2 receptor induced constitutive apoptosis is specific for fibroblast cells or not is unknown.

A specific conformation other than cell membrane expression was sufficient for ANGII independent apoptosis (Miura and Karnik, 2000a). In the present study both CHO-AT2-GFP and CHO-Myc-AT2 stable cells exhibited apoptosis after serum starvation which indicated that the AT2 receptor variants expressed in our cell system are the AT2 receptor of correct conformation.

3.5.2 AT2 receptor inhibited cell growth

It should be noted that apoptosis is considered to be an extreme form of anti-growth signaling (Miura and Karnik, 2000b). Therefore it is not surprising that growth inhibition was also reported in the cell lines which had been reported to undergo apoptosis. For example in AT2 receptor-transfected smooth muscle cells, PC12W cells and R3T3 cells, cell proliferation was reduced (Meffert et al., 1996b; Tsuzuki et al., 1996; Yamada et al., 1995). In all these studies, the cells were serum starved and treated with ANGII together with other growth factors such as epidermal growth factor (EGF),

basic fibroblast growth factor (bFGF). AT2 receptor inhibited cell proliferation induced by these growth factors.

However, serum starvation or even ANGII is not necessary for AT2 receptor mediated-growth inhibition. For example, in NG108-15 cells ANGII inhibited cell proliferation and promoted cell differentiation in presence of serum (Laflamme et al., 1996); cultured mesangial cells (MC) from normotensive Wistar-Kyoto rats (WKY) grew slower than MC from stroke-prone spontaneously hypertensive rats (SHRSP), in which AT2 expression was much lower than WKY rats (Goto et al., 1997); primary cultured fetal vascular smooth muscle cells (VSMC) from wild-type mice grew slower than VSMC from AT2 null mice (Akishita et al., 1999). In fact the latter two reports could be early evidences of constitutive activity of AT2 receptor. However, in these cells the effect of AT1 receptor and locally-produced ANGII still exist. In 2003 a research group stably expressed AT2 receptor in immortalized rat fibroblast cell line Rat1. They found that AT2 receptor inhibits cell growth in these cells and the growth inhibition was due to negative regulation on cell cycle progression from G1 phase to S phase. (Gingras et al., 2003)

In present study, in PC12 cells and HEK cells AT2 receptor expression inhibited cell growth as reported in transfected Rat1 cells. Cell cycle analysis indicated that a higher percentage of AT2-transfected HEK293 cells were found in G1 phase. It is also consistent to that of transfected Rat1 cells. However in PC12 cells, a higher percentage

of AT2-transfected cells were found in S phase. Both G1 phase arrest and S phase accumulation can cause cell growth inhibition. Why the same AT2 receptor induced different results of cell cycle analysis in PC12 and HEK cells is not clear. It is reported that FK778, a novel immunosuppressive agent, mediated growth inhibition either by leading to cell cycle arrest in G1 or cells accumulation in S phase. The differential response was linked to the phosphorylation status of a protein called pRb (Hoppe-Seyler et al., 2009). In present study, AT2 receptor variants may interact with different proteins in different cell types and subsequently resulted in different cell cycle arrest.

Inhibition of ERK 1/2 activity is commonly linked to ANGII/AT2 receptor-induced cell growth inhibition. It has been demonstrated that AT2 receptor inhibited activity of ERK1/2 through activation of protein phosphatases such as tyrosine phosphatase SHP-1 in N1E 115 cells, serine-threonine phosphatase PP2A in rat brain neuronal cultures, or MAPK phosphatase MKP1 in PC12W cells and R3T3 cells (Chamoux et al., 1999). Even in the ANGII-independent growth inhibition of cultured fetal VSMC, the effect of AT2 receptor was mediated through decreased ERK1/2 activity (Akishita et al., 1999). However there are also reports that AT2 receptor activates ERK1/2. For example, in AT2 receptor-endogenously expressed neuronal cell lines such as NG108-15 and PC12W cells, stimulation of AT2 receptor with ANGII induced a delayed but sustained activation of ERK1/2 (Beaudry et al., 2006). In AT2 receptor over-expressing COS7 and NIH3T3 cells, ANGII stimulation also activated ERK1/2 through AT2 receptors (De Paolis et al., 2002; Hansen et al., 2000).

In present study, ERK1/2 activity was increased in HEK-AT2-GFP cells but not in other AT2 receptor-expressing HEK293 cells. ERK1/2 activity was decreased in PC12-Myc-AT2 cells compared to vector control cells. This implicated that :1) ERK1/2 might be not involved in AT2 receptor-induced proliferation inhibition in these cell lines; 2) ERK1/2 indeed affected the cell growth in these cell lines, but the difference between different tagged AT2 receptor and different cell line is still unknown.

In summary AT2 receptor variants expressed in our stable cell lines are constitutively active. Data was consistent with previous reports from primary cultured and transfected cells.

Chapter 4

Co-immunoprecipitation to determine whether AT2 receptor was modified by SUMO and/or ubiquitin

4.1 Introduction

4.1.1 AT2 receptor and SUMO

SUMO protein was discovered in studies in nuclear import of RanGap1 (Matunis et al., 1996). Non-modified RanGap1 resides in cytosol and sumoylated one is associated with nuclear pore complex. Until now one of the most important functions for sumoylation is still cytosol/nuclear trafficking. Sumoylation also targets protein into specific region in nucleus, such as sumoylation on acute promyelocytic leukaemia protein (PML) (Duprez et al., 1999). However sumoylation is not just restricted to nuclear compartment, more and more membrane and cytosolic proteins have been discovered to be modified by sumoylation (Geiss-Friedlander and Melchior, 2007). The first reported sumoylated membrane protein was the K2P1 potassium-leak channel. Sumoylation on K2P1 is sufficient to silence the receptor. The plasma membrane voltage-gated potassium channel Kv1.5 and plasma membrane glutamate receptor 6 (GluR6) were sequentially found to be regulated through sumoylation (Geiss-Friedlander and Melchior, 2007). Sumoylated GluR6 regulated the receptor internalization into cytosol. A GPCR, metabotropic glutamate receptor 8 (mGluR8), also reported to be SUMOylated (Tang et al., 2005), but the function was unknown.

As described in Chapter 1 a putative sumoylation site was predicted in AT2 receptor by SUMOplot ^{TM} based on the consensus motif for sumoylation. In cell cultures and animal tissues AT2 receptor expressed mainly in cytosol and on cell membrane (de Godoy and Rattan, 2006). Normally activated AT2 receptor does not internalize into cytosol, but

there is a report claimed that AT2 receptor internalized into perinuclear region with PLZF after ANGII treatment (Senbonmatsu et al., 2003). Recently, nuclear AT2 receptor, which had a lower MW compared to membrane AT2 receptor, was discovered in sheep kidney (Gwathmey et al., 2009). There is a possibility that membrane expressed AT2 receptor is sumoylated and desumoylated form of AT2 receptor is able to internalize into cells and at last into nucleus.

Presence of consensus motif for sumoylation is not sufficient enough to indicate that a protein is sumoylated (Wilkinson et al., 2008). It is always demonstrated by co-expression and co-immunoprecipitation in cells. The stable cell lines expressing AT2 receptor variants had been established as described in Chapter 2. The next step was to express SUMO protein in those cell lines.

PHM6-HA-SUMO1 and pHMV6-HA-SUMO3 vector were kind gifts from Dr. Shannon Au. However in preliminary study, anti-HA antibody from Santa Cruz failed to pull down HA-tagged SUMO protein in immunoprecipitation. Thereafter a His_6 tag was added between the HA and SUMO protein. AT2-SUMO complex, if any, will be pulled down using Nickel-NTA agarose and specific anti-tag antibody. AT2 and SUMO proteins were detected by respective epitope tag antibody.

4.1.2 AT2 receptor and ubiquitin

Ubiquitination was traditionally linked to proteasomal degradation, but now is well known for other functions, such as signal transduction, endocytotic trafficking and DNA repair. More and more literature reports indicated that ubiquitin affected GPCR

internalization and downregulation. For example ubiquitin negatively regulates protease-activated receptor 1 (PAR1) internalization into cells (Wolfe et al., 2007). Ubiquitination on CXCR4 serves as a signal for endosome entry and in long term for down regulation of the receptor (Marchese, 2009).

Co-expression of a GPCR and a tagged ubiquitin construct in a heterologous expression system is commonly used to confirm receptor ubiquitination (Wojcikiewicz, 2004). Ubiquitination of the agonist-activated GPCR is detected by immunoprecipation and subsequent immunoblotting for the tagged-ubiquitin.

PHM6-HA-ubiquitin vector was also a kind gift from Dr. Shannon Au. After transient transfection, expression of ubiquitin were confirmed by immunofluorescence and western blot. Then immunoprecipitation was performed to confirm a tight association between AT2 receptor and ubiquitin.

MG132, a potent, membrane-permeable proteasome inhibitor, is commonly used in ubiquitination studies. Ubiquitinated protein is usually subjected to 26S proteasome for degradation. MG132 specially block the activity of the 26S proteasome and cause accumulation of ubiquitinated protein. Besides, both sumoylation and ubiquitination are dynamic process, so N-ethymaleimide (NEM), an inhibitor of deubiquitination and desumoylation enzymes, was included in all immunoprecipitation assays.

4.2 Materials

4.2.1 Chemicals

F12-Nutrient power (Cat.21700-075), Dulbecco's Modified Eagle Medium power (Cat.12100-046), fetal bovine serum (Cat.10270-106), penicillin/streptomycin (Cat. 15140-122), Lipofectomine 2000 (Cat. 11668-019), Ni-NTA agrose, all primers, dNTP, 1kb/1kb plus DNA marker, electrophoresis grade agarose were purchased from Invitrogen (Carlsbad, CA, USA). G418 sulfate was from Chemsonic (Germany). Nitrocellulose transfer membrane was from Whatman (Hahnestrabe 3, Dassel, Germany). Amersham ECL™ Western Blotting Detection reagents was from G.E (Healthcare, UK). Medical X-ray film was from FUJI (Japan). Precision Plus Protein Standards were from Bio-Rad (Berkeley, CA, USA). Yeast extract; Bacto Tryptone and agar Nobel were from B.D (Sparks, MD, USA). ProteinA agarose, NBT/BCIP and Protease inhibitor cocktail tablets were from Roche (Roche Diagnostics Corporation, IN.USA). MG132, NEM and all other chemicals and reagents were from Sigma-Aldrich (St.Louis, MO, USA).

4.2.2 Enzymes

Pfu DNA polymerase was from Promega (Madison, WI, USA). All restriction enzyme was from New England Biolabs (Beverley, MA, USA). T4 ligase was from Invitrogen (Carlsbad, CA, USA).

4.2.3 Kits and Instruments

Gel extraction kit was from G.E Healthcare (UK). Plasmid DNA purification kit was from INtRon (Korea). Bicinchoninic Acid (BCA) protein assay kit was from Thermo (HK). Humidified cell culture incubators was form Thermo (HK). TCS SP5 confocal microscope was from Leica (German). Quant microplate reader was from Bio-Tek Instruments Inc (Winnoski, VT, USA)

4.2.4 Antibodies

Mouse monoclonal (Cat.632381) and rabbit polyclonal anti-GFP antibody (Cat.632460) were from Clontech (Mountain View, CA, USA). Mouse monoclonal anti-Myc antibody (Cat. sc-40), mouse monoclonal anti-HA antibody (sc-7392) and mouse anti-ubiquitin antibody (sc-8017) were from Santa Cruz Biotechnology (CA, USA).

4.3 Methods

4.3.1 Construction of pHM6-HA-His_6-SUMO1 (or-SUMO3) expression vector

4.3.1.1 Amplify His_6-SUMO1 and His_6-SUMO3 fragments by PCR

His_6-SUMO1 fragment was amplified from pHM6-HA-SUMO1 vector with forward primer F1343 (5' TAT GGT ACC CAT CAT CAT CAT CAT CAT GCA GCT ATG TCT GAC CAG GAG GCA 3') and reverse primer F1344 (5' ATA AGA ATG CGG CCG CCT AAC CCC CCG TTT GT 3'). His_6-SUMO3 fragment was amplified from pHM6-HA-SUMO3 vector with forward primer F1345 (5' ATT GGT ACC CAT CAT CAT CAT CAT CAT GCA GCT ATG TCC GAG GAG AAG CC 3') and reverse primer F1346 (5' ATA AGA ATG CGG CCG CCT AAC CTC CCG TCT GCT GCT 3') Red characters represent His_6 tag and the underlined nucleotides were Kpn I and Not I restriction cutting sites in the corresponding primers. The PCR reaction was performed in a mixture containing 10× Pfu buffer (2.5 μl), 10 mM dNTP (1 μl), 10 μM primer (1 μl for each primer), pHM6-HA-SUMO1 (or-SUMO3) plasmid (10 ng) as template, 1 μl of Pfu DNA polymerase (2.5 U/μl) and nano pure water to a final volume of 25 μl. Applied Biosystems Elmer Gene Amp 9700 PCR machine was used to initiate the PCR reaction. After denaturing at 94 °C for 5 minutes, PCR reaction was running for 30 cycles with a denature temperature at 94 °C for 30 seconds, an annealing temperature at 56°C for 30 seconds, and an extension temperature at 72 °C for 30 seconds. Following extended incubation for 7 minutes at 72 °C, the mixture was kept at 4 °C.

4.3.1.2 Agarose gel electrophoresis and gel extraction of PCR products

Agarose gel electrophoresis and gel extraction of PCR products were performed as described in section 2.3.1.2 and 2.3.1.3.

4.3.1.3 Restriction enzyme digestion

After gel extraction, purified His_6-SUMO1 or His_6-SUMO3 fragments (~50 μg) was digested in a mixture containing 10 μl of 10× NEB buffer 2, 1 μl of 10 mg/ml BSA, 2 μl of Kpn I (20 U/ μl), 2 μl of Not I (20 U/ μl) in a final volume of 100 μl. The digestion was carried out at 37 °C overnight and confirmed by agarose gel electrophoresis. PHM6-HA-SUMO1 (or-SUMO3) vector (~50 μg) was digested by the same step as described above.

4.3.1.4 Ligation of His_6-SUMO1 or His_6-SUMO3 fragments into pHM6 vector

The vector and fragment were ligated at 1:3 (mol/mol) ratio. The size of pHM6 vector and His_6-SUMO1 (or-SUMO3) fragment are about 5.4 kb and 0.3 kb respectively. The ligation mixture consisted of 5× ligation buffer (4 μl) , T4 ligase (1U/μl) (1 μl) and solution of pHM6 vector and His_6-SUMO1 (or-SUMO3) fragment at a ratio of 1:3. Ligation was performed at 16°C water bath overnight. The vector map of PHM6-HA-His6-SUMO1/SUMO3 was shown in Figure 4.1.

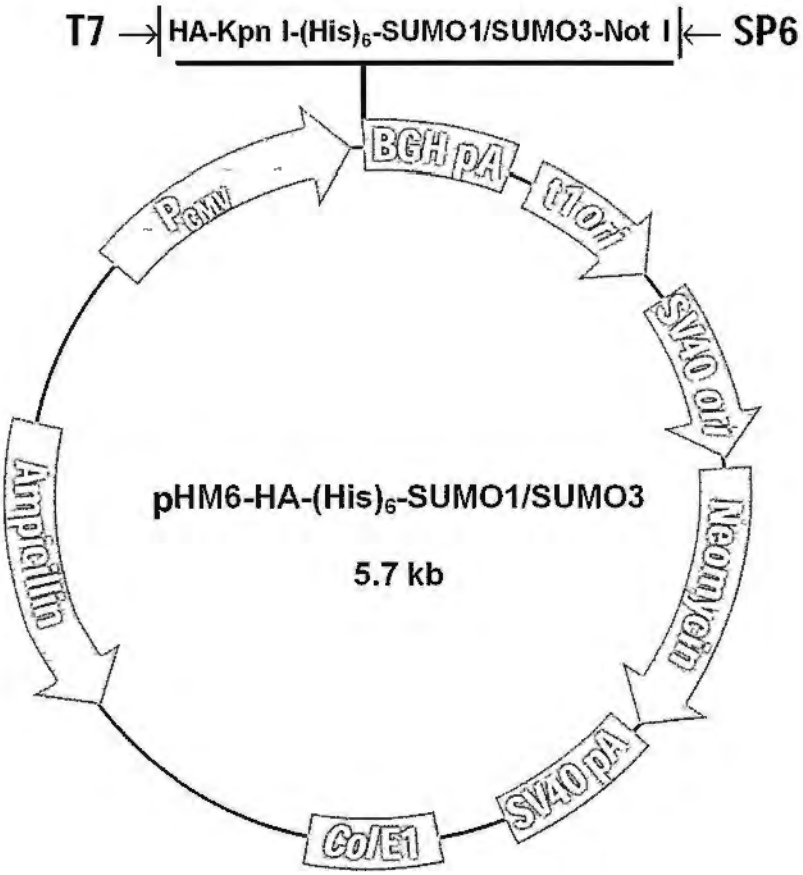

Fig 4.1 Vector map of pHM6-HA-His_6-SUMO1/SUMO3. The fragment of His_6-SUMO1/SUMO3 was amplified by PCR and inserted into Kpn I and Not I restriction cutting sites in pHM6-HA vector. SUMO expression was controlled by a CMV promoter. The expression vector encoded ampicillin and neomycin resistant gene for selection in bacteria or mammalian hosts. The vector map was modified form the vector map of pHM6-HA from Roche.

4.3.1.5 Bacteria transformation, mini-preparation of plasmid and DNA sequencing

Bacteria transformation, mini-preparation of plasmid and DNA sequencing were performed as described in 2.3.1.8, 2.3.1.9, 2.3.1.10.

4.3.2 Co-expression AT2 and SUMO/ubiquitin proteins in different cells

SUMO1 or SUMO3 expression vector was transiently transfected into AT2 receptor stably expressing cell lines with Lipofectamine 2000 as described in section 2.3.3.3. Tagged AT2 receptor stably expressing cells (2×10^6) were seeded on 100 mm dish and cultured at 37 °C until 80% confluence. During transient transfection, DNA and Lipofectamine 2000 were mixed at a ratio of 1:2. Usually, 5 μg of DNA and 10 μl of Lipofectamine 2000 mixture were added to the cells on 100 mm dish. When co-transfection was performed, 10 μg DNA (AT2 6 μg + SUMO/ubiquitin 4 μg) and 20 μl Lipofectamine 2000 were mixed and added to a 100 mm dish. Following 4 hours post-transfection, the medium was discarded and changed to fresh culture medium with 10% fetal calf serum.

4.3.3 Immunofluoresecence and confocal microscopy to detect SUMO1/3 expression in AT2 receptor-expressing cell lines

Indirected immunofluorescence and confocal microscopy was performed as described in section 2.3.6.1 and 2.3.6.2. GFP was excited at 488 nm by Ar/Kr laser and fluorescence was detected at 525±50 nm wavelength. CY3 (anti-HA detection for SUMO) was excited at 561 nm and red fluorescence was captured at 590 nm.

4.3.4 Immunoprecipitation

Immunoprecipitation was performed as described in 2.3.7. NEM was added to the RIPA buffer in a final concentration of 20 mM.

4.3.5 Nickel-NTA (NI-NTA) pull down under native condition

Usually, 24 hours after transfection, cells were harvested by scraper and washed by PBS solution once. The cell pellet was resuspended in 800 µl of a native binding buffer [50 mM NaH_2PO_4, pH 8.0, 0.5 M NaCl, 0.1% Triton, 0.2 mM PMSF, 1 mM Na_3VO_4, 40 µl/ml of protease inhibitor cocktail (1 tablet in 2 ml of nano pure water as store solution), 20 mM NEM (N-ethylmaleimide)]. The cells were frozen and thawed by putting into liquid nitrogen and 37 °C water bath for 5 cycles. DNA was broken down by passing through a 1 ml syringe needle. After centrifuged at 3000 g for 10 minutes, the supernatant of cell lysate was transferred to a new tube. Then 10 µl of the supernatant was taken out for BCA assay as described in section 2.3.7. NI-NTA agarose (50 µl) was added to the remaining supernatant of cell lysate and the mixture was shaken at 4°C overnight. Washing step lasted for 40 minutes (10 minutes × 4 times) by a native wash buffer (50 ml native binding buffer containing 335 µl of 3M imidazole, pH 8.0). NI-NTA agarose was collected by centrifuge at 800g for 1 minute. Then, 45 µl of native elution buffer (15ml native binding buffer containing 1.25ml of 3M imidazole, pH 8.0) was added to the agarose and kept on ice for 10 minutes. Finally 15 µl of 4 × sample buffer (8% SDS, 40% glycerol, 40µl/ml β-mercaptoethanol and 0.01% bromphenol blue in 200 mM Tris-HCl, pH6.8) was added to the pellet and boiled for 10 minutes. Protein sample was analyzed with SDS-PAGE and western blot as described in 2.3.8.

4.3.6 NI-NTA agarose pull down under denatured condition

Usually, 24 hours after SUMO transfection, cells were collected by scraper and washed once by PBS solution. The cell pellet was lysed in 1 ml of guanidinium lysis buffer (6 M guanidine hydrochloride, 20 mM sodium phosphate, pH 7.8, 500 mM NaCl) containing 40 µl/ml of protease inhibitor cocktail (1 tablet in 2 ml of nano pure water as stock solution) and 20 mM NEM. Cell lysate was sonicated at power 5 for 30 seconds and centrifuged at 3000 g for 15 minutes. Then 50 µl of NI-NTA agarose was added to cell lysate and kept shaken at 4°C overnight. The agarose was firstly washed by a denaturing binding buffer (8 M urea,20 mM sodium phosphate pH 7.8, 500 mM NaCl) for 20 minutes (10 minutes × 2 times) and then washed by a denaturing washing buffer (8 M urea, 20 mM sodium phosphate, pH 6.0, 500 mM NaCl) for 20 minutes (10 minutes × 2 times). Then 60 µl of denature elution buffer (8 M urea, 20 mM sodium phosphate, pH 4.0, 500 mM NaCl) and 20 µl of 4× sample buffer was added to the agarose. Sample was boiled for 10 minutes and analyzed with western blot as described in section 2.3.7.

4.3.7 Mouse embryo tissue preparation and immunoprecipitation with anti-AT2 antibody

Mouse embryo tissue preparation and immunoprecipitation with anti-AT2 antibody was performed as described in section 2.3.9.

4.4 Results

4.4.1 AT2 receptor and SUMO

4.4.1.1 Construction of pHM6-HA-His_6-SUMO1 (or-SUMO3) expression vector

According to the sequencing results in Figure 5.2 A and B, His_6 tag was successfully inserted between HA-tag and SUMO protein. DNA sequence was converted into protein sequence by translation software. The results also proved that the sequence was in correct reading frame (Figure 5.2 C, D). The calculated MW of HA-His_6-SUMO1 and HA-His_6-SUMO3 was 14.15 kDa and 14.23 kDa , respectively.

Figure 4.2 DNA sequence alignment and amino acid sequence of tagged SUMO1 and SUMO3

A). Multiple alignment of DNA sequence of HA-his$_6$-SUMO1. The sequence result of HA-his$_6$-SUMO1 was identical to human SUMO1 sequence, HA tag and 6×His tag. HA tag was shown with red box, 6×His tag was underlined with blue color. The start codon and stop codon were shown with black box. Other sequence in between was multiple cloning sites.

B). Multiple alignment of DNA sequence of HA-his$_6$-SUMO3. The sequence result of HA-his$_6$-SUMO3 was identical to human SUMO3 sequence, HA tag and 6×His tag. HA tag was shown with red box, 6×His tag was underlined with blue color. The start codon and stop codon were shown with black box. Other sequence in between was multiple cloning sites.

C). Amino acid sequence of HA-his$_6$-SUMO1. Blue color represents the amino acid sequence of HA tag; red color represents 6×His tag; green color represents the human SUMO1 protein. Additional amino acids in between (color in black) resulted from multiple cloning sites. The fusion protein contains totally 125 amino acids with a predicted MW 14.15 kDa using on ExPASy (http://au.expasy.org/tools/pi_tool.html).

D). Amino acid sequence of HA-his$_6$-SUMO3. Blue color represents the amino acid sequence of HA tag; red color represents 6×His tag; green color represents the human SUMO3 protein. Additional amino acids in between (color in black) resulted from multiple cloning sites. The fusion protein contains totally 127 amino acids with a predicted MW 14.23 kDa using on ExPASy (http://au.expasy.org/tools/pi_tool.html).

A


HA-His-SUMO1 ATGTACCCATACGACGTCCCAGACTACGCTGGAAGCTTGGGTACCCATCATCATCATCAT 60
SUMO1 ----------
HA-His-SUMO1 CATGCAGCTATGTCTGACCAGGAGGCAAAACCTTCAACTGAGGACTTGGGGGATAAGAAG 120
SUMO1 ---------ATGTCTGACCAGGAGGCAAAACCTTCAACTGAGGACTTGGGGGATAAGAAG 51
****
HA-His-SUMO1 GAAGGTGAATATATTAAACTCAAAGTCATTGGACAGGATAGCAGTGAGATTCACTTCAAA 180
SUMO1 GAAGGTGAATATATTAAACTCAAAGTCATTGGACAGGATAGCAGTGAGATTCACTTCAAA 111
****
HA-His-SUMO1 GTGAAAATGACAACACATCTCAAGAAACTCAAAGAATCATACTGTCAAAGACAGGGTGTT 240
SUMO1 GTGAAAATGACAACACATCTCAAGAAACTCAAAGAATCATACTGTCAAAGACAGGGTGTT 171
****
HA-His-SUMO1 CCAATGAATTCACTCAGGTTTCTCTTTGAGGGTCAGAGAACTGCTGATAATTCATACTCCA 300
SUMO1 CCAATGAATTCACTCAGGTTTCTCTTTGAGGGTCAGAGAACTGCTGATAATTCATACTCCA 231
****
HA-His-SUMO1 AAAGAACTGGGAATGGAGGAAGAAGATGTGATTGAAGTTTATCAGGAACAAACGGGGGGT 360
SUMO1 AAAGAACTGGGAATGGAGGAAGAAGATGTGATTGAAGTTTATCAGGAACAAACGGGGGGT 291
****
HA-His-SUMO1 CATTCAACAGTTTAG 375
SUMO1 CATTCAACAGTTTAG 306
****

B

C

```
  1   MYPYDVPDYA GSLGTHHHHH HAAMSDQEAK PSTEDLGDKK EGEYIKLKVI GQDSSEIHFK
 61   VKMTTHLKKL KESYCQRQGV PMNSLRFLFE GQRIADNHTP KELGMEEEDV IEVYQEQTGG
121   HSTV-
```

D

```
  1 MYPYDVPDYA GSLGTHHHHH HAAMSEEKPK EGVKTENDHI NLKVAGQDGS VVQFKIKRHT
 61 PLSKLMKAYC ERQGLSMPQI RFRFDGQPIN ETDTPAQLEM EDEDTIDVFQ QQTGGVPESS
121 LAGHSF-
```

4.4.1.2 SUMO1 and SUMO3 expression in AT2 receptor stably-expressing cell lines

CHO-AT2-GFP and GFP cell lines were firstly established and used for confirmation of sumoylation on AT2 receptor. PHM6-HA-His_6-SUMO1 (or-SUMO3) expression vector was transiently transfected into CHO-AT2-GFP or GFP cell lines. Expressed SUMO proteins were concentrated by NI-NTA agarose pull down assay and detected with anti-HA antibody in western blot (Figure 4.3). SUMO3 expressed well in CHO-AT2-GFP and GFP vector control cells with a molecular weight of about 15 kDa. However, SUMO1 expression was only detected in CHO-GFP cell lines but not in CHO-AT2-GFP cells. This was also confirmed by the lack of fluorescent signal in CHO-AT2-GFP cells stained with anti-HA and anti-CY3 conjugated secondary antibody (Figure 4.4). Somehow SUMO1 expression was inhibited in CHO-AT2-GFP cells which made CHO-AT2-GFP impropriate for the following interaction study. Then SUMO1 was transiently transfected into HEK-AT2-GFP and GFP cells. From immunofluorescence results (Figure 4.4), SUMO1 expression was not affected in HEK-AT2-GFP cells. In western blot SUMO1 also expressed as a 15 kDa protein in both CHO and HEK cells.

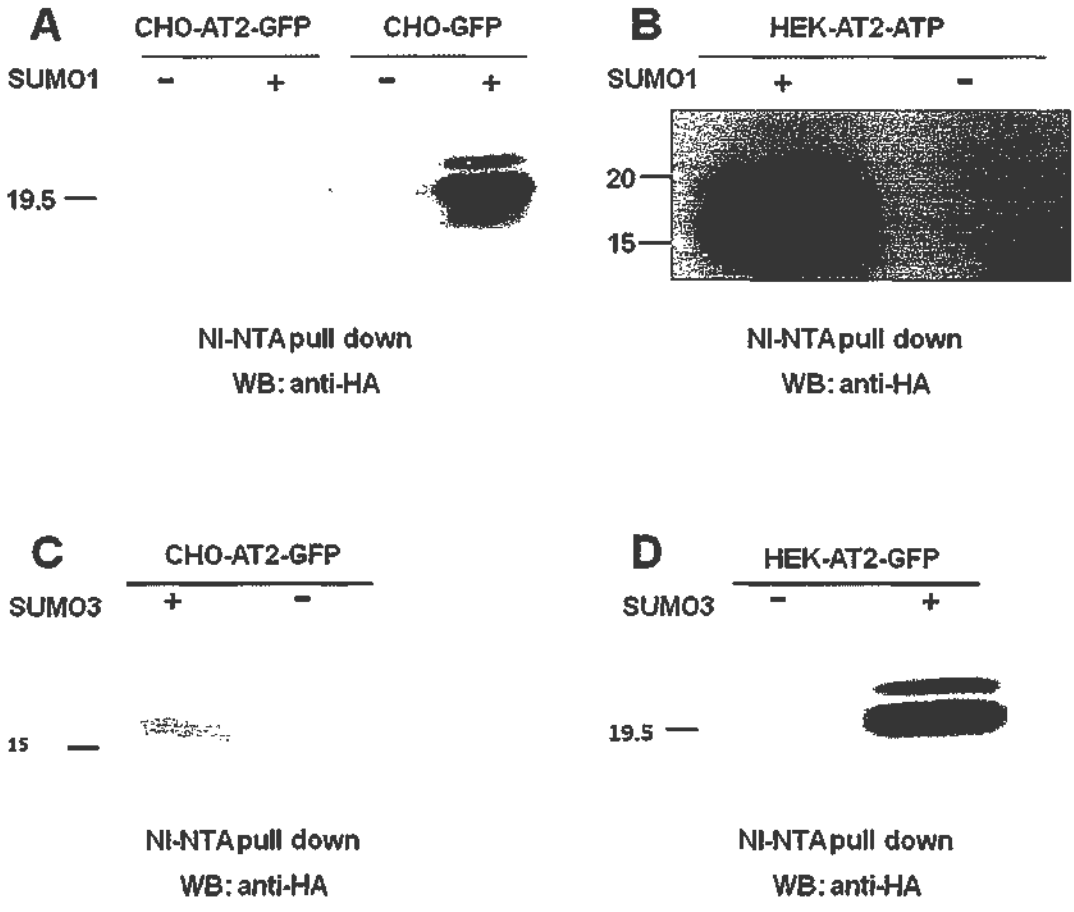

Figure 4.3 SUMO1 and SUMO3 expression detected by western blot. For pull down assay, 5 μg of pHM6-HA-His_6-SUMO1 (A, B) or 5 μg of pHM6-HA-His_6-SUMO3 (C, D) plasmid was transiently transfected into a 100 mm dish with stable cell lines at 90% confluence. After 24 hours, NI-NTA agarose pull down assay under native condition was performed. Precipitated samples were analyzed on 15% SDS-PAGE. SUMO expression was detected with anti-HA antibody in western blot.

Figure 4.4 SUMO1 expression detected by immunofluorescent confocal microscopy. PHM6-HA-$(His)_6$-SUMO1 plasmid (2μg) was transiently transfected into CHO-AT2-GFP (A), CHO-GFP (B), HEK-AT2-GFP (C) and HEK-GFP (D) stable cell lines. Cells were fixed with 4% paraformaldehyde. SUMO1 was labeled with anti-HA primary antibody and then detected with CY3 conjugated secondary antibody. GFP and CY3 were excited at 488 nm and 561 nm, respectively. Green and red fluorescence were collected sequentially. The merge image shows the overlapped images of GFP and CY3. Scale bar is 50 μm.

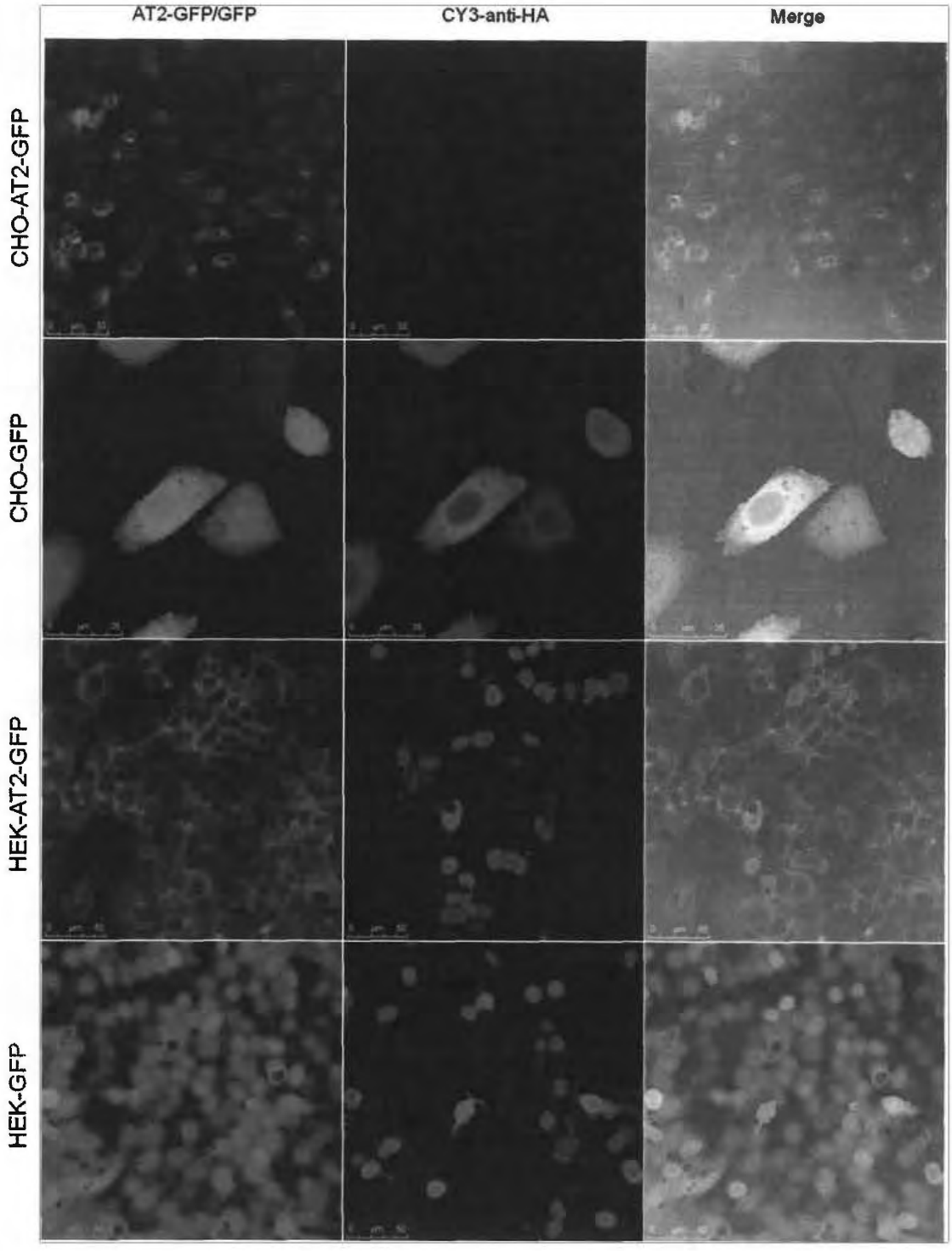
AT2-GFP/GFP
CY3-anti-HA
Merge
CHO-AT2-GFP
CHO-GFP
HEK-AT2-GFP
HEK-GFP

4.4.1.3 Interaction between AT2 receptor and SUMO1

Interaction between AT2 receptor and SUMO1 was initially examined by transiently transfecting HEK-Myc-AT2 stable cells with SUMO1 expressing construct. For co-transfection study, wild-type HEK293 cells was co-transfected with pCMV-Myc-AT2 and pHM6-HA-His_6-SUMO1 plasmid at the same time. In both condition, Myc-AT2 was precipitated with anti-Myc antibody and precipitated sample was detected with anti-HA antibody. Nothing but heavy chain and light chain of antibodies was detected by mouse anti-HA antibody (Figure 4.5 A). However, under the same condition, Myc-AT2 was successfully precipitated as indicated by the staining of anti-Myc antibody (Figure 4.5 B).

On the other hand, SUMO1 transiently transfected HEK-AT2-GFP was subjected to immunoprecipitation with an polyclonal anti-GFP antibody. Still no specific staining was detected in western blot using anti-HA antibody (Figure 4.5 C). Similarly, AT2-GFP was successfully precipitated as shown the strong immunoreactive bands with anti-GFP antibody (Figure 4.5 D).

In both HEK-Myc-AT2 and HEK-AT2-GFP stable cell lines, the cells were treated with ANGII after SUMO1-transfection. However, ANGII failed to induce interactions between AT2 receptor and SUMO1.

Figure 4.5 Interaction between AT2 receptor and SUMO1 detected by co-immunoprecipitation.

A,B). For Myc-tagged AT2 receptor, 5 μg plasmid of pHM6-HA-His_6-SUMO1 was transiently transfected into HEK-Myc-AT2 stable cell lines in a 100 mm dish. In co-transfection, 4 μg plasmid of pHM6-HA-His_6-SUMO1 and 6 μg of pCMV-Myc-AT2 were cotransfected into a 100 mm dish with wild type HEK cells. After transfection for 48 hours, HEK-Myc-AT2 stable cell lines were treated with or without 1 μM ANGII for 20 minutes. Cells were lysed in a RIPA buffer and precipitated with anti-Myc antibody. Precipitated samples were separated on 10% SDS-PAGE and detected with anti-HA antibody in western blot (A). After detection with anti-HA antibody, the membrane was stripped and reprobed with anti-Myc antibody (B).

C,D). For GFP tagged AT2 receptor, 5 μg plasmid of pHM6-HA-His_6-SUMO1 was transiently transfected into HEK-AT2-GFP stable cell lines on a 100 mm dish. After transfection for 48 hours, the cells were treated with or without 1 μM ANGII for 20 minutes. Cells were lysed in a RIPA buffer and precipitated with polyclonal anti-GFP antibody. Precipitated samples were separated on 10% SDS-PAGE and detected with anti-HA antibody in western blot (C). After detection with anti-HA antibody, the membrane was stripped and reprobed with monoclonal anti-GFP antibody (D).

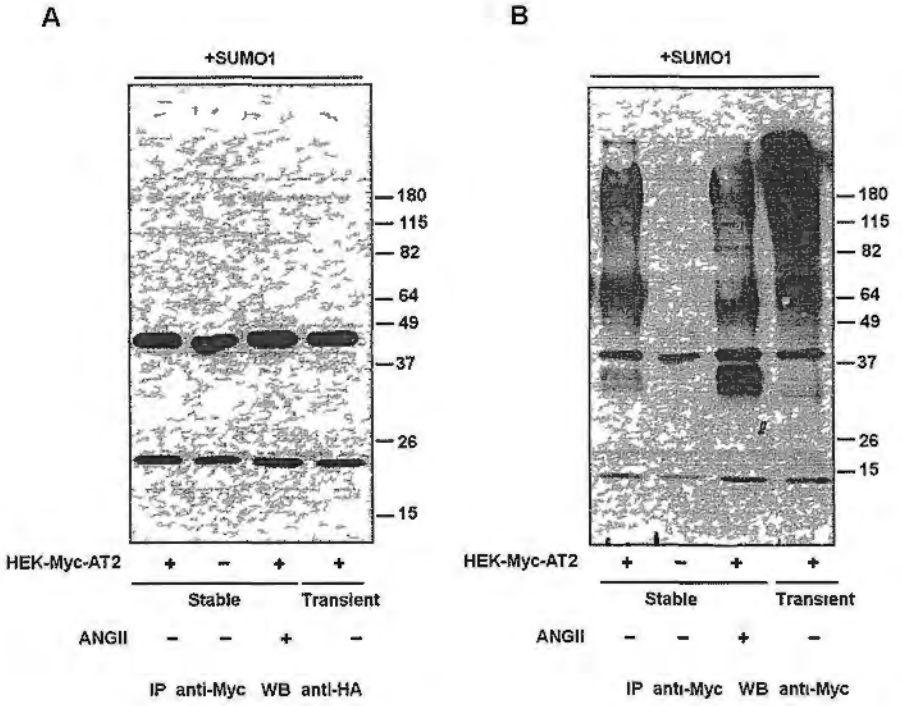
A
+SUMO1
180
115
82
64
49
37
26
15
HEK-Myc-AT2 + − + +
Stable
Transient
ANGII − − + −
IP anti-Myc WB anti-HA
B
+SUMO1
180
115
82
64
49
37
26
15
HEK-Myc-AT2 + − + +
Stable
Transient
ANGII − − + −
IP anti-Myc WB anti-Myc

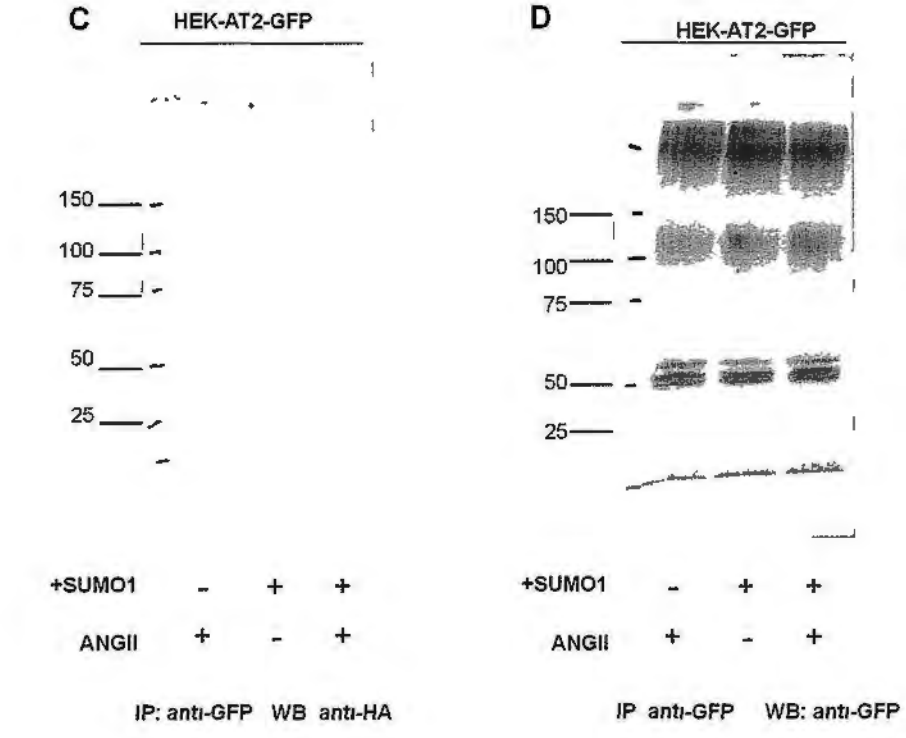
C
HEK-AT2-GFP
150
100
75
50
25
+SUMO1 − + +
ANGII + − +
IP: anti-GFP WB anti-HA
D
HEK-AT2-GFP
150
100
75
50
25
+SUMO1 − + +
ANGII + − +
IP anti-GFP WB: anti-GFP

4.4.1.4 Interaction between AT2 and SUMO3

SUMO3 expressed normally in CHO-AT2-GFP cell lines so SUMO3 transiently expressed in CHO-AT2-GFP was examined first. PHMV-HA-His_6-SUMO3 was transient transfected into CHO-AT2-GFP cells. AT2-GFP was precipitated with a polyclonal anti-GFP antibody. However, no specific staining was detected by anti-HA antibody in the precipitated samples (Figure 4.6). Under the same condition AT2-GFP was successfully precipitated detected by anti-GFP antibody (Chapter 2, Figure 2.10). SUMO3 was then transiently expressed in HEK-Myc-AT2 stable cell lines or transiently co-transfected with pCMV-Myc-AT2 into wild-type HEK cells. In both condition, no specific bands were seen in western blot after immunoprecipitation with an anti-Myc antibody (Figure 4.6).

Figure 4.6 Interaction between AT2 receptor and SUMO3 detected with immunoprecipitation.

A). For Myc tagged AT2 receptor, 5 μg plasmid of pHM6-HA-His_6-SUMO3 was transiently transfected into HEK-Myc-AT2 stable cells on a 100 mm dish. For co-transfection, 4 μg plasmid of pHM6-HA-His_6-SUMO3 and 6 μg of pCMV-Myc-AT2 were co-transfected into 100 mm dish of wild type HEK cells. After transfection for 48 hours, HEK-Myc-AT2 stable cells were treated with or without 1μM of ANGII for 20 minutes. Cells were lysed in RIPA buffer and precipitated with an anti-Myc antibody. Precipitated samples were separated on 10% SDS-PAGE and detected with anti-HA antibody in western blot

B). For GFP tagged AT2 receptor, 5 μg plasmid of pHM6-HA-His_6-SUMO3 was transiently transfected into CHO-AT2-GFP stable cells in 100 mm dish. After transfection for 48 hours, cells were lysed in RIPA buffer and precipitated with polyclonal anti-GFP antibody. Precipitated samples were separated on 10% SDS-PAGE and detected with anti-HA antibody in western blot .

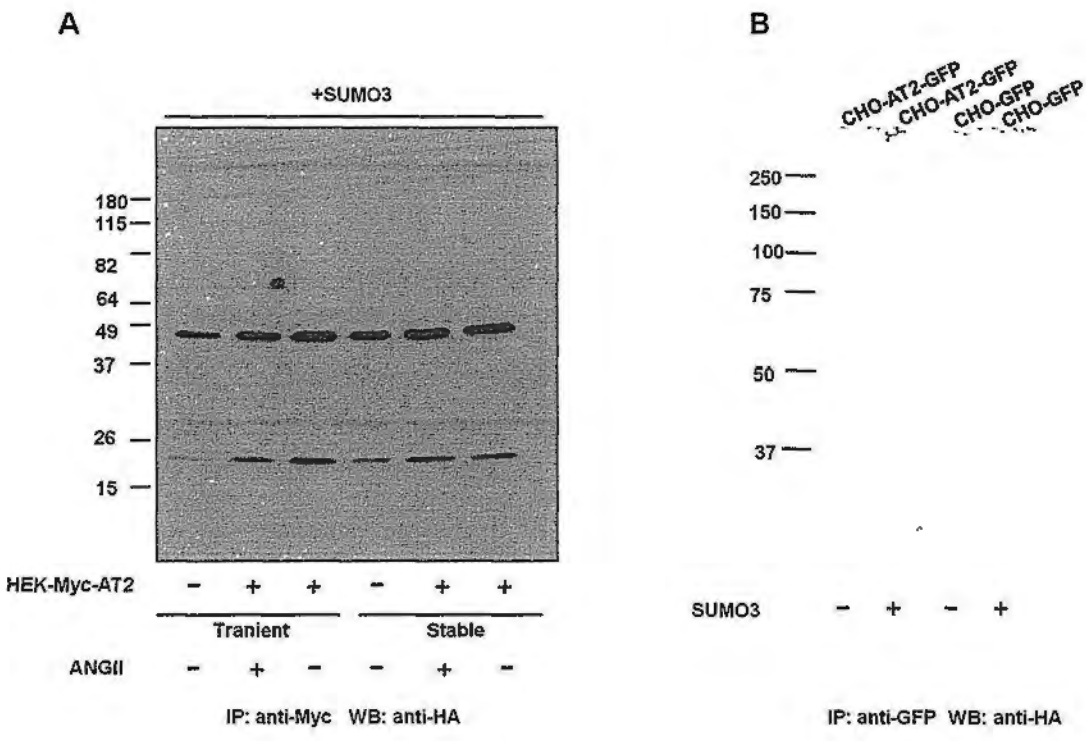
A
+SUMO3
180
115
82
64
49
37
26
15
HEK-Myc-AT2 - + + - + +
Tranient
Stable
ANGII - + - - + -
IP: anti-Myc WB: anti-HA
B
CHO-AT2-GFP
CHO-AT2-GFP
CHO-GFP
CHO-GFP
250
150
100
75
50
37
SUMO3 - + - +
IP: anti-GFP WB: anti-HA

4.4.1.5 Interaction between AT2 and SUMO3 detected by NI-NTA agarose pull down

Since a 6×His tag was added between HA-tag and SUMO protein, NI-NTA agarose pull down assay was also performed to confirm whether AT2 receptor was modified by SUMO3 protein. PHMV-HA-His_6-SUMO3 was transiently expressed in CHO-AT2-GFP and CHO-GFP stable cells. SUMO3 and SUMOylated protein were concentrated with Ni-NTA agarose under both native and denatured condition. Under native condition, non-specific binding was found in both SUMO3 transfected cells and non-transfected cells (Figure 4.7 A). It might be due to none specific binding on the Nickel agarose. Under denatured condition, no specific binds were shown in western blot (Figure 4.7 C). To prove the method is workable, P53 which has been proved modified by SUMO1 was used as a control (Figure 4.7 B).

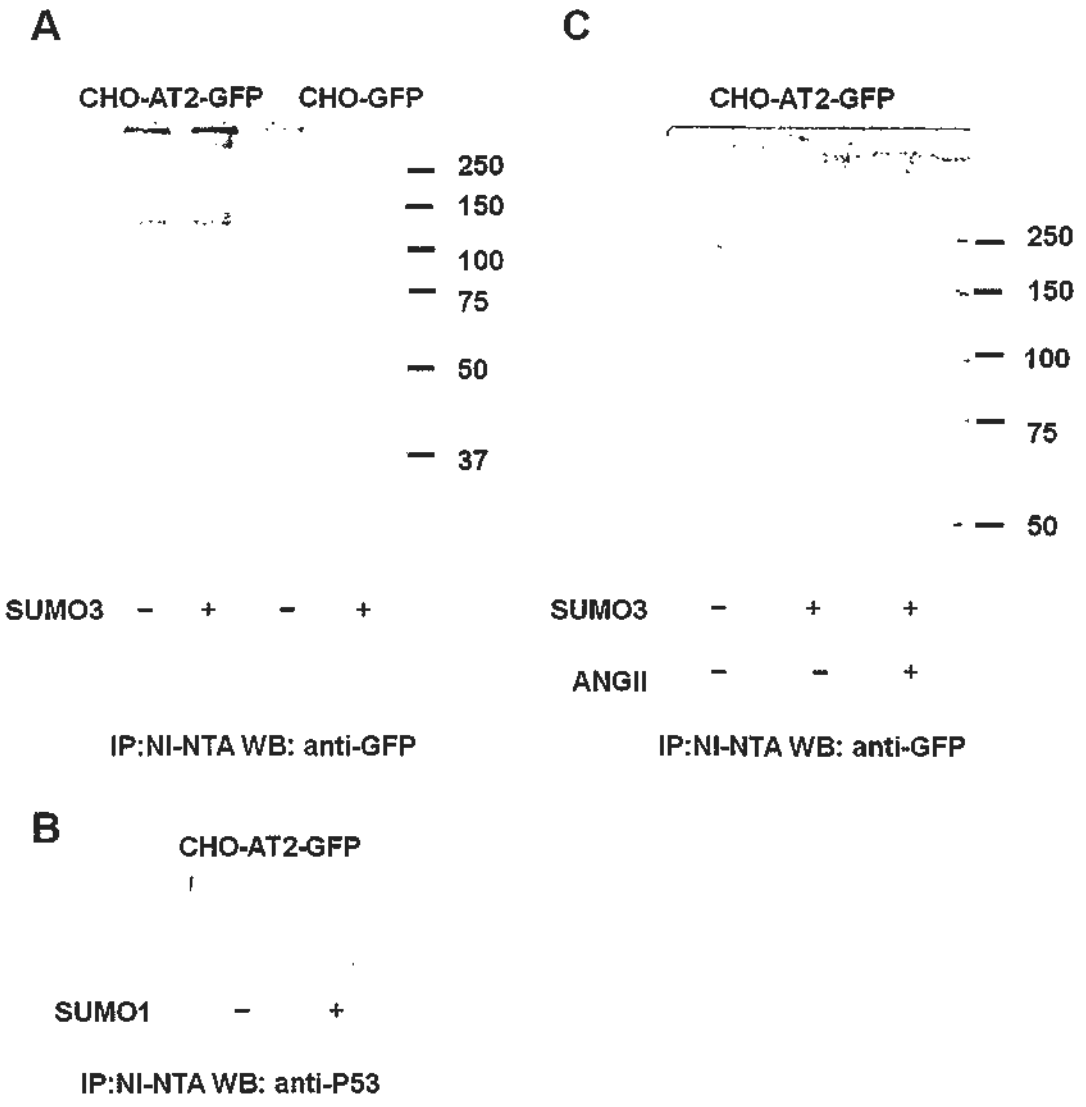

Figure 4.7 Interaction between AT2 receptor and SUMO3 detected by NI-NTA agarose pull down assay. Plasmid of pHMV-HA-His_6-SUMO3 was transiently transfected into CHO- AT2-GFP and GFP stable cells in a 100 mm dish. After transfection for 48 hours, the cells were lysed in RIPA buffer and precipitated by Ni-NTA agarose under native (A) or denatured (C) conditions. Samples prepared under native condition were immunoblotted with anti-P53 as a system control (B).

4.4.2 AT2 receptor and ubiquitin

4.4.2.1 Ubiquitin expression

Expression of ubiquitin was detected by western blot and immunofluorescent confocal microscopy. PHMV6-HA-ubiquitin was transiently transfected into HEK-Myc-AT2 and empty vector control cells. Total cell lysate was analyzed by western blot (Figure 4.8 A). An immunoreactive band close to the predicted MW of HA-ubiquitin (12.5 kDa) was detected in both cell lines which implied that ubiquitin expression was not affected by AT2 receptor expression. Immunofluorescence staining was also performed when pHMV6-HA-ubiquitin was transiently transfected into HEK293 cells. HA-ubiquitin mainly expressed in cytosol of HEK cells (Figure 4.8 B).

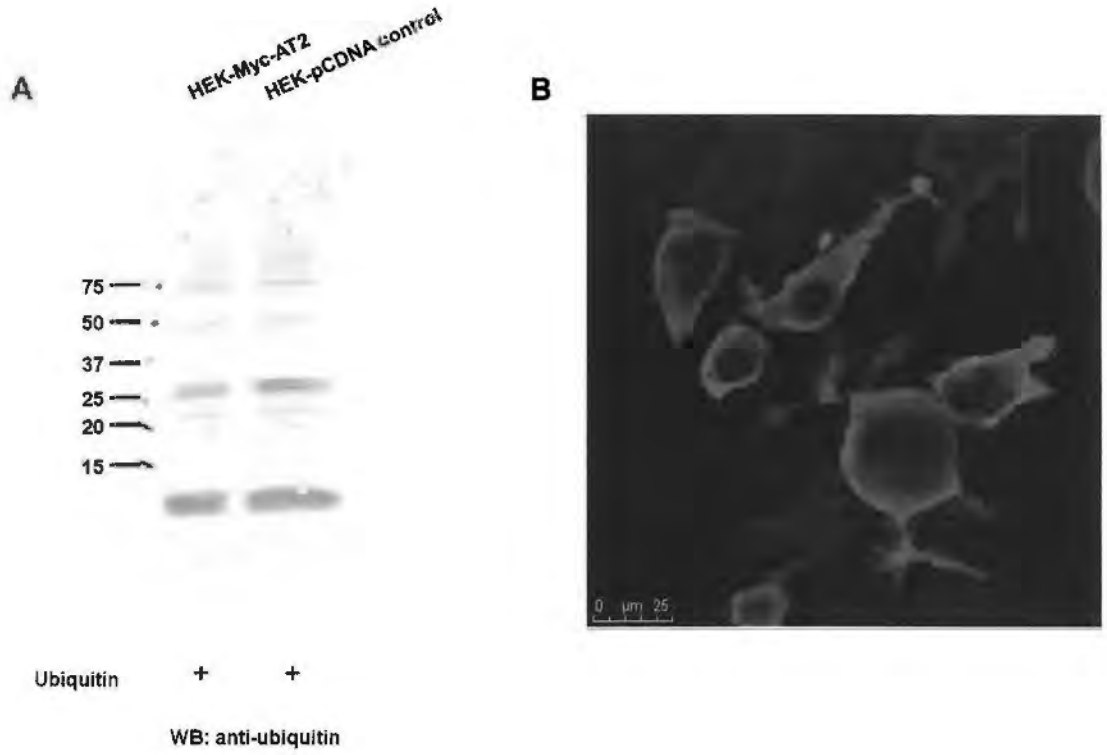

Figure 4.8 Ubiquitin expression detected by western blot and confocal imaging.

A). PHMV6-HA-ubiquitin (5 µg) was transiently transfected into a 100 mm dish of HEK-Myc-AT2 or empty vector control cells. Cells were lysed in RIPA buffer and boiled for 10 minutes. Total cell lysate were separated on 15% SDS-PAGE and detected with anti-ubiquitin antibody.

B). PHMV6-HA-ubiquitin (2 µg) was transiently transfected into wild-type HEK 293 cells seeded on a 25 mm coverslip. Ubiquitin expression was revealed with an anti-HA antibody and FITC-conjugated secondary antibody using confocal microscopy.

4.4.2.2 Interaction between AT2 receptor and Ubiquitin

Myc-AT2 expressing constructs and HEK293 cells were firstly used for examining the the interaction between AT2 and ubiquitin. PHMV6-HA-ubiquitin was transiently transfected into HEK-Myc-AT2 stable cells. Alternatively, pCMV-Myc-AT2 and pHM6-HA-ubiquitin plasmid were co-transfected into wild type HEK293 cells at the same time. In both conditions, Myc-AT2 was precipitated with an anti-Myc antibody and precipitated sample was detected with anti-HA antibody. Surprisingly, Myc-AT2 was detected to be modified by ubiquitin only in co-transfection system but not in HEK-Myc-AT2 stable cell lines (Figure 4.9 A). Myc-AT2 was successfully pulled down under the same condition reflected by anti-Myc antibody staining on the same membrane (Figure 4.9 B).

AT2-GFP was also co-expressed with ubiquitin in HEK cells. PHMV6-HA-ubiquitin was transiently transfected into HEK-AT2-GFP stable cells. Alternatively, pEGFP-AT2 and pHM6-HA-ubiquitin plasmid were co-transfected into wild type HEK 293 cells at the same time. Cell lysate were precipitated with a polyclonal anti-GFP antibody and detected with both anti-HA and anti-ubiquitin antibody. The results were similar to that of Myc-AT2: ubiquitination on AT2-GFP was only detected when AT2-GFP and ubiquitin were co-expressed in wild type HEK cells (Figure 4.9 C, D).

Figure 4.9 Interaction between AT2 receptor and ubiquitin.

A,B). For Myc tagged AT2 receptor, 5 μg plasmid of pHMV6-HA-ubiquitin was transiently transfected into HEK-Myc-AT2 stable cells seeded on a 100 mm dish. For co-transfection, 4 μg plasmid of pHMV6-HA-uibiquitin and 6 μg of pCMV-Myc-AT2 were co-transfected into a 100 mm dish of wild type HEK cells. After 24~48 hours, HEK-Myc-AT2 stable cell lines were treated with or without 1 μM ANGII for 20 minutes. Cells were lysed in RIPA buffer and precipitated with an anti-Myc antibody. Precipitated samples were separated on 10% SDS-PAGE and detected with anti-HA antibody in western blot (A). After detection with anti-HA antibody, the membrane was stripped and reprobed by anti-Myc antibody (B).

C,D). For GFP tagged AT2 receptor, 5 μg plasmid of pHMV6-HA-ubiquitin was transiently transfected into HEK-AT2-GFP stable cells seeded on a 100 mm dish. For co-transfection, 4 μg plasmid of pHMV6-HA-uibiquitin and 6 μg of pEGFP-AT2 were co-transfected into a 100 mm dish of wild type HEK cells. After 48 hours, the cells were lysed in RIPA buffer and precipitated with a polyclonal anti-GFP antibody. Precipitated samples were separated on 10% SDS-PAGE and detected with anti-HA antibody (C). After detection with anti-HA antibody, the membrane was stripped and reprobed with anti-ubiquitin antibody (D).

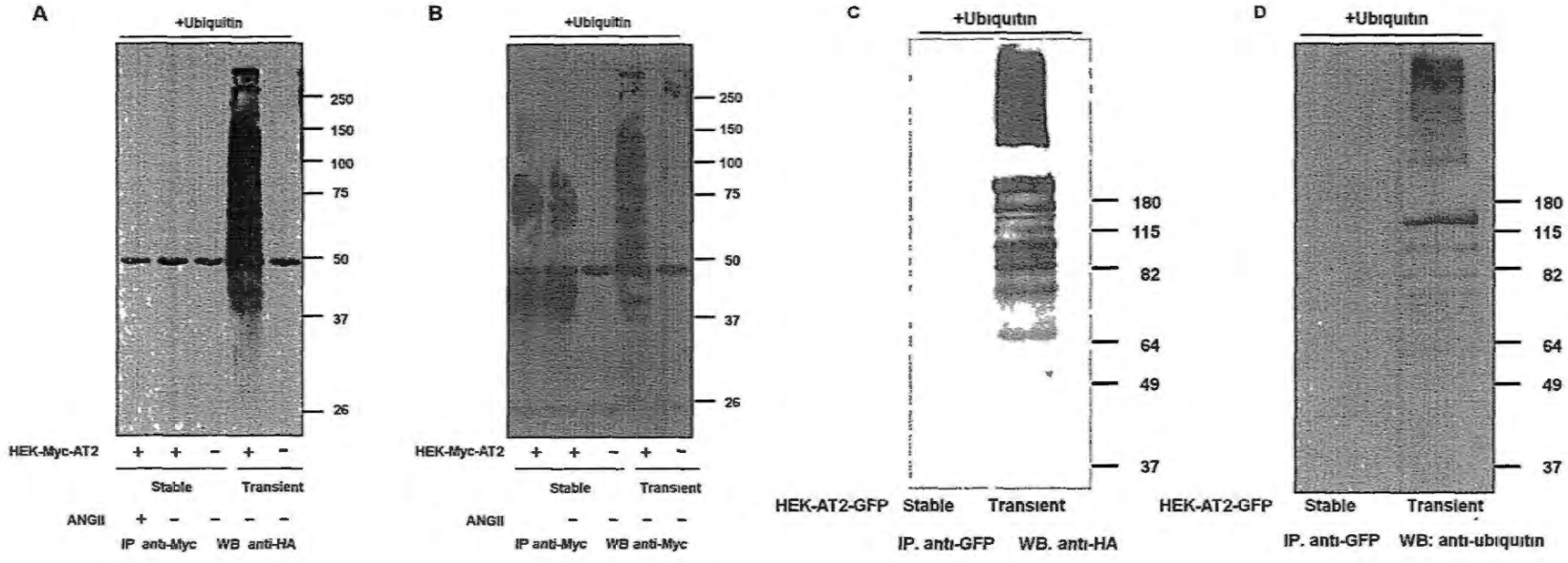
A
+Ubiquitin
250
150
100
75
50
37
26
HEK-Myc-AT2 + + − + −
Stable
Transient
ANGII + − − − −
IP anti-Myc WB anti-HA
B
+Ubiquitin
250
150
100
75
50
37
26
HEK-Myc-AT2 + + − + −
Stable
Transient
ANGII − − − − −
IP anti-Myc WB anti-Myc
C
+Ubiquitin
180
115
82
64
49
37
HEK-AT2-GFP Stable Transient
IP. anti-GFP WB. anti-HA
D
+Ubiquitin
180
115
82
64
49
37
HEK-AT2-GFP Stable Transient
IP. anti-GFP WB: anti-ubiquitin

4.4.2.3 Interaction between AT2 receptor and ubiquitin in mouse embryo tissue

Anti-AT2 antibody has been demonstrated to precipitate AT2 receptor expressed in mouse embryo tissue in Chapter 2. Whether AT2 receptor was modified by ubiquitin in embryo tissues was determined. As shown in figure 4.10, in mouse embryo brain membrane, series of protein bands were detected with anti-AT2 antibody when precipitated with anti-AT2 antibody (Figure 4.10 lane 1). The membrane was stripped and reprobed with anti-ubiquitin antibody. Series of immunoreactive bands were detected with anti-ubiquitin antibody suggesting a possible polyubiquitination on AT2 receptor (Figure 4.10 lane 2).

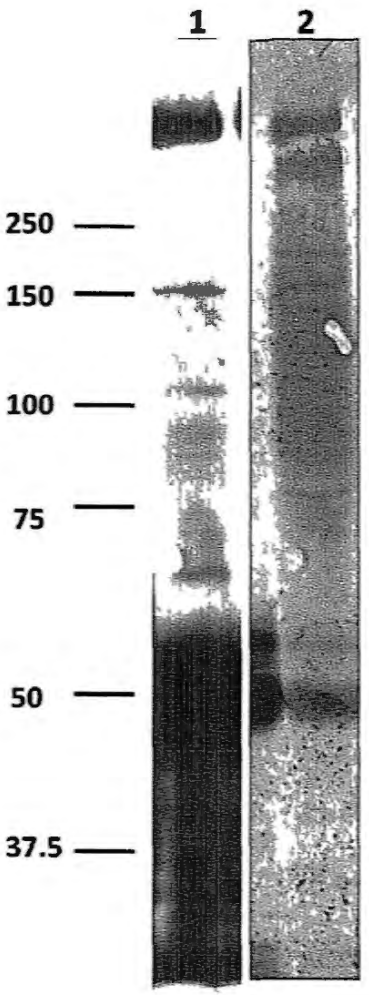

Figure 4.10 AT2 receptor and ubiquitin in mouse embryo brain tissue

Mouse embryo on day 19 was removed and homogenized in TE buffer. Membrane fraction was prepared as described in Methods and lysed in RIPA buffer. Cell lysate was immunoprecipitated with 8 μg of anti-AT2 antibody overnight. Precipitated proteins were separated on 10% SDS-PAGE and detected with an anti-AT2 antibody with ECL (lane1). After stripped, the membrane was reprobed with anti-ubiquitin antibody and detected with NBT/BCIP detection system (lane 2).

4.5 Discussion

4.5.1 AT2 receptor and SUMO

It is not surprising that AT2 receptor was not modified by sumoylation. Most discovered sumoylated targets are nuclear proteins (Anckar and Sistonen, 2007). Until now four membrane proteins were reported to be sumoylated. Only one GPCR (mGluR8) was modified by sumoylation so far (Tang et al., 2005). Besides mGluR8 belongs to group III GPCR while AT2 receptor belongs group I GPCR.

In present study, standard experiment procedure for sumoylation was performed. AT2 receptor variants were transiently and stably expressed in HEK and CHO cells. SUMO1 and SUMO3 were both considered and constructed with an HA and 6×His tag. Expression of SUMO proteins was confirmed by western blot and immunofluorescent confocal microscopy. AT2 receptor was pull down by different anti-tag antibody. SUMO and sumoylated proteins were pulled down by NI-NTA agarose pull down through the 6×His tag. No interaction between AT2 receptor and SUMO protein was detected no matter whether the cells were stimulated by ANGII or not.

In conclusion, AT2 was not modified by sumoylation in our cell expression system.

4.5.2 AT2 receptor and Ubiquitin

The relationship between GPCR and ubiquitin has been reviewed extensively (Hanyaloglu and von Zastrow, 2008). Firstly ubiquitin acts as an internalization signal. PAR1 is deubiquitinated and internalized after agonist stimulation. Internalization of an

ubiquitin-deficient mutant of PAR1 was enhanced (Wolfe et al., 2007). Secondly, activated and internalized GPCR could be modified by ubiquitin and subjected into lysosome for degradation in mammalian cells. The β2AR was the first mammalian GPCR reported to be ubiquitinated after agonist stimulation. A mutant in which all Lys residues were converted to Arg internalized normally but failed to be downregulated (Shenoy et al., 2001). Thirdly, ubiquitination plays an important role in GPCR biosynthesis control. Polyubiquitination and degradation of misfolded GPCRs by the proteasomes have been demonstrated in many GPCRs including rhodopsin, δ -opioid receptor and TRHR (Marchese et al., 2008).

Ubiquitination on GPCR has been confirmed in transient transfection system before. For example, ubiquitination on PAP1 receptor was confirmed by transient co-expression of the receptor with HA-ubiquitin in wild type HEK293 cells (Wolfe et al., 2007); CXCR4 was shown to be ubiquitinated by co-expressing HA-CXCR4 and FLAG-ubiquitin in wild type HEK cells (Marchese and Benovic, 2001).

There are also reports showing ubiquitination of GPCRs in stable cell lines. For example, β2-Adrenergic receptor was ubiquitinated after agonist stimulation in Chinese hamster fibroblast cells (CHW-1102) stably expressing β2-AR (Shenoy et al., 2001); activated PAR2 was mono-ubiquitinated and degraded in lysosomes after agonist stimulation in PAR2-stably expressing HEK293 cells (Jacob et al., 2005).

To my knowledge, there are no literature reports regarding on the controversy between stable expression and transient expression. The reasons why ubiquitination was only detected in co-transfection system are not clear at present. It may due to the typical nature of AT2 receptor. GPCR mentioned above are all typical GPCRs, which will bind to β-arrestin and quickly internalize into cell after agonist stimulation. The internalized GPCR either go back to cell membrane (short term) or be degraded (Hanyaloglu and von Zastrow, 2008). However AT2 receptor is not such a GPCR. Normally AT2 receptor is not internalized. Even when co-expressed and internalized with PLZF, the process was much slower than other GPCR (3 hours after agonist treatment for AT2 receptor, no more than 10 minutes for most GPCRs) (Senbonmatsu et al., 2003). In present study ANGII treated cells for only 20 minutes. The time period might be too short to detect the effect of ubiquitination on AT2 receptor. Furthermore, in transient transfection, protein robustly expressed in the cells. Misfolded protein could cause ER stress and ER stress induces ubiquitin-proteasome degradation pathway (Shenkman et al., 2007). In this process ubiquitin served as a regulator of protein biosynthesis.

In summary through immunoprecipitation and followed by western blot, AT2 receptor was demonstrated to be modified by ubiquitin when the two proteins were transient co-expressed in HEK293 cells; ubiquitination on AT2 receptor was not detected when ubiquitin expressed in AT2 receptor stably expressing cell lines.

Chapter 5

Factors affecting AT2 receptor membrane expression

5.1 Introduction

In Chapter 2 it has been demonstrated that cell membrane expression of AT2 receptor variants was affected by cell type. In both transient and stable expression system, the best cell membrane expression was obtained in HEK293 cells. Potential effects of sumoylation and ubiquitination on AT2 receptor cell membrane expression were considered in Chapter 4. Besides SUMOylation and ubiquitination, GPCRs are also modified by other posttranslational modifications, like glycosylation and oligomerization. AT2 receptors undergo extensive glycosylation in different tissues, primary cultured cells and AT2 receptor endogenously-expressed cell lines (Ouali et al., 1993; Servant et al., 1994, 1996). However, it has been demonstrated that glycosylation did not affect AT2 receptor cell membrane expression in PC12W cells (Servant et al., 1996). Homodimer and oligomer of AT2 receptor have been reported in the brain sample of Alzheimer's disease (AD) patients, AT2 receptor stably-transfected CHO cells and AT2 receptor endogenously-expressed PC12W cells (AbdAlla et al., 2009; Miura et al., 2005). It has been demonstrated that homodimer affected AT2-GFP cell membrane expression in stably-transfected CHO cells (Miura et al., 2005). The effects of glycosylation, homodimer or oligomer on plasma membrane expression of AT2 receptor variants were examined in our stable cell lines.

To study the factors affecting AT2 receptor cell membrane expression, cell surface immunoprecipitation and subcellular fractionation were performed to concentrate cell membrane expressed AT2 receptor. Both methods are commonly used in detection of

membrane-expressed protein including GPCRs (Michineau et al., 2006; Servant et al., 1996). Cell surface immunoprecipitation requires specific antibody, but has high purity for the target proteins. Subcellular fractionation collects membrane fraction through series of centrifugation steps, but in this situation it is impossible to remove other membrane proteins in the membrane fraction.

Serum starvation could increase total expression of AT2 receptor in R3T3 cells and membrane expression of AT2 receptor in stably-transfected CHO cells (Dudley and Summerfelt, 1993; Miura et al., 2005). ANGII, the recognized ligand for AT2 receptor, prevented AT2 degradation in R3T3 cells but decreased the expression of AT2 receptor in fetal sheep (Csikos et al., 1998; Robillard et al., 1995). In present study, the effects of serum starvation and ANGII stimulation on AT2 receptor membrane expression were determined.

To look for interacting proteins of AT2 receptor and confirm the posttranslational modification on the receptor, mass spectrometry analysis of immunoprecipitated samples were performed. Mass spectrometry (MS) is an analytical technique that measures the mass-to-charge ratio of charged particles. In biology it is used for protein characterization, identification of posttranslational modification including glycosylation, phosphorylation and so on.

5.2 Chemicals

5.2.1 Chemicals

F12-Nutrient power (Cat.21700-075), Dulbecco's Modified Eagle Medium power (Cat.12100-046), fetal bovine serum (Cat.10270-106), penicillin/streptomycin (Cat. 15140-122), Lipofectomine 2000 (Cat. 11668-019) were purchased from Invitrogen (Carlsbad, CA, USA). G418 sulfate was from Chemsonic (Germany). Nitrocellulose transfer membrane was from Whatman (Hahnestrabe 3, Dassel, Germany). Amersham ECL™ Western Blotting Detection reagents were from G.E (Healthcare, UK). Medical X-ray film was from FUJI (Japan). Precision Plus Protein Standards were from Bio-Rad (Berkeley, CA, USA). ProteinA agarose, NBT/BCIP and Protease inhibitor cocktail tablets were from Roche (Roche Diagnostics Corporation, IN.USA). Tunicamycin, MG132 and all other chemicals and reagents were from Sigma-Aldrich (St.Louis, MO, USA).

5.2.2 Kits and Instruments

Bicinchoninic Acid (BCA) protein assay kit was from Thermo (HK). 37 ° C humidified cell culture incubators was form Thermo (HK). TCS SP5 confocal microscope was from Leica (German). Quant microplate reader was from Bio-Tek Instruments Inc (Winnoski, VT, USA).

5.2.3 Antibodies

Mouse monoclonal (Cat.632381) and rabbit polyclonal anti-GFP antibody (Cat.632460) were from Clontech (Mountain View, CA, USA). Mouse monoclonal anti-Myc antibody (Cat. sc-40), mouse monoclonal anti-HA antibody (Cat. sc-7392) were from Santa Cruz Biotechnology (CA, USA). Mouse monoclonal anti-β-actin antibody (A-5441) mouse and monoclonal anti-β-tubulin antibody (T5201) were from Sigma-Aldrich (St.Louis, MO, USA).

5.3 Methods

5.3.1 Cell surface immunoprecipitation

PCDNA3-Myc-AT2 or pCDNA3 empty vector stably-transfected HEK293 cells (2×10^6 cells) were seeded on 100 mm dish which had been treated with 0.1% poly-lysine (dissolved in nano pure water and filtered with 0.22 μm membrane). The cells were cultured in a 37 °C humidified cell culture incubator for 72 hours. Cells were transferred into serum free medium (containing 1% penicillin/streptomycin) and cultured for another 24 hours. ANGII was added to the culture medium to a final concentration of 1 μM and incubated with the cells at 37 °C for 40 minutes. The culture medium was discarded and the cells were washed by PBS solution twice. The following procedure was conducted at 4 °C. The dish with cells was incubated with 3 ml of blocking buffer [PBS with 0.2% BSA (W/V)] for 30 minutes to eliminate non-specific binding. Then the blocking buffer was discarded and 2 ml of blocking buffer containing 4 μl anti-Myc of antibody was incubated with the dish for 2 hours with gentle shaking. The dish with the cells was washed by blocking buffer twice (10 minutes each time) and then washed with PBS solution once. Cells were collected by cell scraper and lysed in 1 ml of RIPA buffer [0.1 M Tris pH 7.4, 150 mM NaCl, 1% sodium deoxycholate, 1% Triton X-100, 5 mM EDTA, 40 μl/ml of protease inhibitor cocktail (1 tablet in 2 ml of nano pure water as store solution)]. Cell lysate was incubated on ice for one hour and then centrifuged at 10621 g for 10 minutes. Protein concentration of the supernatant was measured by BCA kit as described in section 2.3.7 to make sure equal amount of protein in each sample. Afterwards 50 μl of protein A agarose was added to cell lysate and shaken overnight. Protein A agarose was spun down at 800 g for 1 minute and washed by the RIPA buffer

for 4 times (10 minutes × 4 times). In the end, 50~80 µl of a sample buffer (2% SDS, 10% glycerol, 40 µl/ml β-mercaptoethanol and 0.01% bromphenol blue in 50 mM Tris-HCl, pH6.8) was added to the agarose pellet and boiled for 10 minutes. Proteins were separated on 10% SDS-PAGE (14 cm ×16 cm) and analyzed by western blot as described in section 2.3.8.

5.3.2 Band intensity and statistic analysis with GraphPad Prism software

Band intensity and statistic analysis with GraphPad Prism software was performed as described in section 3.3.2.

5.3.3 Subcellular fractionation

AT2 receptor variants and respective empty vector stably transfected HEK293 cells (2 $\times 10^6$ cells) were seeded on 0.1% poly-lysine treated 100 mm dish. The cells were kept cultured in a 37 °C humidified cell culture incubator for 72 hours until 95% confluence. Then the cells were washed with PBS once and collected into a 15 ml falcon tube by trypsinization as described in section 2.3.3.2. The cell pellet was resuspended in 1 ml of an extraction buffer (20 mM Tris-HCl, pH 7.5, 2 mM EDTA, 2 mM PMSF and 40 µl/ml of protease inhibitor cocktail) and kept on ice for 15 minutes. The cells were frozen and thawed for 5 cycles by putting in liquid N_2 and 37 °C water bath. Cell lysate was centrifuged at 1500g for 8 minutes to remove remaining cell debris. The supernatant was transferred to a new 1.5 ml tube and further centrifuged at 100,000g for 1 hour at 4 ° C.

The resulting membrane pellet was dissolved in 150 µl of the sample buffer and boiled for 10 minutes. Samples were separated on 10% SDS-PAGE (8 cm × 9 cm) and analyzed by western blot as described in section 2.3.8.

5.3.4 Immunoprecipitation

Immunoprecipitation of total cell lysate was performed as described in section 2.3.7.

5.3.5 Silver staining and sample preparation for mass spectrometry

SDS-PAGE gel was fixed overnight in solution A (40% ethanol, 10% acetic acid and 50% water). On the next day the gel was washed with solution B (30% ethanol, 4.1% Na acetate anhydrous, 0.2% Na thiosulfate) for 45 minutes in room temperature. Then the gel was washed with water for another 30 minutes (10 minutes ×3 times). Afterwards the gel was stained with 0.1% silver nitrate (dissolved in water) for 40 minutes at 4° C in dark. After rinsed twice with water the gel was developed in developing buffer (2.5% Na_2CO3 and 40 µl of 37% formaldehyde in 100 ml water) for up to 15 minutes. The reaction was terminated by a stop solution (1.46 % EDTA-Na_2 in water). The gel was preserved in water until used.

Target bands were cut into small pieces with a blade. The color resulted from silver staining was removed by adding 50 µl of a destaining solution (potassium ferrcyanide and sodium thiosulphate 1:1 freshly mixed). When the color was completely removed

the gel was washed by water once. Then the gel was equilibrated in 200 mM of NH_4HCO_3 for 10 minutes. After the supernatant was removed, the gel pieces were dehydrated with 25 µl of acetonitrile (ACN) for 3 times (10 minutes ×3 times). The gel was dried in speed vacuum for 5 minutes and then incubated with 10 µl of DTT solution (10 mM in 50 mM NH_4HCO_3) at 60° C for 30 minutes. Then 10 µl of iodoacetamide (55 mM in 50 mM NH_4HCO_3) was added to the gel solution and incubated at room temperature for 30 minutes. The gel pieces were washed with 500 µl of 50 mM NH_4HCO_3 for 10 minutes and then dehydrated again with 25 µl ACN for 3 times (10 minutes ×3 times). The gel pieces were dried in speed vacuum for 5 minutes and rehydrated with 10 µl of trypsin solution (40 ng/ul trypsin in 50 mM NH_4HCO_3). After incubated on ice for 30 minutes the gel-trypsin solution was incubated at 30° C overnight.

The gel-trypsin solution was incubated with 20 µl of 50 mM NH_4HCO_3 and sonicated for 10 minutes. Then 20 µl of 50% CAN / 5% TFA was added to the gel pieces and sonicated for 10 minutes. This step was repeated once. The gel solution was transferred to a new 1.5 ml tube, mixed with 10 µl of absolute ACN and sonicated for 10 minutes. The gel solution was dried with speed vacuum to dust like powder.

Zip Tip was rinsed with 50% ACN/ 0.1%TFA and equilibrated with 0.1% TFA. The dried sample was resuspended in 0.1% TFA and loaded to Zip Tip by pipetting up and down for 10 times. The Zip Tip was washed with 0.1% TFA for 5 times. Protein samples

were eluted with 2 μl of 50% ACN/0.1%TFA and transferred into a clean PCR tube. After mixed with 2 μl of matrix, the sample was submitted for mass spectrometry analysis immediately.

5.4 Results

5.4.1 Cell surface expressed AT2 receptor

5.4.1.1 Cell surface immunoprecipitation

The N-terminus of GPCR is located at outside of cells. The Myc-tag was attached to the N-terminus of AT2 receptor which made it possible to use specific antibody to precipitated cell membrane expressed AT2 receptor. Confocal imaging study in Chapter 2 indicated that membrane expression of Myc-AT2 in HEK293 and PC12 stable cells were clearer than that in CHO cells, so the two cell lines were employed in cell surface immunoprecipitation. For the expression of Myc-AT2 was quite low in PC12 cells, the cells were cultured with serum free medium for 12 hours before immunoprecipitataion to increase the expression of AT2 receptor (Miura et al., 2005).

Anti-Myc antibody was incubated with live cells of HEK-Myc-AT2 and PC12-Myc-AT2. Non-specific bound antibodies were washed away before cell lysis. Thus, AT2 receptor expressed in cytosol will not bind to the antibody. As shown in Figure 5.1, compared to total cell lysate immunoprecipitation (Figure 2.10 in Chapter 2), cell membrane expressed Myc-AT2 was mainly focused at the higher MW region (between 70~110 kDa). In contrast, the 45 kDa protein band in total cell lysate immunoprecipitation was lost. The cell surface expressed Myc-AT2 could be the dimer formation or other posttranslational modification.

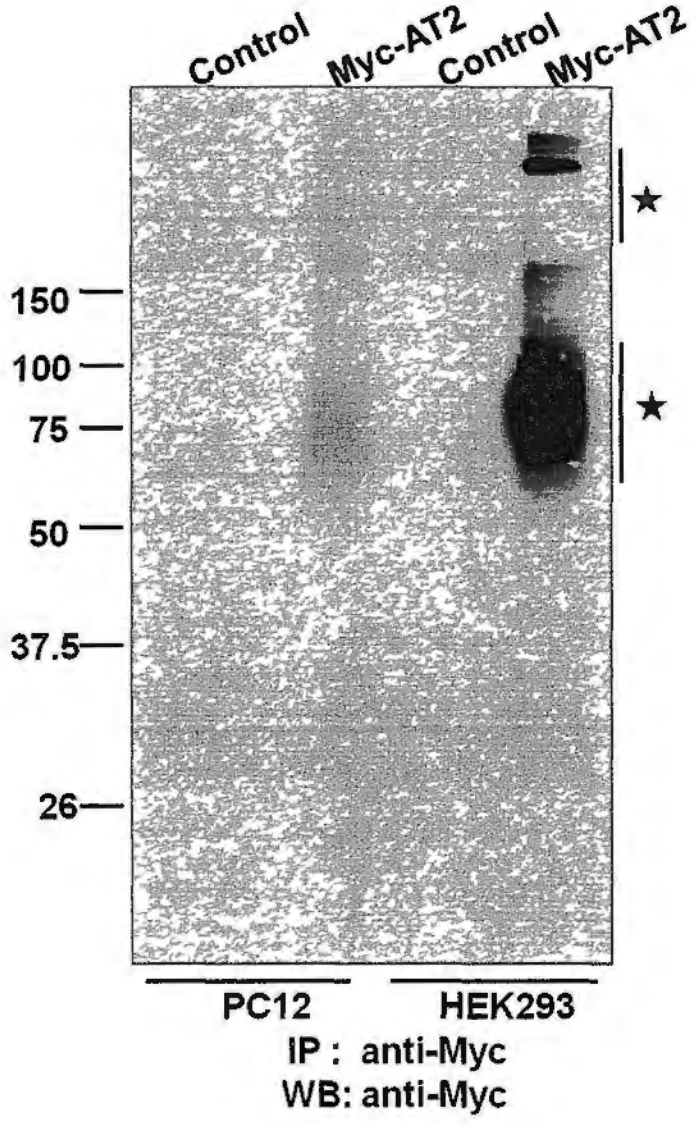

Figure 5.1 Cell surface immunoprecipitation of membrane-expressing Myc-AT2. Stably transfected HEK293 (2×10^6 cells) and PC12 cells (2×10^6 cells) were seeded on 100 mm dish and cultured at 37 °C for 4 days. Culture medium was changed into serum free medium 12 hours before cell lysate. Cell surface-expressing AT2 receptor was immunoprecipitated as described in Methods. Precipitated samples were separated on 10% SDS-PAGE and detected with an anti-Myc antibody in western blot.

5.4.1.2 Subcellular fractionation

Crude membrane fraction of cells including plasma membrane, endosome membrane and mitochondria membrane can be isolated by high speed centrifuge (Nahmias et al., 1995). Crude membrane fraction of Myc-AT2 stably-expressing cell lines and AT2-GFP or GFP stably-expressing HEK293 cells were prepared by high speed centrifuge. Serum-free culture for 12 hours was also introduced to increase the expression of Myc-AT2. Consistent to cell surface immunoprecipitation results, membrane expressed Myc-AT2 in HEK293 and CHO cells were those variants of higher MW (Figure 5.2 A). No specific bands were detected in PC12 cells. It might be due to the lower expression level of Myc-AT2 in PC12 cells. The concentrating effect of subcellular fractionation was not as good as immunoprecipitation.

In HEK-AT2-GFP and GFP cells, compared to total cell lysate (Figure 2.10 in Chapter 2), only the immuno-reactive band above 200 kDa was detected in membrane fraction. In HEK-GFP cells there was still cytosolic protein (GFP) contamination in crude membrane fraction (Figure 5.2 B).

Figure 5.2 Cell fractionation of AT2 receptor stably-expressing cell lines.

A, Myc-AT2 and pCDNA3 empty vector stably-transfected CHO, HEK293 and PC12 cells were seeded on 100 mm dish and cultured until confluence. Cell culture medium was changed into serum-free medium and cultured for another 12 hours. Crude membrane fraction was prepared as described in Methods. Protein samples were separated on 10% SDS-PAGE and detected with an anti-Myc antibody on western blot

B, AT2-GFP and GFP stably-expressed HEK293 cells were seeded on 100 mm dish and cultured until confluence. Crude membrane fraction was prepared as described in Methods. Proteins were separated on 10% SDS-PAGE and detected with an anti-GFP antibody on western blot.

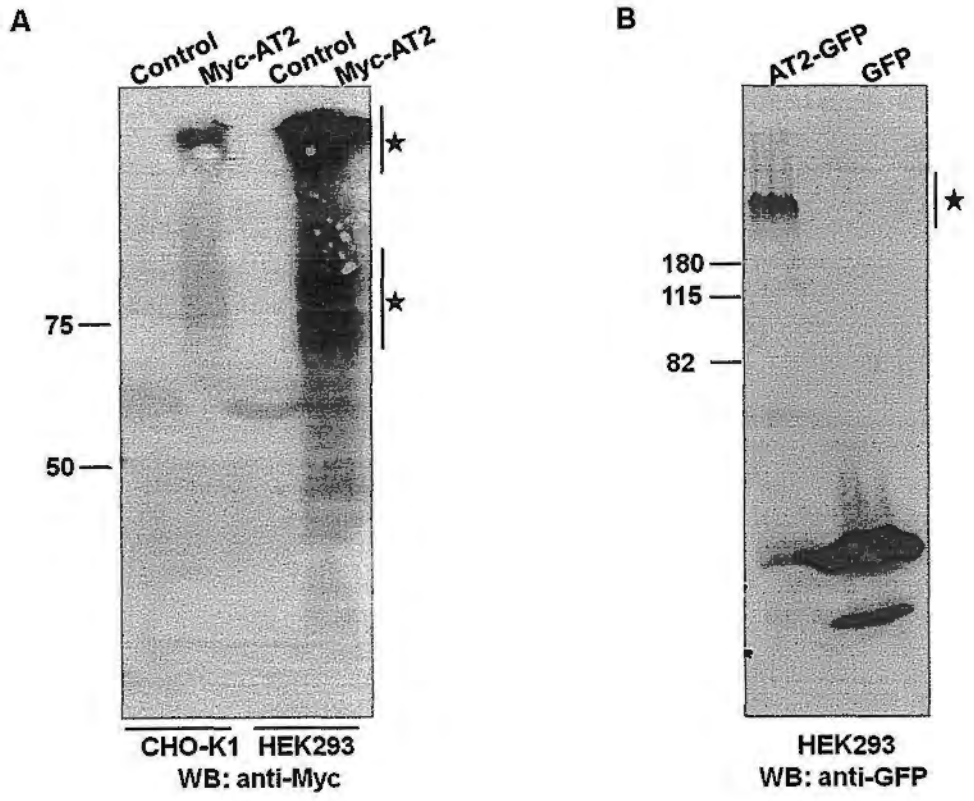
A
Control
Myc-AT2
Control
Myc-AT2
75
50
CHO-K1
HEK293
WB: anti-Myc
B
AT2-GFP
GFP
180
115
82
HEK293
WB: anti-GFP

5.4.2 Dimer and oligomer of AT2 receptor

Cell surface expressed AT2 receptor variants were only detected at higher MW region which could be dimer or oligomer of AT2 receptor variants. AT2 receptor formed dimer in transfected CHO cells and dimer formation affected AT2 receptor cell membrane expression (Miura et al., 2005). Whether the AT2 receptor variants could form dimer in present study was proved by co-expression of two different tagged AT2 receptor variants in HEK293 cells.

AT2-GFP and pCMV-Myc-AT2 were transiently co-transfected into HEK293 cells. AT2-GFP was precipitated with a polyclonal anti-GFP antibody. Precipitated proteins were detected with an anti-Myc antibody on western blot. Monomer form of Myc-AT2 at 45 kDa was detected which indicated that AT2-GFP indeed interacted with Myc-AT2 in present system. Protein bands at quite high MW region (>200 kDa) were also detected. It could be the oligomer formed between AT2-GFP and Myc-AT2 (Figure 5.3).

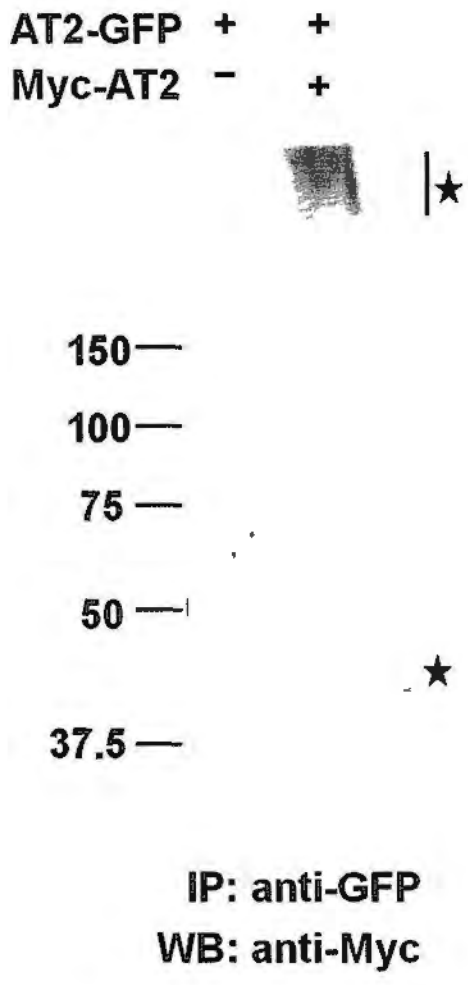

Figure 5.3 Dimer formation between different tagged AT2 receptor variants. Plasmid of AT2-GFP (5 µg) was transiently transfected into HEK 293 cells together with or without plasmid of pCMV-Myc-AT2 (5 µg). After 48 hours, cells were lysed in RIPA buffer and precipitated with a polyclonal anti-GFP antibody. Precipitated samples were separated on 10% SDS-PAGE and detected with an anti-Myc antibody on western blot.

5.4.3 Glycosylation of AT2 receptor

Tunicamycin is a kind of antibiotic which inhibits a series of enzymes involved in synthesis of N-linked glycoproteins (Liao and Chan, 2001). It is commonly used to block glycosylation of proteins (Kamitani and Sakata, 2001). HEK-AT2-GFP and HEK-Myc-AT2 stable cell lines were cultured with or without tunicamycin treatment. The polyclonal anti-GFP and monoclonal anti-Myc antibodies were used to precipitate AT2-GFP and Myc-AT2, respectively.

Compared to non-treated cells, higher MW protein bands of Myc-AT2 decreased dramatically after deglycosylation treatment. The 45 kDa band also migrated to about 34 kDa, which was reported as the original non-modified MW of AT2 receptor (Servant et al., 1994). However in HEK-AT2-GFP cells the expression of AT2-GFP was not changed on western blot after deglycosylation treatment (Figure 5.4).

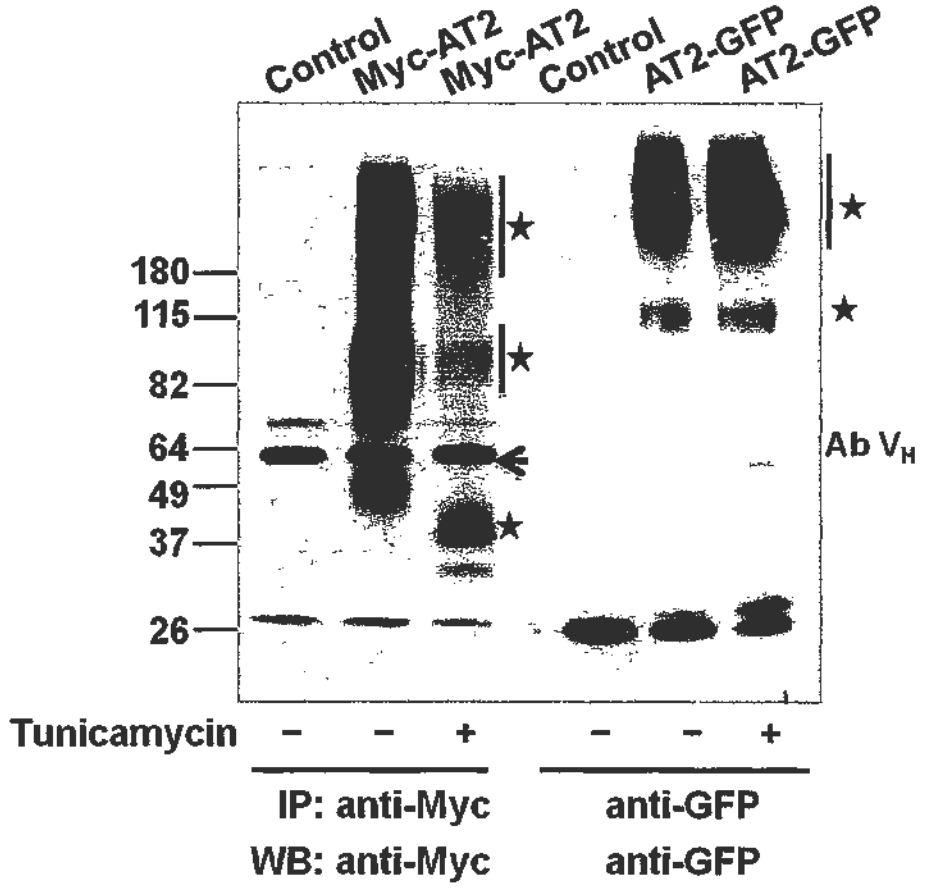

Figure 5.4 AT2 receptor expression after tunicamycin treatment. HEK-AT2-GFP, HEK-GFP, HEK-Myc-AT2 and HEK-PCDNA stable cells were seeded on 100 mm dish and cultured until 90% cell confluence. Then the cells were cultured with or without 1 μg/ml (final concentration) tunicamycin for 24 hours. The cells were lysed in RIPA buffer and immunoprecipitated with anti-GFP and anti-Myc antibody respectively. Precipitated samples were separated on 10% SDS-PAGE and detected with anti-GFP and anti-Myc antibody respectively. Data is representative of three independent experiments.

5.4.4 Serum starvation and ANGII stimulation

5.4.4.1 ANGII increase total AT2 receptor metabolism

The effect of ANGII on AT2 receptor expression was firstly examined with CHO-AT2-GFP stable cell lines and they were used as models in these experiments. CHO-AT2-GFP cells were cultured under normal condition. Protein degradation was blocked with MG132, a proteasomal inhibitor. On the other hand, protein synthesis was blocked by cycloheximide (CHX), a reagent affected protein translation step. As shown in Figure 5.5 A, in the presence of MG132, AT2 receptor expression was increased after ANGII treatment which indicated that ANGII promoted AT2 receptor biosynthesis. In contrast, when protein synthesis was blocked by CHX, AT2 receptor expression was decreased after ANGII treatment which suggested that ANGII accelerated AT2 degradation (Figure 5.5 A, B). There was no significant change of AT2 receptor expression in absence of any blockers in 5 hours (data not shown).

Of interest, when the cells were cultured with extended ANGII treatment (12 hours), AT2 receptor expression was increased. It indicated the overall effect of ANGII was increasing AT2 expression in long term (Figure 5.5 C, D).

Figure 5.5 ANGII increases AT2 receptor metabolism.

A, CHO-AT2-GFP cells were seeded on 100 mm dish and cultured till 95% confluence. MG132 of a final concentration of 10 μg/ml and cychloheximide of a final concentration of 20 μg/ml was added to the culture medium, recepectively, and incubated at 37 °C for half hour. Then ANGII was added into the indicated cells to a final concentration of 5 μM. All the cells were cultured for another 5 hours. Cells were lysed in RIPA buffer and precipitated with an anti-GFP antibody. Precipitated samples were separated on 10% SDS-PAGE and detected with anti-GFP antibody in western blot.

B. The immunoreactive bands in panel A were digitalized using a flat-bed scanner and the UN-SCAN-IT$_{TM}$ software. Band intensity was calculated as described in Methods. The graph was created in GraphPad Prism software. Data of lane 1 and 2 was from one experiment; data of lane 3 and 4 was from two independent experiments.

C, CHO-AT2-GFP cells were seeded on 100 mm dish and cultured till 80% confluence. ANGII was added to cell culture medium to a final concentration of 1 μM. After 12 hours, cells were lysed in RIPA buffer. Protein concentration was determined by BCA assay and equal amount of protein was separated on 10% SDS-PAGE and detected with an anti-GFP antibody in western blot.

D, The immunoreactive bands in panel C were digitalized using a flat-bed scanner and the UN-SCAN-IT$_{TM}$ software. Band intensity was calculated as described in Methods. The graph was created in GraphPad Prism software. Data was from two independent experiments.

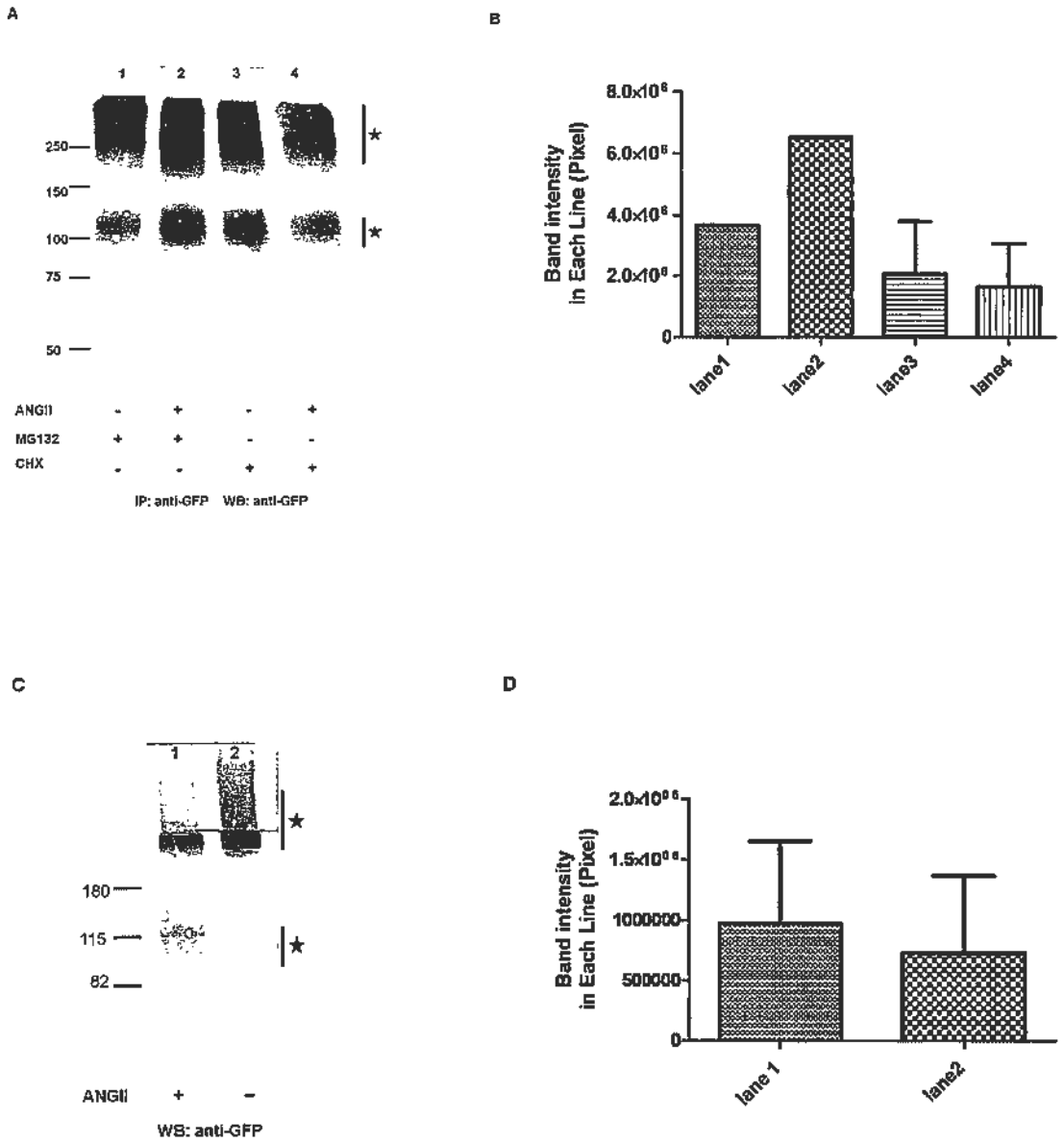
A
1
2
3
4
250
150
100
75
50
ANGII - + - +
MG132 + + - -
CHX - - + +
IP: anti-GFP WB: anti-GFP
B
Band intensity in Each Line (Pixel)
8.0x10^6
6.0x10^6
4.0x10^6
2.0x10^6
0
lane1
lane2
lane3
lane4
C
1
2
180
115
82
ANGII + -
WB: anti-GFP
D
Band intensity in Each Line (Pixel)
2.0x10^6
1.5x10^6
1000000
500000
0
lane 1
lane2

5.4.4.2 Effects of serum and ANGII on plasma membrane expression of AT2 receptor

The effect of serum starvation on AT2 membrane expression was firstly investigated by confocal imaging. In CHO-AT2-GFP cells, AT2 receptor expressed on cell membrane and accumulated at perinuclear region like many other GPCRs. As shown in Figure 5.6A, After serum starvation for 12 hours, AT2-GFP mainly expressed on cell membrane while the expression at perinuclear region decreased. However, ANII treatment did not enhance this effect.

Serum starvation also increased Myc-AT2 cell membrane expression. Cell surface expressed Myc-AT2 was concentrated by cell surface immunoprecipitataion. As shown in Figure 5.6 B and C, cell membrane expressed Myc-AT2 increased after serum starvation for 24 hours. At the same time in the cells which had been cultured in serum free medium for 24 hours, ANGII decreased cell membrane expression of Myc-AT2. It implied that ANGII could induce AT2 receptor internalization in this condition.

Figure 5.6 Effect of serum and ANGII on AT2 membrane expression.

(A) CHO-AT2-GFP cells (1×10^5) were seeded on 25 mm coverslips and cultured for 24 hours. The cells were continued cultured for 12 hours with serum-free medium or with complete medium containing 10% serum. ANGII treated cells were incubated with 1 μM ANGII for 15 min at 37°C. Live cells were examined with confocal microscope. Data is representative of two independent experiments.

(B) HEK-Myc-AT2 cells (1×10^6) were seeded on 100 mm dish and cultured till 90% cell confluence. Culture medium of two dishes of cells were changed into serum-free medium and incubated at 37 °C for 24 hours (lane 1 and lane 3). ANGII was added to one of the two dishes to a final concentration of 1 μM and incubated at 37 °C for 30 minutes before immunoprecipitation (lane 1). Cell surface immunoprecipitation was performed as described in Methods. Precipitated samples were separated on 10% SDS-PAGE and detected with an anti-Myc antibody in western blot.

(C) The immunoreactive bands in panel C were digitalized using a flat-bed scanner and the UN-SCAN-IT$_{TM}$ software. Normalized band intensity was calculated as described in Methods. The graph was created in GraphPad Prism software. Data was from three independent experiments.

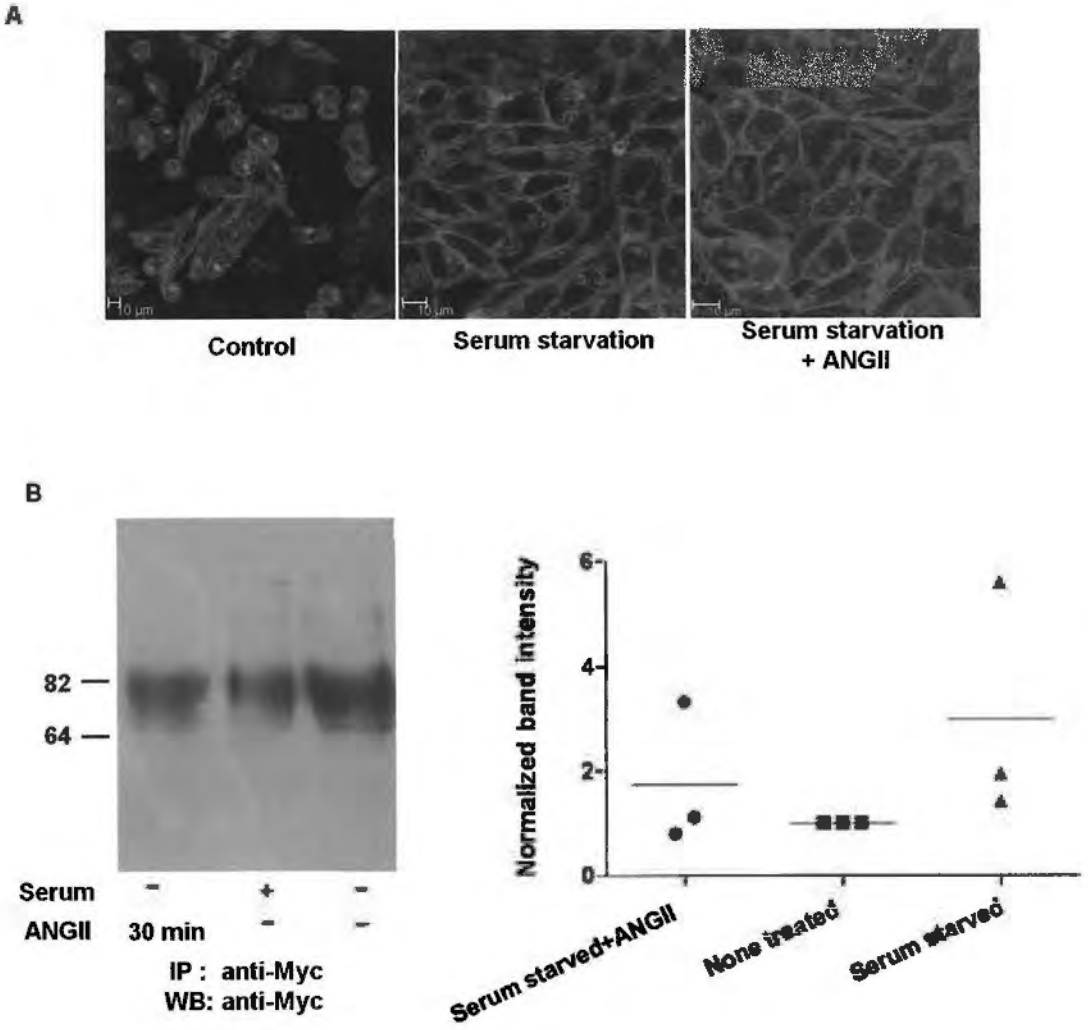
A
Control
Serum starvation
Serum starvation
+ ANGII
B
82
64
Serum
ANGII
30 min
IP : anti-Myc
WB: anti-Myc
Normalized band intensity
6
4
2
0
Serum starved+ANGII
None treated
Serum starved

5.4.5 AT2 receptor interacted with β-actin

Besides studies on postranslational modification, immunoprecipitation and mass-spectrometry were performed trying to find the interacting protein of AT2 receptor. Myc-AT2 was transiently and stably expressed in HEK293 cells, in which all AT2 receptor variants showed highest expression. Myc-AT2 was precipitated with an anti-Myc antibody and the precipitated samples were separated on 10% SDS-PAGE. After silver staining, the proteins bands shown in HEK-Myc-AT2 stable cell lines were similar to that of HEK-pCDNA control cells. In pCMV-Myc-AT2 transiently-transfected cells, several protein bands were considered as potential targets and sent for mass spectrometry analysis. Most of the protein bands were not identified because the protein amount was quite low. The only protein identified was β-actin (Figure 5.7 A).

To prove that it was not due to contamination during sample preparation, the interaction was confirmed by immunoprecipitataion and western blot (Figure 5.7 B). Myc-AT2 was transiently and stably expressed in HEK cells. β-actin was detected in precipitated samples of Myc-AT2 transiently-transfected HEK cells but not in the stable cell lines. Interestingly, the interaction decreased after ANGII treatment.

Another important component of cytoskeleton, β-tubulin, the protein that make up microtubules, was also investigated in present study. There was no interaction between AT2 receptor and β-tubulin detected by immunoprecipitataion and western blot (Figure

5.7 C). It implied that the interaction between AT2 receptor variants and β-actin was not due to contamination in precipitation or non-specific binding to cytoskeleton.

Figure 5.7 AT2 receptor interacts with β-actin.

A, Stable cell lines of HEK-Myc-AT2, HEK-PCDNA and wild type HEK 293 were seeded on 100 mm dish and cultured until 90% confluence. PCMV-Myc-AT2 (5 μg) was transfected into HEK cells as described in section 2.3.3. After 24 hours, cells were lysed in RIPA buffer and immunoprecipitated with an anti-Myc antibody. Precipitated proteins were separated on 10% SDS-PAGE and then subjected to silver staining. Target protein bands were cut and prepared for mass spectrometry as described in Methods.

B, HEK 293 (2×dish) were transfected with 5μg of pCMV-Myc-AT2, stable cell lines HEK-Myc-AT2, HEK-PCDNA were cultured till 90% confluence. After 24 hours, cell culture medium was changed into serum-free medium and incubated at 37 °C for 8 hours. ANGII was added to the indicated cells to a final concentration of 1 μM and incubated at 37 °C for 20 minutes before cell lysis. Samples precipitated with anti-Myc antibody were separated on 10% SDS-PAGE and detected with a mouse monoclonal anti-β-actin antibody in western blot. Data is representative of three independent experiments.

C, Cells were seeded and transfected as described in panel A. After 24 hours, cell culture medium was changed into serum-free medium and incubated at 37 °C for 8 hours. ANGII was added to the indicated cells to a final concentration of 1 μM and incubated at 37 °C for 20 minutes before cell lysis. Samples precipitated with anti-Myc antibody were separated on 10% SDS-PAGE and detected with a mouse monoclonal anti-β-tubulin antibody in western blot.

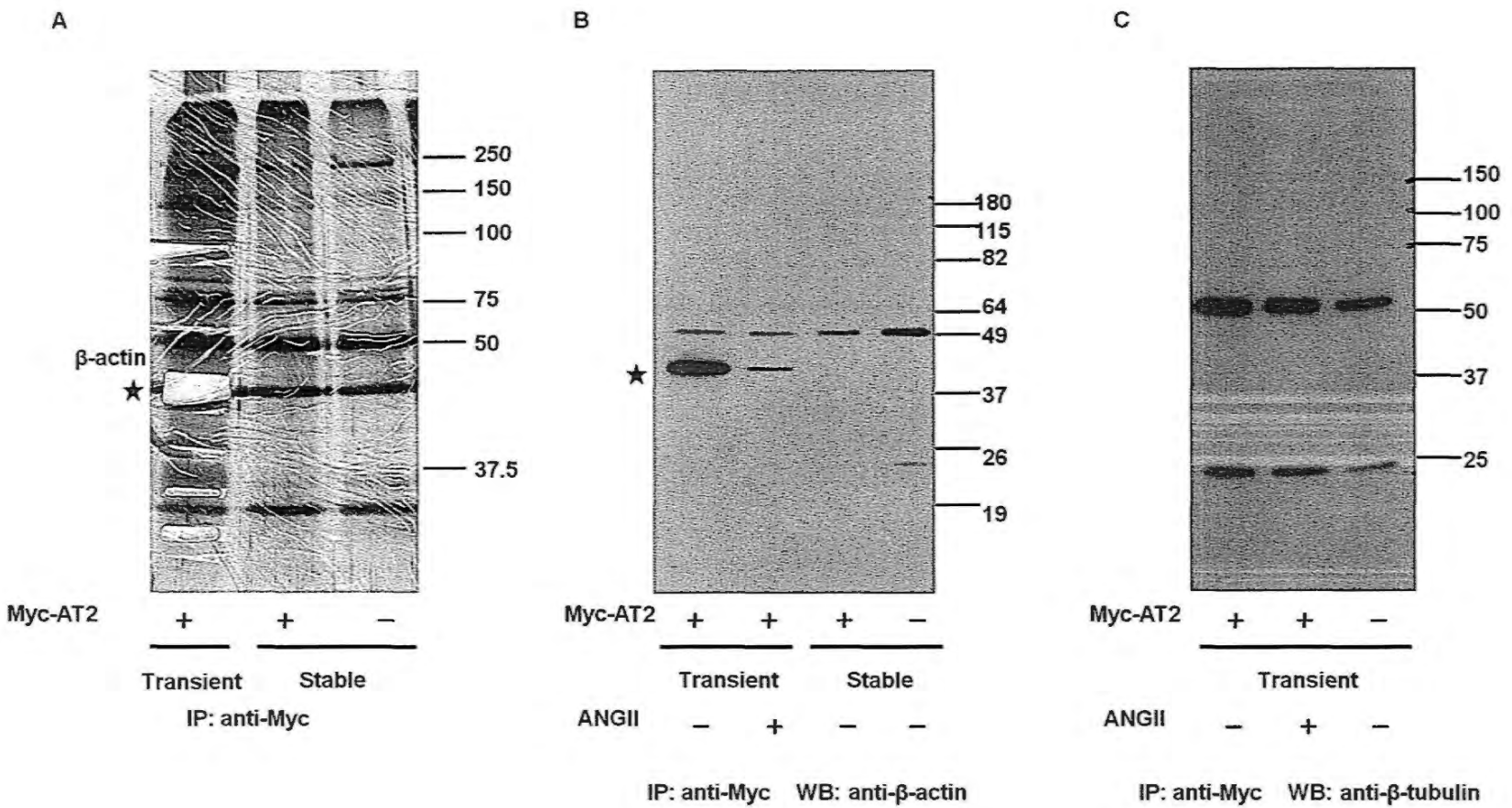
A
250
150
100
75
50
β-actin
★
37.5
Myc-AT2
+
+
–
Transient
Stable
IP: anti-Myc
B
180
115
82
64
49
★
37
26
19
Myc-AT2
+
+
+
–
Transient
Stable
ANGII
–
+
–
–
IP: anti-Myc
WB: anti-β-actin
C
150
100
75
50
37
25
Myc-AT2
+
+
–
Transient
ANGII
–
+
–
IP: anti-Myc
WB: anti-β-tubulin

5.5 Discussion

5.5.1 Dimer and oligomer of AT2 receptor

Homodimer and oligomer of AT2 receptor were detected in brain tissues of Alzheimer Disease patients and model mice which indicated a potential role of AT2 receptor in Alzheimer disease (AbdAlla et al., 2009). Miura et al. proposed a hypothesis that AT2 receptor homodimer, which was formed through disulfide bond, affected cell surface expression of AT2 receptor and ligand-independent AT2 receptor-mediated apoptosis in transfected CHO cells (Miura et al., 2005). As shown by Miura and his co-workers, the molecular weight of AT2-GFP in CHO was around 120 kDa which was similar to that of AT2-GFP in present study. However, in the publication when samples were pretreated with DTT before SDS-PAGE, AT2-GFP was mainly detected as monomer (Miura et al., 2005). In present study although all the samples were prepared with β-mercaptoethanol, a reducing reagent equivalent to DTT, AT2-GFP was still detected as dimer and oligomer. The difference between previous and present study is not clear. It has been reported that some GPCR dimers were resistant to reducing reagent (Lee et al., 2003). Dimer and oligomer of AT2 receptor detected in the brain tissue of Alzheimer Disease patients and mice were also resistant to urea and β-mercaptoethanol in western blot. The molecular weight of AT2 receptor oligomer was larger than 250 kDa in western blot (AbdAlla et al., 2009). It implied that besides disulfide bond some other covalent interaction might be involved in AT2 dimer formation.

It is a commonly used method to prove GPCR dimer formation with different tagged receptor. For example, AT2-GFP and AT2-DsRed were co-expressed to verify the homodimer formation of AT2 receptor by overlap images in confocal microscopy and western blot analysis of immunoprecipitated samples (Miura et al., 2005). In present study AT2-GFP and Myc-AT2 were co-expressed in HEK293 cells. Western protein analysis of immunoprecipitated samples confirmed that the two tagged AT2 receptor variants interacted with each other in present system.

From subcellular fractionation assay and western protein analysis of tunicamycin treated cells, cell membrane expression of AT2-GFP but not Myc-AT2 was affected by oliogomer formation in HEK293 cells. It indicated that different tagged AT2 receptor variants differed in the same cells. As discussed in Chapter 2, N-terminal tagged AT2 receptors were easier to form dimer or oligomer.

In conclusion, in present study, AT2 formed homodimer and oligomer. Dimer and oligomer formation affected AT2-GFP cell membrane expression in HEK293 cells.

5.5.2 Glycosylation

The crucial evidence regarding effects of glycosylation on plasma membrane expression of AT2 receptor was reported in 1996 (Servant et al., 1996). In the publication, tunicamycin-treated PC12W cells were labled with I^{125}-ANGII. Cell membrane fraction

were prepared and analyzed on western blot. AT2 receptor was still detected by autoradiography in the membrane fraction of tunicamycin-treated cells but the molecular weight was decreased. The author believed that without glycosylation AT2 receptors still localized on cell membrane (Servant et al., 1996). In present study, tunicamycin treatment had different effects in different cell lines. In HEK-Myc-AT2 stable cell lines, the majority of higher molecular weight bands of Myc-AT2 decreased on SDS-PAGE. Based on cell surface immunoprecipitation results, the higher molecular weight bands of Myc-AT2 accounted for the cell membrane expressed AT2 receptor. It indicated that in HEK-Myc-AT2 cells, glycosylation indeed affected plasma membrane expression of Myc-AT2. However in HEK-AT2-GFP stable cell lines, tunicamycin had no effects on AT2-GFP expression reflected on western blot. It implied that glycosylation were not involved in membrane expression of AT2-GFP.

The reasons for the difference between the previous and present study might be: different tagged AT2 receptors expressed in different cells behaves differently. For instance in PC12W cells which endogenously expressed AT2 receptor, the molecular weight of AT2 receptor is about 200 kDa (Servant et al., 1996), which could be the oligomer form of AT2 receptor. In fact, AT2 receptor formed dimer and oligomer in PC12W cells (Miura et al., 2005). Therefore in the case of PC12W cells, cell membrane expression of AT2 receptor was affected by oligomerization but not by glycosylation. However, as discussed in Chapter 2, AT2 receptor in some cells and tissues are of 40~70 kDa (Hakam et al., 2006; Harada et al., 2010; Hoffmann and Cool, 2003; Nora et al., 1998; Wehbi et al., 2001; Zahradka et al., 1998), whether AT2 receptor homodimer

exists in these cells is still a question. Results in present study provided us a possibility that in some cells and tissues, glycosylation affected AT2 receptor membrane expression.

In conclusion, glycosylation affected Myc-AT2 but not AT2-GFP plasma membrane expression in HEK293 cells.

5.5.3 Serum starvation and ANGII stimulation affected AT2 receptor plasma membrane expression

Serum starvation increased plasma membrane expression of AT2-GFP in stably transfected CHO-K1 cells. After serum starvation AT2-GFP mainly localized on cell membrane examined by confocal microscopy (Miura et al., 2005). In present study, AT2-GFP expressed in CHO cells behaved in the same way as reported. Myc-AT2 was also used to investigate the effects of serum starvation on AT2 receptor membrane expression using cell surface immunoprecipitation. After serum starvation, cell membrane expressed Myc-AT2 was increased. The possible reasons for an increase of AT2 receptor membrane expression c be: 1) serum starvation increased total AT2 receptor expression including membrane expression, as demonstrated in R3T3 cells (Dudley and Summerfelt, 1993); 2) serum starvation induces the transport of cytosolic AT2 receptors to cell membrane. Why serum starvation affected AT2 receptor expression in AT2 receptor transfected and endogenously expressed cell lines are still unknown.

The effects of ANGII on AT2 expression were complicated. Incubation the R3T3 cells with specific agonist of AT2 receptor including ANGII for 24 hours cause up-regulation of AT2 binding sites (Csikos et al., 1998; Dudley and Summerfelt, 1993). The results were concluded from radioactive ligand binding which reflect cell membrane expression of AT2 receptor. In contrast, continuous i.v. infusion of ANGII in kidney for 24 hours decreased the AT2 receptor expression in fetal sheep (Robillard et al., 1995). The results were obtained from RNA expression level in Northern blot which reflected total expression of AT2 receptor in gene level. In present study, ANGII treatment increase turnover of AT2 receptor variants in short-term (5 hours). However, the effect of biosynthesis should be a little bigger than that of degradation because the overall effect of ANGII was increasing AT2 expression in long term (12 hours treatment of ANGII).

In present study, ANGII stimulation for 20 minutes caused AT2 receptor internalization in serum-starved cells. ANGII induced internalization hasn't been reported before. It is commonly believed that AngII-stimulated AT2 receptors do not internalize (Pucell et al., 1991). The reason for the difference could be that in previous studies the internalization of AT2 receptor was analyzed at 10~60 minutes after ANGII treatment. For normal GPCRs the receptor internalizes into cells very quickly (Oakley et al., 2000). AT2 receptor does not belong to these GPCRs. AT2 receptors underwent a quite slow internalization (3 hours after stimulation) when co-expressed with a protein called PLZF. However, in this time period AT2 receptor did not internalize by itself (Senbonmatsu et

al., 2003). It indicated that the internalization of AT2 receptor could be a quite long process. The internalization could be observed only when the majority of expressed AT2 receptors were located on cell membrane such as in the condition of serum starvation.

5.5.4 β-actin and AT2 receptor

The cytoskeleton is formed by three types of high molecular weight polymers: microtubules, microfilaments, and intermediate filaments. All three types of cytoskeletal elements are intimately associated with cytoplasmic organelles, particularly mitochondria, lysosomes, and secretary vesicles. All cytoskeletetal elements also interact with the nucleus and plasma membrane. Cytoskeletal fibers play an important role in cell motility and various forms of intracellular movements including axonal transport and receptor endocytosis (Feuilloley and Vaudry, 1996). Actin is the monomeric subunit of microfilaments. There are three kinds of actin proteins: α-actins exist in muscle tissues and are major components of the contractile apparatus. β and γ actins co-exist in most cell types as components of the cytoskeleton.

Actin fibers are primary targets of ANGII activation. ANGII stimulation induced a rapid translocation of Gαq/α11, microfilaments and microtubules to the membrane in adrenal glomerulosa cells, facilitating second messenger production (Cote et al., 1997). ANGII stimulation induced rapid increase in actin fluorescence labeling at the membrane in human fetal adrenal glands, as one of the consequences of ANGII induced apoptosis (Chamoux et al., 1999). ANGII-activated AT2 receptor increased the migration of

NG108-15 cell (a neuronal cell line endogenously expressed AT2) through actin depolymerization at the leading edge of the cells (Kilian et al., 2008). Direct interaction between AT2 receptor and β-actin has not been reported before.

In present study, Myc-AT2 transiently expressed in HEK293 cells interacted with β-actin in basal state. The interaction was specific and decreased after ANGII treatment. It provided a possibility that AT2 receptor might bind to β-actin cytoskeleton at basal state and dissociated from it after ANGII treatment. Whether the β-actin-associated AT2 receptors are plasma membrane expressed or cytosolic needs further investigation. If they are cytosolic, it indicated that AT2 receptor does not translocate with β-actin upon ANGII treatment. Pulse (1 minute) stimulation with ANGII significantly increased actin fluorescence labeling at the membrane in human fetal adrenal glands (Chamoux et al., 1999). It is possible that after ANGII treatment, β-actin rapidly dissociated from the cytosolic proteins and moved to cell membrane. If β-actin-associated AT2 receptors are membrane expressed receptors, it indicated that AT2 receptor internalized after ANGII stimulation. In present study, the cells were serum starved before ANGII stimulation. As mentioned before, serum starvation increased cell membrane expression of AT2 receptor which made it easier to observe the internalization of AT2 receptor. It is possible that after ANGII treatment, AT2 receptor dissociated from the β-actin near the plasma membrane and moved into cytosol.

Chapter 6 General discussion

To study the relationship between posttranslational modification and cell membrane expression of AT2 receptor, several tagged-AT2 receptor variants subcloned in different expression vectors were firstly constructed in present study. Different expression vectors were transiently and stably expressed in three cell lines. AT2 receptor expression was determined by confocal microscopy and western blot by different tag antibodies and anti-AT2 antibodies.

The activity of expressed AT2 in stable cell lines was confirmed. Consistent to previous report (Miura and Karnik, 2000), AT2 expressed CHO cells displayed apoptosis when cultured in serum free medium. No apoptosis response was detected in HEK293 and PC12 cells. However, cell proliferation of AT2 expressed HEK cells and PC12 cells were slower than respective control cell lines. To try to explain the inhibited proliferation, cell cycle analysis and ERK phosphorylation status were examined.

Posttranslational modification of sumoylation and ubiquitination were also examined. Regardless the AT2 receptor were tagged in N- or C- terminus, no sumoylation was detected on AT2 receptor in either transient transfection or stable cell lines. However, ubiquitination of AT2 receptor was detected in transient transfection but not in stable cell lines.

Cell membrane expressed AT2 receptor was purified by cell surface immunoprecipitation and subcellular fractionation. The results show that cell membrane expressed AT2 mainly consist of the high molecular weight form AT2. Both glycosylation and oligomerization affect AT2 cell membrane expression. Effects of ANGII and serum starvation on AT2 cell membrane expression were also clarified.

6.1 The difference of AT2 expression between different cell types

One of the advantages in present study was that different cells and different tagged AT2 receptor variants were employed to try to avoid false positive results.

Three cell lines were used in the present study. In transient transfection, the highest expression level and the best membrane expression was shown in HEK 293 cells while the lowest expression level and the worst membrane expression was found in PC12 cells. In stable cell lines, membrane expression of Myc-AT2 in PC12 and HEK cells were better compared to that in CHO cells. The difference of expression level was due to transfection efficiency.

Consistent to literature review CHO-AT2-GFP underwent apoptosis after serum starvation. However this is not the case for HEK and PC12 cells. In HEK and PC12 cells only cell proliferation was inhibited. The underlying mechanism might be due to cell

cycle arrest. For HEK cells more AT2-expressed cells stayed in G1 phase, while for PC12 cells more AT2 expressed cells accumulated in S phase.

Western protein analysis indicated that a tagged AT2 variant displayed similar molecular weight in different cell lines, suggesting that posttranslational modification was similar in different cell types. Thus in only HEK and CHO cells were included the following study in posttranslational modification experiments. For example, results of interaction between AT2 and SUMO3 were consistent in HEK and CHO cells.

6.2 The difference of AT2 expression between different tags

In present study, different tags were attached to AT2. At C-terminus of AT2 receptor, GFP tag or FLAG was added. Confocal imaging showed that cell membrane expression of AT2 was not affected by GFP and FLAG tag. However, there were some drawbacks of these two tags. Low expression of AT2-FLAG was detected by western blot and immunofluorescent confocal microscopy in both transient and stable expression. GFP is a big protein especially when considering that the intracellular C terminal is important to GPCR signaling pathway. Therefore, HA or Myc tag was added to the N terminus of AT2 receptor respectively.

Expression level of tagged AT2 variants was quite different in transient transfection. This is surprising, because basically all tagged AT2 used the same promoter: human

cytomegalovirus promoter (CMV). PEGFP-N1, PCMV-HA, PCMV-Myc use the exactly same promoter: CMV early promoter ($P_{CMV\ IE}$). PCDNA3 and PCMV-FLAG use the same promoter: CMV. Despite with the exactly same promoter was used for different constructs, expression of pCMV-Myc-AT2 was several folds higher than pCMV-HA-AT2. Plasmid preparation and transfection was performed by the same standard procure. Although the detection system in present study relayed on immunology which was highly dependent on the specificity of antibodies, the antibodies were tested with other tagged protein and all shown high specificity (data not shown).

The expression level of exogenous gene in stable cell lines mainly depends on the copy of gene combined to genome. It could be tested by Southern blot (did not perform in present study). The molecular weight of the same tagged AT2 variant in different stable cell lines was similar on western blot which indicated that posttranslational modification for the same tagged AT2 variant was similar in different cells. However, in the same cells posttranslational modification of different tagged AT2 variants could be different. As discussed in Chapter 5, tunicamycin changed Myc-AT2 expression profile in HEK cells but did nothing to AT2-GFP expression in HEK cells. Why the same protein undergoes different modification in the same cells is unknown.

6.3 The difference of AT2 expression between transient expression and stable expression

Both transient expression and stable expression are used for protein expression and protein-protein interaction in literature. In transient transfection, exogenous DNA does not integrate into genome and cause a quite high expression in a short time. In stable expression, exogenous DNA will integrate into genome and cause a continued expression of proteins.

Immunofluorescent images indicated that cell membrane expression was clearer in stable cell lines than that in transient transfection. This might be due to the expression level in stable cell lines was much lower than that in transient transfection in a single cell. As mentioned in section 2.4.2.2, when lower amount of AT2 was expressed, AT2 expressed mainly on cell membrane. In contrast, when AT2 expression level was increased more fluorescence aggregated in cells and caused cell toxicity.

In present study, AT2 interaction with ubiquitin and β –actin was only detected in cells transiently expressed AT2. There are two possibilities for this: 1) the interaction was caused by over-expression of AT2 proteins. Over-expressed protein induces ER stress and ER stress targets those proteins for ubiquitin-proteasome degradation (Nakayama et al., 2008). Over-expressed protein diffused everywhere in cytosol which makes interaction with β –actin is easy to understand. 2) Another possible reason is that AT2 transient expressed in cells mimics the real situation in body. AT2 expression in body is also "transient" : in adult and earlier stage of embryo, AT2 expression was quite low or even undetectable; however, during the period before and after birth (for mice one day

before or after birth) the expression was dramatically increased (Grady et al., 1991). In present study, AT2 precipitated with our anti-AT2 antibody in mouse embryo also shows series of protein bands like that shown in HEK transient transfected with PCMV-Myc-AT2. In brain tissues, the series bands were detected by ubiquitin antibody. Although it needs further confirmation, it provided a possibility that AT2 in transient transfection system might mimic the "real" AT2. Expression of AT2 in stable cell lines was stable and cells get used to it. There was no tissue in adult body expressed so much AT2 as that in our stable cell lines. Even with high expression in adult adrenal the expression was still lower than that in fetus. If this is the case, it will open a whole new page for AT2 studies.

6.4 AT2 trafficking in cells

It is reported that in basal state AT2 receptor resided in cytosol in smooth muscle cells. After high concentration of ANGII treatment AT2 receptor moves to cell membrane (de Godoy and Rattan, 2006). Unlike other GPCR, AT2 receptor does not internalize to cytosol after shot-term treatment of ANGII (Pucell et al., 1991). How AT2 traffics in cells and what is the fate of cell membrane AT2 receptor?

Based on present results, a trafficking model of AT2 was proposed (Figure 6.1). After synthesized in ER, AT2 receptors undergo glycosylation or form homo-dimer or oligomer in cytosol. These modifications help AT2 receptor travel to the cell surface. The non-modified AT2 receptors could be ubiquitinated and targeted for protein

degradation in proteasome. The newly synthesized AT2 and cell membrane expressed AT2 receptor are in an equilibrium. Somehow some signals, such as serum starvation or ANGII stimulation, enhance AT2 receptor trafficking onto cell membrane. Thus the equilibrium is broken up and AT2 receptor synthesis is accelerated. With increasing cell membrane expression of AT2, a new equilibrium will form.

When the AT2 receptors on cell membrane are saturated, i.e AT2 receptor cell membrane expression will not be further increased, AT2 receptor will be internalized after ANGII stimulation. For example, when the cells were cultured in serum-free medium overnight, the expression level of AT2 receptor on cell membrane was quite high. At this moment, ANGII stimulation trigger AT2 receptor internalization into cells. The internalized AT2 receptors get back into cytol for recycling (early-endosome) or degradation (proteasome or lysosome). Ubiquitin might be involved in the process of directing AT2 receptor internalization and degradation.

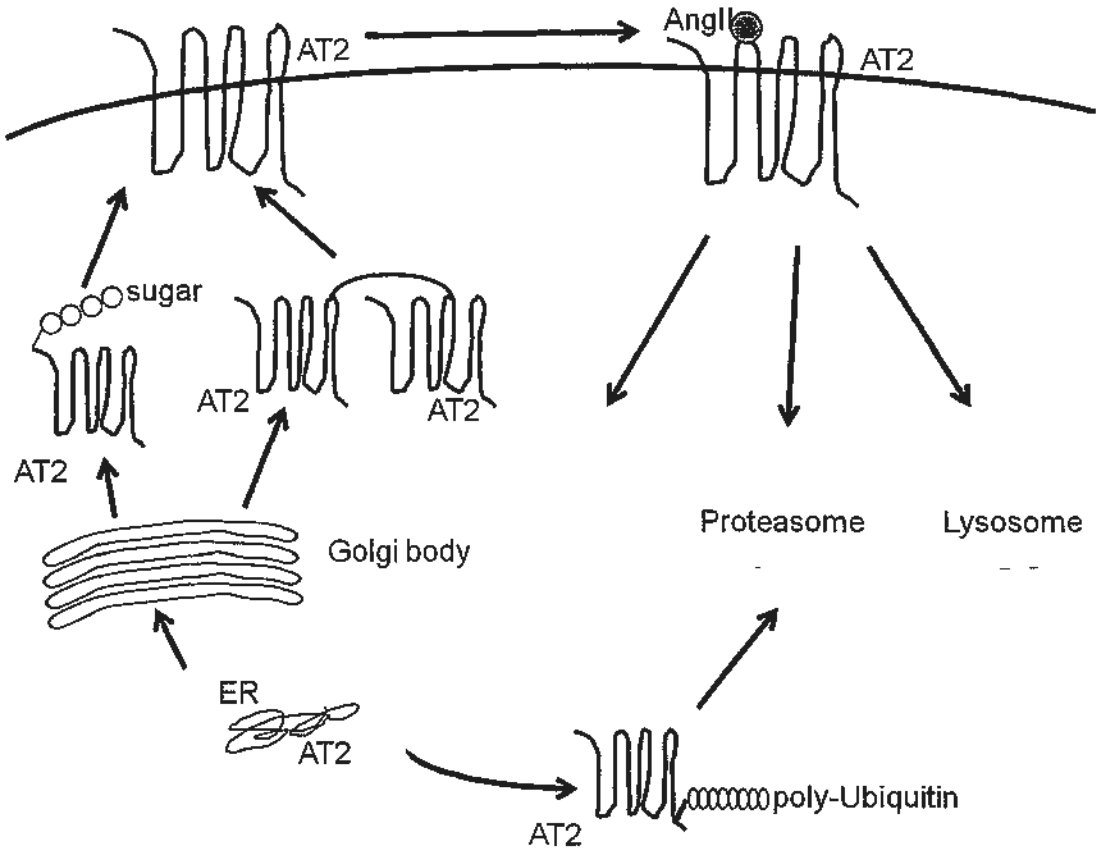

Figure 6.1 AT2 receptor trafficking in cells

6.5 Limitations of present study

In present study different tagged AT2 expressed in different cell lines in both transient and stable way. However from previous discussion AT2 behaved differently in different cell type, with different tag. Even for the same tagged AT2 in the same cells interaction with ubiquitin and β-actin results are different between transient and stable expression. Which is the real condition for physiological AT2? The questions still need to be answered in animal models. In present study, the expression of AT2 and the interaction of AT2 with ubiquitin were tried to be proved by mouse embryo tissue. However for the limited amount of sample the results need to be repeated in the future.

1. AbdAlla, S., Lother, H., Abdel-tawab, A.M. & Quitterer, U. The angiotensin II AT2 receptor is an AT1 receptor antagonist. *J Biol Chem* **276**, 39721-39726 (2001).

2. AbdAlla, S., *et al.* Angiotensin II AT2 receptor oligomers mediate G-protein dysfunction in an animal model of Alzheimer disease. *J Biol Chem* **284**, 6554-6565 (2009).

3. Acconcia, F., Sigismund, S. & Polo, S. Ubiquitin in trafficking: the network at work. *Exp Cell Res* **315**, 1610-1618 (2009).

4. Akishita, M., *et al.* Expression of the AT2 receptor developmentally programs extracellular signal-regulated kinase activity and influences fetal vascular growth. *J Clin Invest* **103**, 63-71 (1999).

5. Aldred, G.P., *et al.* Distribution of angiotensin II receptor subtypes in the rabbit brain. *Regul Pept* **44**, 119-130 (1993).

6. Anckar, J. & Sistonen, L. SUMO: getting it on. *Biochem Soc Trans* **35**, 1409-1413 (2007).

7. Attwood, T.K. & Findlay, J.B. Fingerprinting G-protein-coupled receptors. *Protein Eng* 7, 195-203 (1994).

8. Baldwin, J.M. The probable arrangement of the helices in G protein-coupled receptors. *EMBO J* **12**, 1693-1703 (1993).

9. Beaudry, H., Gendron, L., Guimond, M.O., Payet, M.D. & Gallo-Payet, N. Involvement of protein kinase C alpha (PKC alpha) in the early action of angiotensin II type 2 (AT2) effects on neurite outgrowth in NG108-15 cells: AT2-

receptor inhibits PKC alpha and p21ras activity. *Endocrinology* **147**, 4263-4272 (2006).

10. Belloni, A.S., *et al.* Distribution and functional significance of angiotensin-II AT1- and AT2-receptor subtypes in the rat adrenal gland. *Endocr Res* **24**, 1-15 (1998).

11. Bridges, T.M. & Lindsley, C.W. G-protein-coupled receptors: from classical modes of modulation to allosteric mechanisms. *ACS Chem Biol* **3**, 530-541 (2008).

12. Brown, B. & Hall, A.S. Renin-angiotensin system modulation: the weight of evidence. *Am J Hypertens* **18**, 127S-133S (2005).

13. Cagnol, S. & Chambard, J.C. ERK and cell death: mechanisms of ERK-induced cell death--apoptosis, autophagy and senescence. *FEBS J* **277**, 2-21 (2010).

14. Carey, R.M., Jin, X., Wang, Z. & Siragy, H.M. Nitric oxide: a physiological mediator of the type 2 (AT2) angiotensin receptor. *Acta Physiol Scand* **168**, 65-71 (2000).

15. Chamoux, E., Breault, L., Lehoux, J.G. & Gallo-Payet, N. Involvement of the angiotensin II type 2 receptor in apoptosis during human fetal adrenal gland development. *J Clin Endocrinol Metab* **84**, 4722-4730 (1999).

16. Chappell, M.C., Jacobsen, D.W. & Tallant, E.A. Characterization of angiotensin II receptor subtypes in pancreatic acinar AR42J cells. *Peptides* **16**, 741-747 (1995).

17. Chung, O., Csikos, T. & Unger, T. Angiotensin II receptor pharmacology and AT1-receptor blockers. *J Hum Hypertens* **13 Suppl 1**, S11-20; discussion S33-14 (1999).

18. Cote, M., Payet, M.D., Dufour, M.N., Guillon, G. & Gallo-Payet, N. Association of the G protein alpha(q)/alpha11-subunit with cytoskeleton in adrenal glomerulosa cells: role in receptor-effector coupling. *Endocrinology* **138**, 3299-3307 (1997).

19. Csikos, T., *et al.* Angiotensin AT2 receptor degradation is prevented by ligand occupation. *Biochem Biophys Res Commun* **243**, 142-147 (1998).

20. Cui, T., *et al.* Pivotal role of tyrosine phosphatase SHP-1 in AT2 receptor-mediated apoptosis in rat fetal vascular smooth muscle cell. *Cardiovasc Res* **49**, 863-871 (2001).

21. Dai, X.Q., Kolic, J., Marchi, P., Sipione, S. & Macdonald, P.E. SUMOylation regulates Kv2.1 and modulates pancreatic beta-cell excitability. *J Cell Sci* **122**, 775-779 (2009).

22. D'Amore, A., Black, M.J. & Thomas, W.G. The angiotensin II type 2 receptor causes constitutive growth of cardiomyocytes and does not antagonize angiotensin II type 1 receptor-mediated hypertrophy. *Hypertension* **46**, 1347-1354 (2005).

23. de Godoy, M.A. & Rattan, S. Translocation of AT1- and AT2-receptors by higher concentrations of angiotensin II in the smooth muscle cells of rat internal anal sphincter. *J Pharmacol Exp Ther* **319**, 1088-1095 (2006).

24. De Paolis, P., *et al.* Functional cross-talk between angiotensin II and epidermal growth factor receptors in NIH3T3 fibroblasts. *J Hypertens* **20**, 693-699 (2002).

25. Della Rocca, G.J., Maudsley, S., Daaka, Y., Lefkowitz, R.J. & Luttrell, L.M. Pleiotropic coupling of G protein-coupled receptors to the mitogen-activated

protein kinase cascade. Role of focal adhesions and receptor tyrosine kinases. *J Biol Chem* **274**, 13978-13984 (1999).

26. Denuc, A. & Marfany, G. SUMO and ubiquitin paths converge. *Biochem Soc Trans* **38**, 34-39 (2010).

27. Deshaies, R.J. & Joazeiro, C.A. RING domain E3 ubiquitin ligases. *Annu Rev Biochem* **78**, 399-434 (2009).

28. Dimmeler, S., Rippmann, V., Weiland, U., Haendeler, J. & Zeiher, A.M. Angiotensin II induces apoptosis of human endothelial cells. Protective effect of nitric oxide. *Circ Res* **81**, 970-976 (1997).

29. Dong, C., Filipeanu, C.M., Duvernay, M.T. & Wu, G. Regulation of G protein-coupled receptor export trafficking. *Biochim Biophys Acta* **1768**, 853-870 (2007).

30. Dudley, D.T. & Summerfelt, R.M. Regulated expression of angiotensin II (AT2) binding sites in R3T3 cells. *Regul Pept* **44**, 199-206 (1993).

31. Dupre, D.J., Robitaille, M., Rebois, R.V. & Hebert, T.E. The role of Gbetagamma subunits in the organization, assembly, and function of GPCR signaling complexes. *Annu Rev Pharmacol Toxicol* **49**, 31-56 (2009).

32. Duprez, E., *et al.* SUMO-1 modification of the acute promyelocytic leukaemia protein PML: implications for nuclear localisation. *J Cell Sci* **112 (Pt 3)**, 381-393 (1999).

33. Edwards, R.M. & Aiyar, N. Angiotensin II receptor subtypes in the kidney. *J Am Soc Nephrol* **3**, 1643-1652 (1993).

34. Engelman, D.M. & Steitz, T.A. The spontaneous insertion of proteins into and across membranes: the helical hairpin hypothesis. *Cell* **23**, 411-422 (1981).

35. Feng, Y.H., Sun, Y. & Douglas, J.G. Gbeta gamma -independent constitutive association of Galpha s with SHP-1 and angiotensin II receptor AT2 is essential in AT2-mediated ITIM-independent activation of SHP-1. *Proc Natl Acad Sci U S A* **99**, 12049-12054 (2002).

36. Feng, Y.H., Zhou, L., Sun, Y. & Douglas, J.G. Functional diversity of AT2 receptor orthologues in closely related species. *Kidney Int* **67**, 1731-1738 (2005).

37. Ferreira, J.C., *et al.* The role of local and systemic renin angiotensin system activation in a genetic model of sympathetic hyperactivity-induced heart failure in mice. *Am J Physiol Regul Integr Comp Physiol* **294**, R26-32 (2008).

38. Feuilloley, M. & Vaudry, H. Role of the cytoskeleton in adrenocortical cells. *Endocr Rev* **17**, 269-288 (1996).

39. Franco, R., *et al.* Basic concepts in G-protein-coupled receptor homo- and heterodimerization. *ScientificWorldJournal* **7**, 48-57 (2007).

40. Geiss-Friedlander, R. & Melchior, F. Concepts in sumoylation: a decade on. *Nat Rev Mol Cell Biol* **8**, 947-956 (2007).

41. Gendron, L., *et al.* Signals from the AT2 (angiotensin type 2) receptor of angiotensin II inhibit p21ras and activate MAPK (mitogen-activated protein kinase) to induce morphological neuronal differentiation in NG108-15 cells. *Mol Endocrinol* **13**, 1615-1626 (1999).

42. George, A.J., Thomas, W.G. & Hannan, R.D. The renin-angiotensin system and cancer: old dog, new tricks. *Nat Rev Cancer* **10**, 745-759 (2010).

43. Gether, U. & Kobilka, B.K. G protein-coupled receptors. II. Mechanism of agonist activation. *J Biol Chem* **273**, 17979-17982 (1998).

44. Gingras, B., *et al.* Expression of angiotensin type II receptor downregulates Cdk4 synthesis and inhibits cell-cycle progression. *Oncogene* **22**, 2633-2642 (2003).

45. Goto, M., *et al.* Growth-dependent induction of angiotensin II type 2 receptor in rat mesangial cells. *Hypertension* **30**, 358-362 (1997).

46. Grady, E.F., Sechi, L.A., Griffin, C.A., Schambelan, M. & Kalinyak, J.E. Expression of AT2 receptors in the developing rat fetus. *J Clin Invest* **88**, 921-933 (1991).

47. Gray, J.A., *et al.* Cell-type specific effects of endocytosis inhibitors on 5-hydroxytryptamine(2A) receptor desensitization and resensitization reveal an arrestin-, GRK2-, and GRK5-independent mode of regulation in human embryonic kidney 293 cells. *Mol Pharmacol* **60**, 1020-1030 (2001).

48. Gross, V., Obst, M. & Luft, F.C. Insights into angiotensin II receptor function through AT2 receptor knockout mice. *Acta Physiol Scand* **181**, 487-494 (2004).

49. Gwathmey, T.M., *et al.* Nuclear angiotensin II type 2 (AT2) receptors are functionally linked to nitric oxide production. *Am J Physiol Renal Physiol* **296**, F1484-1493 (2009).

50. Haack, K.K., *et al.* A novel bioassay for detecting GPCR heterodimerization: transactivation of beta 2 adrenergic receptor by bradykinin receptor. *J Biomol Screen* **15**, 251-260 (2010).

51. Haithcock, D., Jiao, H., Cui, X.L., Hopfer, U. & Douglas, J.G. Renal proximal tubular AT2 receptor: signaling and transport. *J Am Soc Nephrol* **10 Suppl 11**, S69-74 (1999).

52. Hakam, A.C., Siddiqui, A.H. & Hussain, T. Renal angiotensin II AT2 receptors promote natriuresis in streptozotocin-induced diabetic rats. *Am J Physiol Renal Physiol* **290**, F503-508 (2006).

53. Hansen, J.L., *et al.* Functional reconstitution of the angiotensin II type 2 receptor and G(i) activation. *Circ Res* **87**, 753-759 (2000).

54. Hanyaloglu, A.C. & von Zastrow, M. Regulation of GPCRs by endocytic membrane trafficking and its potential implications. *Annu Rev Pharmacol Toxicol* **48**, 537-568 (2008).

55. Harada, K., *et al.* Localization of type-2 angiotensin II receptor in adrenal gland. *J Histochem Cytochem* **58**, 585-593 (2010).

56. Hoffmann, A. & Cool, D.R. Angiotensin II receptor types 1A, 1B, and 2 in murine neuroblastoma Neuro-2a cells. *J Recept Signal Transduct Res* **23**, 111-121 (2003).

57. Hoppe-Seyler, K., Weigand, K., Lohrey, C., Hoppe-Seyler, F. & Sauer, P. Cellular growth inhibition by FK778 is linked to G1 arrest or S phase accumulation, dependent on the functional status of the retinoblastoma protein. *Int J Mol Med* **23**, 415-420 (2009).

58. Horiuchi, M., Lehtonen, J.Y. & Daviet, L. Signaling Mechanism of the AT2 Angiotensin II Receptor: Crosstalk between AT1 and AT2 Receptors in Cell Growth. *Trends Endocrinol Metab* **10**, 391-396 (1999).

59. Hunyady, L. & Catt, K.J. Pleiotropic AT1 receptor signaling pathways mediating physiological and pathogenic actions of angiotensin II. *Mol Endocrinol* **20**, 953-970 (2006).

60. Ichiki, T., *et al.* Effects on blood pressure and exploratory behaviour of mice lacking angiotensin II type-2 receptor. *Nature* **377**, 748-750 (1995).

61. Jacob, C., *et al.* c-Cbl mediates ubiquitination, degradation, and down-regulation of human protease-activated receptor 2. *J Biol Chem* **280**, 16076-16087 (2005).

62. Jacobs, L.S. & Douglas, J.G. Angiotensin II type 2 receptor subtype mediates phospholipase A2-dependent signaling in rabbit proximal tubular epithelial cells. *Hypertension* **28**, 663-668 (1996).

63. Kambayashi, Y., *et al.* Molecular cloning of a novel angiotensin II receptor isoform involved in phosphotyrosine phosphatase inhibition. *J Biol Chem* **268**, 24543-24546 (1993).

64. Kamitani, S. & Sakata, T. Glycosylation of human CRLR at Asn123 is required for ligand binding and signaling. *Biochim Biophys Acta* **1539**, 131-139 (2001).

65. Kilian, P., *et al.* Angiotensin II type 2 receptor stimulation increases the rate of NG108-15 cell migration via actin depolymerization. *Endocrinology* **149**, 2923-2933 (2008).

66. Klco, J.M., Lassere, T.B. & Baranski, T.J. C5a receptor oligomerization. I. Disulfide trapping reveals oligomers and potential contact surfaces in a G protein-coupled receptor. *J Biol Chem* **278**, 35345-35353 (2003).

67. Knowle, D., Ahmed, S. & Pulakat, L. Identification of an interaction between the angiotensin II receptor sub-type AT2 and the ErbB3 receptor, a member of the epidermal growth factor receptor family. *Regul Pept* **87**, 73-82 (2000).

68. Koch, T., Wu, D.F., Yang, L.Q., Brandenburg, L.O. & Hollt, V. Role of phospholipase D2 in the agonist-induced and constitutive endocytosis of G-protein coupled receptors. *J Neurochem* **97**, 365-372 (2006).

69. Korolchuk, V.I., Menzies, F.M. & Rubinsztein, D.C. Mechanisms of cross-talk between the ubiquitin-proteasome and autophagy-lysosome systems. *FEBS Lett* **584**, 1393-1398 (2010).

70. Laflamme, L., Gasparo, M., Gallo, J.M., Payet, M.D. & Gallo-Payet, N. Angiotensin II induction of neurite outgrowth by AT2 receptors in NG108-15 cells. Effect counteracted by the AT1 receptors. *J Biol Chem* **271**, 22729-22735 (1996).

71. Lanctot, P.M., Leclerc, P.C., Escher, E., Leduc, R. & Guillemette, G. Role of N-glycosylation in the expression and functional properties of human AT1 receptor. *Biochemistry* **38**, 8621-8627 (1999).

72. Lazard, D., *et al.* Characterization of a membrane glycoprotein having pharmacological and biochemical properties of an AT2 angiotensin II receptor from human myometrium. *Eur J Biochem* **220**, 919-926 (1994).

73. Lee, S.P., O'Dowd, B.F., Rajaram, R.D., Nguyen, T. & George, S.R. D2 dopamine receptor homodimerization is mediated by multiple sites of interaction, including an intermolecular interaction involving transmembrane domain 4. *Biochemistry* **42**, 11023-11031 (2003).

74. Lee, Y.H., Mungunsukh, O., Tutino, R.L., Marquez, A.P. & Day, R.M. Angiotensin-II-induced apoptosis requires regulation of nucleolin and Bcl-xL by SHP-2 in primary lung endothelial cells. *J Cell Sci* **123**, 1634-1643 (2010).

75. Lenkei, Z., Palkovits, M., Corvol, P. & Llorens-Cortes, C. Expression of angiotensin type-1 (AT1) and type-2 (AT2) receptor mRNAs in the adult rat brain: a functional neuroanatomical review. *Front Neuroendocrinol* **18**, 383-439 (1997).

76. Leong, S.P., *et al.* Effect of different fixatives on the localization of human melanoma antigens by immunofluorescence. *Oncology* **36**, 202-207 (1979).

77. Leung, P.S., Chan, H.C., Fu, L.X. & Wong, P.Y. Localization of angiotensin II receptor subtypes AT1 and AT2 in the pancreas of rodents. *J Endocrinol* **153**, 269-274 (1997).

78. Liao, W. & Chan, L. Tunicamycin induces ubiquitination and degradation of apolipoprotein B in HepG2 cells. *Biochem J* **353**, 493-501 (2001).

79. Liu, F. & Walters, K.J. Multitasking with ubiquitin through multivalent interactions. *Trends Biochem Sci* **35**, 352-360 (2010).

80. Longden, J., Cooke, E.L. & Hill, S.J. Effect of CCR5 receptor antagonists on endocytosis of the human CCR5 receptor in CHO-K1 cells. *Br J Pharmacol* **153**, 1513-1527 (2008).

81. Lu, D., Yang, H., Shaw, G. & Raizada, M.K. Angiotensin II-induced nuclear targeting of the angiotensin type 1 (AT1) receptor in brain neurons. *Endocrinology* **139**, 365-375 (1998).

82. Maiato, H. Mitosis: wisdom, knowledge, and information. *Cell Mol Life Sci* **67**, 2141-2143 (2010).

83. Marchese, A. Ubiquitination of chemokine receptors. *Methods Enzymol* **460**, 413-422 (2009).

84. Marchese, A. & Benovic, J.L. Agonist-promoted ubiquitination of the G protein-coupled receptor CXCR4 mediates lysosomal sorting. *J Biol Chem* **276**, 45509-45512 (2001).

85. Marchese, A., Paing, M.M., Temple, B.R. & Trejo, J. G protein-coupled receptor sorting to endosomes and lysosomes. *Annu Rev Pharmacol Toxicol* **48**, 601-629 (2008).

86. Matsubara, H., Mori, Y., Masaki, H. & Inada, M. [Pathophysiological function of angiotensin II AT1 and AT2 receptors and clinical application of AT1 antagonists]. *Nippon Rinsho* **56**, 1912-1918 (1998).

87. Matsubara, H., Murasawa, S., Suzuki, J., Urakami, M. & Inada, M. [Angiotensin II receptor gene transcription is tissue-specifically regulated in central and cardiovascular systems]. *Jpn Circ J* **57 Suppl 4**, 1136-1138 (1993).

88. Mattiazzi, A. Positive inotropic effect of angiotensin II. Increases in intracellular Ca2+ or changes in myofilament Ca2+ responsiveness? *J Pharmacol Toxicol Methods* **37**, 205-214 (1997).

89. Matunis, M.J., Coutavas, E. & Blobel, G. A novel ubiquitin-like modification modulates the partitioning of the Ran-GTPase-activating protein RanGAP1 between the cytosol and the nuclear pore complex. *J Cell Biol* **135**, 1457-1470 (1996).

90. Meffert, S., Stoll, M., Steckelings, U.M., Bottari, S.P. & Unger, T. The angiotensin II AT2 receptor inhibits proliferation and promotes differentiation in PC12W cells. *Mol Cell Endocrinol* **122**, 59-67 (1996).

91. Menard, L., *et al.* Synergistic regulation of beta2-adrenergic receptor sequestration: intracellular complement of beta-adrenergic receptor kinase and beta-arrestin determine kinetics of internalization. *Mol Pharmacol* **51**, 800-808 (1997).

92. Michineau, S., Alhenc-Gelas, F. & Rajerison, R.M. Human bradykinin B2 receptor sialylation and N-glycosylation participate with disulfide bonding in surface receptor dimerization. *Biochemistry* **45**, 2699-2707 (2006).

93. Millan, M.A., Jacobowitz, D.M., Aguilera, G. & Catt, K.J. Differential distribution of AT1 and AT2 angiotensin II receptor subtypes in the rat brain during development. *Proc Natl Acad Sci U S A* **88**, 11440-11444 (1991).

94. Miura, S. & Karnik, S.S. Ligand-independent signals from angiotensin II type 2 receptor induce apoptosis. *EMBO J* **19**, 4026-4035 (2000).

95. Miura, S., Karnik, S.S. & Saku, K. Constitutively active homo-oligomeric angiotensin II type 2 receptor induces cell signaling independent of receptor conformation and ligand stimulation. *J Biol Chem* **280**, 18237-18244 (2005).

96. Miura, S., Matsuo, Y., Kiya, Y., Karnik, S.S. & Saku, K. Molecular mechanisms of the antagonistic action between AT1 and AT2 receptors. *Biochem Biophys Res Commun* **391**, 85-90 (2010).

97. Miura, S.I. & Karnik, S.S. Ligand-independent signals from angiotensin II type 2 receptor induce apoptosis. *Embo Journal* **19**, 4026-4035 (2000).

98. Miyata, N., Park, F., Li, X.F. & Cowley, A.W., Jr. Distribution of angiotensin AT1 and AT2 receptor subtypes in the rat kidney. *Am J Physiol* **277**, F437-446 (1999).

99. Mukoyama, M., Horiuchi, M., Nakajima, M., Pratt, R.E. & Dzau, V.J. Characterization of a rat type 2 angiotensin II receptor stably expressed in 293 cells. *Mol Cell Endocrinol* **112**, 61-68 (1995).

100. Muller, D.N., *et al.* NF-kappaB inhibition ameliorates angiotensin II-induced inflammatory damage in rats. *Hypertension* **35**, 193-201 (2000).

101. Munzenmaier, D.H. & Greene, A.S. Opposing actions of angiotensin II on microvascular growth and arterial blood pressure. *Hypertension* **27**, 760-765 (1996).

102. Nahmias, C., *et al.* Angiotensin II AT2 receptors are functionally coupled to protein tyrosine dephosphorylation in N1E-115 neuroblastoma cells. *Biochem J* **306 (Pt 1)**, 87-92 (1995).

103. Nakajima, M., Mukoyama, M., Pratt, R.E., Horiuchi, M. & Dzau, V.J. Cloning of cDNA and analysis of the gene for mouse angiotensin II type 2 receptor. *Biochem Biophys Res Commun* **197**, 393-399 (1993).

104. Nakayama, H., *et al.* ER stress is the initial response to polyglutamine toxicity in PC12 cells. *Biochem Biophys Res Commun* **377**, 550-555 (2008).

105. Nelson, D.M., *et al.* Coupling of DNA synthesis and histone synthesis in S phase independent of cyclin/cdk2 activity. *Mol Cell Biol* **22**, 7459-7472 (2002).

106. New, D.C. & Wong, Y.H. Characterization of CHO cells stably expressing a G alpha 16/z chimera for high throughput screening of GPCRs. *Assay Drug Dev Technol* **2**, 269-280 (2004).

107. Nikcevic, G., Kovacevic-Grujicic, N. & Stevanovic, M. Improved transfection efficiency of cultured human cells. *Cell Biol Int* **27**, 735-737 (2003).

108. Nora, E.H., Munzenmaier, D.H., Hansen-Smith, F.M., Lombard, J.H. & Greene, A.S. Localization of the ANG II type 2 receptor in the microcirculation of skeletal muscle. *Am J Physiol* **275**, H1395-1403 (1998).

109. Nowak, M. & Hammerschmidt, M. Ubc9 regulates mitosis and cell survival during zebrafish development. *Mol Biol Cell* **17**, 5324-5336 (2006).

110. Oakley, R.H., Laporte, S.A., Holt, J.A., Caron, M.G. & Barak, L.S. Differential affinities of visual arrestin, beta arrestin1, and beta arrestin2 for G protein-coupled receptors delineate two major classes of receptors. *J Biol Chem* **275**, 17201-17210 (2000).

111. Olivares-Reyes, J.A., Jayadev, S., Hunyady, L., Catt, K.J. & Smith, R.D. Homologous and heterologous phosphorylation of the AT(2) angiotensin receptor by protein kinase C. *Mol Pharmacol* **58**, 1156-1161 (2000).

112. Ostasov, P., Krusek, J., Durchankova, D., Svoboda, P. & Novotny, J. Ca2+ responses to thyrotropin-releasing hormone and angiotensin II: the role of plasma membrane integrity and effect of G11alpha protein overexpression on homologous and heterologous desensitization. *Cell Biochem Funct* **26**, 264-274 (2008).

113. Ouali, R., LeBrethon, M.C. & Saez, J.M. Identification and characterization of angiotensin-II receptor subtypes in cultured bovine and human adrenal fasciculata cells and PC12W cells. *Endocrinology* **133**, 2766-2772 (1993).

114. Pernollet, M.G., Devynck, M.A., Macdonald, G.J. & Meyer, P. Plasma renin activity and adrenal angiotensin II receptors in fetal, newborn, adult and pregnant rabbits. *Biol Neonate* **36**, 119-127 (1979).

115. Pucell, A.G., Hodges, J.C., Sen, I., Bumpus, F.M. & Husain, A. Biochemical properties of the ovarian granulosa cell type 2-angiotensin II receptor. *Endocrinology* **128**, 1947-1959 (1991).

116. Pulakat, L., *et al.* Ligand-dependent complex formation between the Angiotensin II receptor subtype AT2 and Na+/H+ exchanger NHE6 in mammalian cells. *Peptides* **26**, 863-873 (2005).

117. Pulakat, L., *et al.* Role of C-terminal cytoplasmic domain of the AT2 receptor in ligand binding and signaling. *FEBS Lett* **524**, 73-78 (2002).

118. Rabkin, S.W. The angiotensin II subtype 2 (AT2) receptor is linked to protein kinase C but not cAMP-dependent pathways in the cardiomyocyte. *Can J Physiol Pharmacol* **74**, 125-131 (1996).

119. Robillard, J.E., *et al.* Differential gene expression and regulation of renal angiotensin II receptor subtypes (AT1 and AT2) during fetal life in sheep. *Pediatr Res* **38**, 896-904 (1995).

120. Savoia, C., *et al.* Angiotensin II/AT2 receptor-induced vasodilation in stroke-prone spontaneously hypertensive rats involves nitric oxide and cGMP-dependent protein kinase. *J Hypertens* **24**, 2417-2422 (2006).

121. Senbonmatsu, T., *et al.* A novel angiotensin II type 2 receptor signaling pathway: possible role in cardiac hypertrophy. *EMBO J* **22**, 6471-6482 (2003).

122. Servant, G., Dudley, D.T., Escher, E. & Guillemette, G. The marked disparity between the sizes of angiotensin type 2 receptors from different tissues is related to different degrees of N-glycosylation. *Mol Pharmacol* **45**, 1112-1118 (1994).

123. Servant, G., Dudley, D.T., Escher, E. & Guillemette, G. Analysis of the role of N-glycosylation in cell-surface expression and binding properties of angiotensin II type-2 receptor of rat pheochromocytoma cells. *Biochem J* **313 (Pt 1)**, 297-304 (1996).

124. Shaul, Y.D. & Seger, R. The MEK/ERK cascade: from signaling specificity to diverse functions. *Biochim Biophys Acta* **1773**, 1213-1226 (2007).

125. Shenkman, M., Tolchinsky, S. & Lederkremer, G.Z. ER stress induces alternative nonproteasomal degradation of ER proteins but not of cytosolic ones. *Cell Stress Chaperones* **12**, 373-383 (2007).

126. Shenoy, S.K., McDonald, P.H., Kohout, T.A. & Lefkowitz, R.J. Regulation of receptor fate by ubiquitination of activated beta 2-adrenergic receptor and beta-arrestin. *Science* **294**, 1307-1313 (2001).

127. Shirai, H., Takahashi, K., Katada, T. & Inagami, T. Mapping of G protein coupling sites of the angiotensin II type 1 receptor. *Hypertension* **25**, 726-730 (1995).

128. Siragy, H.M. & Carey, R.M. The subtype 2 (AT2) angiotensin receptor mediates renal production of nitric oxide in conscious rats. *J Clin Invest* **100**, 264-269 (1997).

129. Smith, J.A. & Martin, L. Do cells cycle? *Proc Natl Acad Sci U S A* **70**, 1263-1267 (1973).

130. Smith-Clerc, J. & Hinz, B. Immunofluorescence detection of the cytoskeleton and extracellular matrix in tissue and cultured cells. *Methods Mol Biol* **611**, 43-57 (2010).

131. Song, K., Allen, A.M., Paxinos, G. & Mendelsohn, F.A. Mapping of angiotensin II receptor subtype heterogeneity in rat brain. *J Comp Neurol* **316**, 467-484 (1992).

132. Stoll, M., *et al.* The angiotensin AT2-receptor mediates inhibition of cell proliferation in coronary endothelial cells. *J Clin Invest* **95**, 651-657 (1995).

133. Su, H.L. & Li, S.S. Molecular features of human ubiquitin-like SUMO genes and their encoded proteins. *Gene* **296**, 65-73 (2002).

134. Subramaniam, S. & Unsicker, K. ERK and cell death: ERK1/2 in neuronal death. *FEBS J* **277**, 22-29 (2010).

135. Tamura, K., *et al.* Effect of genetic deficiency of angiotensinogen on the renin-angiotensin system. *Hypertension* **32**, 223-227 (1998).

136. Tang, Z., El Far, O., Betz, H. & Scheschonka, A. Pias1 interaction and sumoylation of metabotropic glutamate receptor 8. *J Biol Chem* **280**, 38153-38159 (2005).

137. Tjio, J.H. & Puck, T.T. Genetics of somatic mammalian cells. II. Chromosomal constitution of cells in tissue culture. *J Exp Med* **108**, 259-268 (1958).

138. Tsuzuki, S., Eguchi, S. & Inagami, T. Inhibition of cell proliferation and activation of protein tyrosine phosphatase mediated by angiotensin II type 2 (AT(2)) receptor in R3T3 cells. *Biochem Bioph Res Co* **228**, 825-830 (1996).

139. Tsuzuki, S., *et al.* Molecular cloning and expression of the gene encoding human angiotensin II type 2 receptor. *Biochem Biophys Res Commun* **200**, 1449-1454 (1994).

140. Turu, G., *et al.* Differential beta-arrestin binding of AT1 and AT2 angiotensin receptors. *FEBS Lett* **580**, 41-45 (2006).

141. Velez, J.C. The importance of the intrarenal renin-angiotensin system. *Nat Clin Pract Nephrol* **5**, 89-100 (2009).

142. Vervoort, V.S., *et al.* AGTR2 mutations in X-linked mental retardation. *Science* **296**, 2401-2403 (2002).

143. Volpe, M. & De Paolis, P. Angiotensin II AT2 subtype receptors: an emerging target for cardiovascular therapy. *Ital Heart J* **1**, 96-103 (2000).

144. Watson, I.R. & Irwin, M.S. Ubiquitin and ubiquitin-like modifications of the p53 family. *Neoplasia* **8**, 655-666 (2006).

145. Webb, M.L., *et al.* Molecular characterization of angiotensin II type II receptors in rat pheochromocytoma cells. *Peptides* **13**, 499-508 (1992).

146. Wehbi, G.J., Zimpelmann, J., Carey, R.M., Levine, D.Z. & Burns, K.D. Early streptozotocin-diabetes mellitus downregulates rat kidney AT2 receptors. *Am J Physiol Renal Physiol* **280**, F254-265 (2001).

147. Weidekamm, C., *et al.* Effects of AT1 and AT2 receptor blockade on angiotensin II induced apoptosis of human renal proximal tubular epithelial cells. *Wien Klin Wochenschr* **114**, 725-729 (2002).

148. Wickner, W.T. & Lodish, H.F. Multiple mechanisms of protein insertion into and across membranes. *Science* **230**, 400-407 (1985).

149. Wilkinson, K.A., Nishimune, A. & Henley, J.M. Analysis of SUMO-1 modification of neuronal proteins containing consensus SUMOylation motifs. *Neurosci Lett* **436**, 239-244 (2008).

150. Wojcikiewicz, R.J. Regulated ubiquitination of proteins in GPCR-initiated signaling pathways. *Trends Pharmacol Sci* **25**, 35-41 (2004).

151. Wolf, G., Schroeder, R. & Stahl, R.A. Angiotensin II induces hypoxia-inducible factor-1 alpha in PC 12 cells through a posttranscriptional mechanism: role of AT2 receptors. *Am J Nephrol* **24**, 415-421 (2004).

152. Wolfe, B.L., Marchese, A. & Trejo, J. Ubiquitination differentially regulates clathrin-dependent internalization of protease-activated receptor-1. *J Cell Biol* **177**, 905-916 (2007).

153. Wong, P.F., Lee, S.S. & Cheung, W.T. Immunohistochemical colocalization of type II angiotensin receptors with somatostatin in rat pancreas. *Regul Pept* **117**, 195-205 (2004).

154. Woo, C.H. & Abe, J. SUMO--a post-translational modification with therapeutic potential? *Curr Opin Pharmacol* **10**, 146-155 (2010).

155. Wruck, C.J., *et al.* Regulation of transport of the angiotensin AT2 receptor by a novel membrane-associated Golgi protein. *Arterioscler Thromb Vasc Biol* **25**, 57-64 (2005).

156. Wyllie, A.H. "Where, O death, is thy sting?" A brief review of apoptosis biology. *Mol Neurobiol* **42**, 4-9 (2010).

157. Xu, Y., Menon, V. & Jugdutt, B.I. Cardioprotection after angiotensin II type 1 blockade involves angiotensin II type 2 receptor expression and activation of protein kinase C-epsilon in acutely reperfused myocardial infarction in the dog. Effect of UP269-6 and losartan on AT1 and AT2-receptor expression and IP3 receptor and PKCepsilon proteins. *J Renin Angiotensin Aldosterone Syst* **1**, 184-195 (2000).

158. Yamada, K., *et al.* Gene-Transfer of Human Angiotensin-Converting Enzyme (Ace) into Thf Rat-Brain Causes Sustained Blood-Pressure Elevation. *Hypertension* **26**, 557-557 (1995).

159. Yamada, T., *et al.* Angiotensin II type 2 receptor mediates vascular smooth muscle cell apoptosis and antagonizes angiotensin II type 1 receptor action: an in vitro gene transfer study. *Life Sci* **63**, PL289-295 (1998).

160. Yamada, T., Horiuchi, M. & Dzau, V.J. Angiotensin II type 2 receptor mediates programmed cell death. *Proc Natl Acad Sci U S A* **93**, 156-160 (1996).

161. Yee, D.K., Reagan, L.P., Moga, C.N., Siemens, I.R. & Fluharty, S.J. Angiotensin II stabilizes a multimeric type 2 (AT2) receptor complex in murine neuroblastoma N1E-115 cells. *Regul Pept* **54**, 355-366 (1994).

162. Yurchenko, V., Xue, Z., Gama, V., Matsuyama, S. & Sadofsky, M.J. Ku70 is stabilized by increased cellular SUMO. *Biochem Biophys Res Commun* **366**, 263-268 (2008).

163. Zahradka, P., *et al.* Modulation of the vascular smooth muscle angiotensin subtype 2 (AT2) receptor by angiotensin II. *Biochem Biophys Res Commun* **252**, 476-480 (1998).

164. Zhang, J. & Pratt, R.E. The AT2 receptor selectively associates with Gialpha2 and Gialpha3 in the rat fetus. *J Biol Chem* **271**, 15026-15033 (1996).

165. Zhao, Y., *et al.* Contribution of bradykinin and nitric oxide to AT2 receptor-mediated differentiation in PC12 W cells. *J Neurochem* **85**, 759-767 (2003).

166. Zhu, H. & Zhou, J.N. SUMO1 enhances 17-beta estradiol's effect on CRH promoter activation through estrogen receptors. *Neuro Endocrinol Lett* **29**, 230-234 (2008).